

Shackleton Prospector

A proposal for the Lunar Exploration Regolith
Analysis (LERA) Mission

Team Penguins

Nathan Long	Tony Nguyen
Samuel Dowling	Stevie Nuss-Soeharto
Alain Haddad	Maria Pantelidi
Hyacinth Jimenez	Nilkumar Shah
Kit-Ho Kwok	Ramez Wassef





Prof. Pier Marzocca
 Head of the Aviation and Aerospace
 Engineering Discipline
 RMIT University, Bundoora VIC 3083



Nathan Long
 936883



Dr. Graham E. Dorrington
 Project Supervisor
 937074



Samuel Dowling
 936970



Alain Haddad
 936967



Hyacinth Jimenez
 937016



Kit-Ho Kwok
 936984



Tony Nguyen
 936983



Stevie Nuss-Soeharto
 937014



Maria Pantelidi
 937017



Nilkumar Shah
 591179



Ramez Wassef
 937015

1 Acknowledgements

This report could not have been completed without the efforts of other students and academics. We appreciate their hard work and are thankful for their good will to include their work in our submission.

We would like to thank first and foremost, Professor Graham Dorrington and Professor Pier Marzocca, for their continuous support and encouragement. Both professors allowed for our ideas to mature into a complete concept we could be proud to submit.

We would also like to thank Matthew Williamson for his contribution to the launcher segment and for completing the calculations for the orbital mechanics. All STK simulations and STK figures were produced by Matthew, and he has given explicit written consent for their use in this report for the AIAA Space Design Competition.

The Falcon 9 CAD was taken from GrabCAD and modified by Johnathan O'Neil-Donnellon with full permission given by Johnathan to use his modified version for use in this report for the AIAA Space Design Competition.

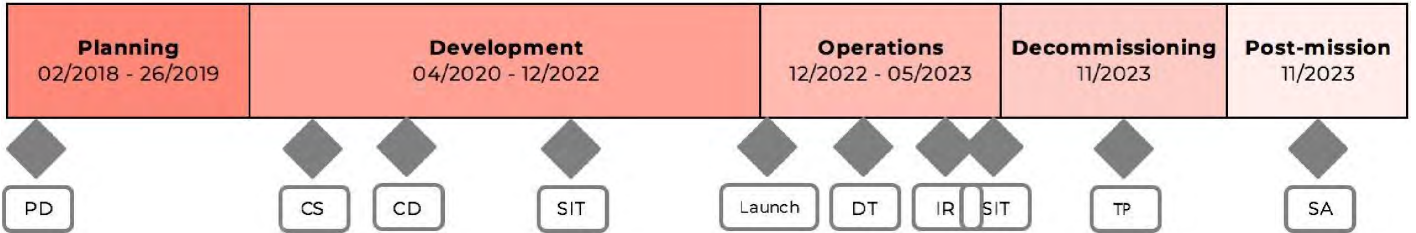
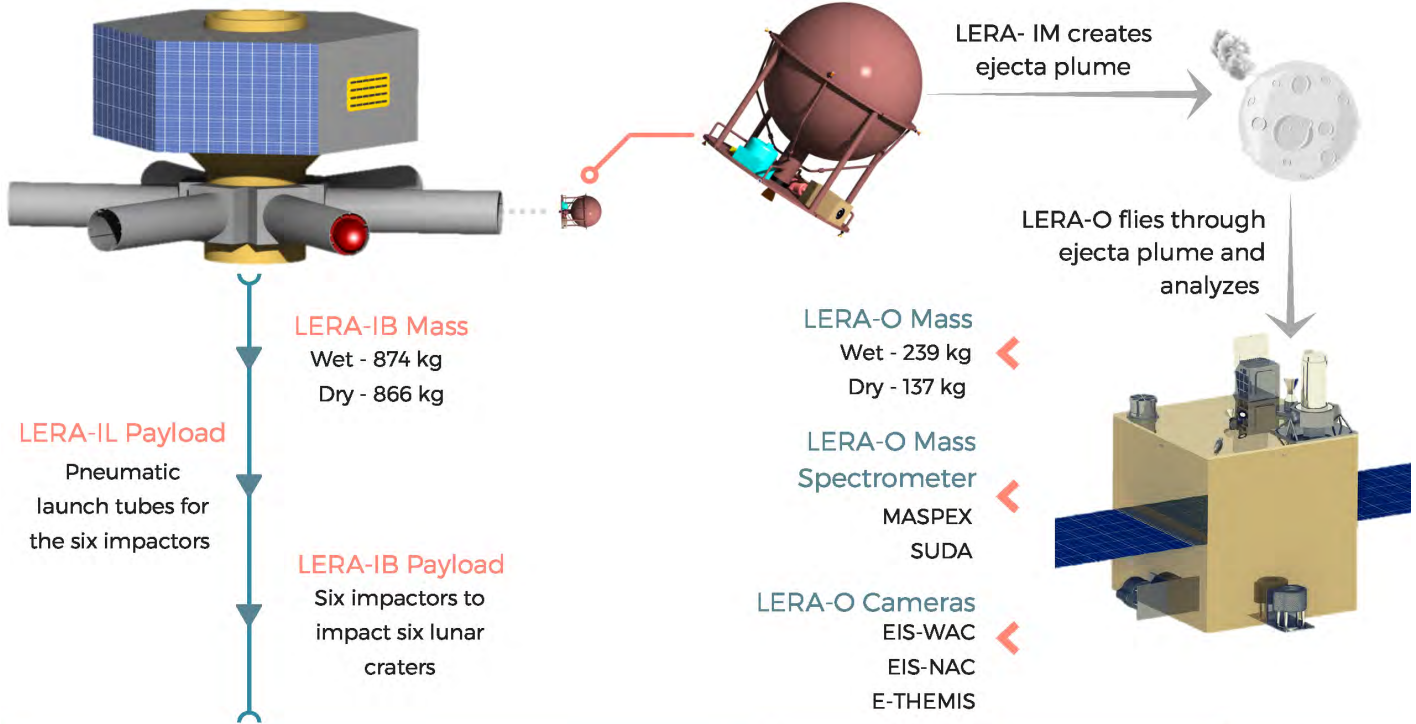
The penetrator design concept was contributed by an internal RMIT University design team (L1) in the mission trade off-study.



Mission Goals

- Measure and determine the ratio of water to regolith on the Moon
- Explore potential for scientific breakthrough on location and extent of water within the Moon's South Pole craters
- Generate a design that does not exceed US \$500M (FY17)

LERA Mission Architecture		
Launch Vehicle	Falcon 9	
Mission Target	Moon	
Mission Duration (All phases)	six years	
Ground Station Network	Swedish Space Corporation (SSC)	
	LERA-O	LERA-IB
Mission Trajectory	Circular lunar orbit	Cislunar orbit
System Architecture	Orbiting satellite	Orbiting satellite



Contents

1	Acknowledgements	2
2	Acronyms	10
3	Executive Summary	12
4	LERA Mission	14
4.1	Motivation and Mission Objectives	14
4.2	Mission Trade Study	14
4.3	Mission Requirements	17
4.4	System Breakdown Structure	18
4.5	Cost Estimation	19
4.5.1	Work Breakdown Structure (WBS)	19
4.5.2	Mission Insurance	20
4.5.3	Mission Contingency Cost	20
4.5.4	Requirement Compliance	20
4.6	Mass Estimation	21
4.7	Concept of Operations	21
4.7.1	Telecommunications	21
4.7.2	LERA-IB	24
4.7.3	Mission Schedule	24
4.8	Integration	26
5	Science Investigation	27
5.1	Science Goals and Objectives	27
5.1.1	Science Overview	27
5.1.2	Specimen Analysis	27
5.1.3	Objectives and Requirements	28
5.2	Science Instrumentation	32
5.2.1	Payload	32
5.2.2	Mass Spectrometers	32
5.2.3	Imaging Systems	34
5.2.4	Instrument Testing, Integration, and Calibration	39
5.3	Science Mission	41
5.3.1	Pre lunar orbit	41

5.3.2	Lunar orbit insertion	41
5.3.3	Impacts 1 – 3	42
5.3.4	Data collection & transfer	42
5.3.5	Change in orbital plane	42
5.3.6	Mission end	42
6	Launch System	42
7	Mission Breakdown	44
7.1	LERA-O Mission Overview	45
7.2	LERA-IB Mission Overview	45
7.3	Trajectory Modeling	46
8	LERA-O	47
8.1	Overview	47
8.2	LERA-O System Architecture	48
8.3	Structure	49
8.3.1	Spacecraft Bus	49
8.3.2	Thermal	49
8.4	Propulsion	49
8.4.1	Mission Requirements	50
8.4.2	LERA-O Propellant Trade Study	51
8.4.3	Propulsion System Summary	53
8.4.4	Propellant Thermal Management	55
8.4.5	Risks	55
8.5	Attitude Determination and Control System (ADCS)	55
8.5.1	Sensors	58
8.5.2	Actuators	60
8.5.3	ADCS Overview	61
8.5.4	(Δv) Budget	61
8.5.5	Fuel Mass Estimation	62
8.6	Command and Data Handling	62
8.6.1	Hardware	62
8.6.2	Software	64
8.6.3	Risk Aversion	64
8.6.4	Architecture	64

8.7	Power	65
8.7.1	Primary Power Source: Solar Panels	66
8.7.2	Secondary Power Source: Li-Ion Batteries	68
9	LERA-IB	69
9.1	LERA-IB System Architecture	69
9.2	LERA-IB Requirements	70
9.3	Target Characteristics	71
9.3.1	Lunar Composition	71
9.3.2	Crater Selection	71
9.4	Plume	72
9.4.1	Background	72
9.4.2	Characterization of the LERA Impact Plume	73
9.5	LERA-IB Design	77
9.5.1	LERA-IB	77
9.5.2	LERA-IM Design	78
9.5.3	Δv Requirements	78
9.5.4	Contamination Considerations	78
9.5.5	Initial Mass	79
9.5.6	Propellant Tank Design	79
9.5.7	Navigation and Control Instruments	81
9.5.8	Thruster Design	81
9.5.9	LERA-IL Design	82
9.5.10	Pressure-Tank Sizing	84
9.5.11	Impactor Detachment Effect	85
9.6	Risk and Mitigation Strategies	86
Appendix A	Pressure Tank Design	93
Appendix B	Thruster Design Equations	95
Appendix C	LERA-O Propulsion	96
C.1	Parameters	96
C.2	Maneuvers	96
C.3	Tank requirements	97
C.4	Propellant thermal management	98

List of Figures

1	System breakdown structure	18
2	LERA Mission Cost Schedule	19
3	Ground Control system layout [72]	24
4	SpaceX Falcon 9 Fairing	27
5	LCROSS Mission - NASA/JPL - This image or video was catalogued by Jet Propulsion Laboratory of the United States National Aeronautics and Space Administration (NASA).	28
6	Mass spectrum from a graphite target with a series of carbon cluster lines - LAMA [87]	29
7	1 – 10 Score trade-off study comparing similar mission instrumentation for gas particle mass spectrometers	32
8	1 – 10 Score trade-off study comparing similar mission instrumentation for dust particle mass spectrometers	33
9	1 – 10 Score trade-off study comparing similar mission instrumentation for narrow angle camera instrumentation	35
10	1 – 10 Score trade-off study comparing similar mission instrumentation for wide angle camera instrumentation	36
11	1 – 10 Score trade-off study comparing similar mission instrumentation for thermal imaging instrumentation	38
12	LERA-O Science Instruments	39
13	SUDA spectra of a pyroxene particle impact on a silver target and of a latex particle on a gold target [55]	40
14	Mission Flowchart	41
15	Launch system trade study	43
16	Falcon 9 upper-stage and payload	44
17	LERA mission breakdown	44
18	LERA-O mission breakdown	45
19	LERA-IB mission breakdown	46
20	LERA-O System Architecture	48
21	LERA-O system architecture	48
22	LERA-O system bus	50
23	Aerojet prototype GR-22 thruster [59]	53
24	Propulsion system	53
25	QinetiQ T5 thrusters mounted on LERA-O bus	61
26	Onboard computer trade study	62
27	Data bus trade study	63
28	CDH architecture flowchart	65
29	Electrical power subsystem and its functions [12]	65
30	LERA-IM and LERA-IL Subsystems Attached to LERA-IB System	69

31	LERA-IB system architecture	70
32	Lunar composition on the Moon [61]	71
33	Selected craters and their orbital planes	72
34	Definition of plume parameters	73
35	Ejecta mass obtained above the specified altitudes in terms of impactor mass	74
36	Predicted surface volume ejecta moving faster than velocity v for LERA and plume height for given velocities for LCROSS	75
37	Morphology of the low-angle component of a synthetic plume	76
38	LERA-IB cross section	77
39	LERA-IM design	78
40	LERA-IM Design Characteristics	80
41	LERA-IL Configuration	83
42	LERA-IL Configuration	83
43	LERA-IL pressure and stress performance	84
44	LERA-IL mass and shear stress characteristics	85
45	Dimensions of pressure tank at design point $r = 0.332 [m]$, $t = 10 [mm]$	85

List of Tables

1	Possible mission architectures considered for LERA	15
2	Costing of previous missions similar to LERA	16
3	Total LERA mission cost breakdown	20
4	Breakdown of the cost estimation for LERA	21
5	Antenna frequency band specifications	23
6	Antenna gain specifications	23
7	LERA-O telecommunications system specifications	23
8	Mission schedule	25
9	LERA's science objectives and the suitability of hardware to the top-level mission requirements and goals.	31
10	Mass spectrometer instrument overview	34
11	Performance specifications	34
12	Narrow angle camera trade study	35
13	Wide angle camera trade study	36
14	Thermal imaging camera trade study	37
15	Thermal imaging camera instrument overview	38
16	LERA-O science instruments	39

17	Δv budget for orbital maneuvers	47
18	Comparison between heritage batteries and the impact of using Li-ion Saft batteries [35]	49
19	LERA-O propulsion system highlights	50
20	Δv budget and fuel requirements	51
21	Propellant suitability evaluation	51
22	Toxicity testing results of AF-M315E and hydrazine [17]	53
23	GPIM AF-M315E GR-22 thruster technical data	54
24	LERA-O propulsion system mass breakdown	54
25	Technology readiness of propulsion system components	55
26	Propulsion system risks	55
27	Attitude control modes during the mission [86]	56
28	ADCS subsystem requirements	56
29	Attitude control methods [86]	56
30	Types of sensor for attitude determination [99]	57
31	Attitude determination and control instruments	57
32	Potential star trackers for the LERA-O ADCS [51, 80, 93, 94]	58
33	Potential sun sensors for LERA-O ADCS [62–65, 91]	59
34	Potential IMUs for the LERA-O ADCS [26, 28, 43, 79]	59
35	Reaction wheels considered for the LERA-O ADCS [4, 23, 66, 95]	60
36	xenon reaction control thrusters that were taken into consideration for the attitude determination and control system of the LERA-O [19, 34, 36]	60
37	Attitude determination and control system overview	61
38	Given the mechanical properties of the chosen material the following characteristics relating to the xenon fuel tank were defined	62
39	LERA-O instrument data rates	63
40	Power requirements for LERA-O	65
41	Power budget for LERA-O	66
42	Comparison of silicon and gallium arsenide solar cells	67
43	Comparison of silicon and gallium arsenide solar cells [89]	67
44	Heritage batteries and useful characteristics [20]	68
45	Saft Li-ion cell technical specifications [35]	69
46	Details of six selected craters	72
47	Comparison of LERA-IM propellants	79
48	Mass properties for LERA-IM	80

49	LERA-IM propellant tank properties	80
50	Navigation and control instruments onboard the LERA-IM	81
51	LERA-IM thruster design	82
52	Material properties of Aluminum-6061	84
53	LERA-IB risk and mitigation strategies	86
54	LERA-O propulsion parameters	96

2 Acronyms

Acronym	Definition
ADCS	Attitude Determination and Control System
AIAA	American Institute of Aeronautics and Astronautics
AMO	Air Mass Zero
AVGR	Ames Vertical Range Gun
BER	Bit Error Rate
BIRCHES	Broadband Infrared Compact High Resolution Explorer Spectrometer
BOL	Beginning of Life
BWG	Beam Wave Guide
CAD	Computer Aided Design
CCSDS	Consultative Committee for Space Data Systems
CDH	Command and Data Handling
CMG	Control Moment Gyros
COMA	Cometary Mass Analyzer
COSIMA	Cometary Secondary Ion Mass Analyzer
COTS	Commercial Off-The-Shelf
EIS	Europa Imaging System
EMC/EMI	Electromagnetic Compatibility/Interference
EPS	Electrical Power System
EPS	Electronic Power System
E-THEMIS	Europa - THERmal EMISSION Imaging System
FAA	Federal Aviation Administration
FY	Financial Year
GAN	Ground Antenna Network
GEO	Geostationary Earth Orbit
GPIM	Green Propellant Infusion Mission
GTO	Geostationary transfer orbit
HAN	Hydroxyl Ammonium Nitrate
HGA	High Gain Antenna
IMU	Inertial Measurement Unit
IPCU	Ion Propulsion Control Unit
ISRO	Indian Space Research Organisation
ISS	International Space Station
ITA	Ion Thruster Assembly
JEM	Japanese Experimental Module
LADEE	Lunar Atmosphere Dust and Environment Explorer
LCROSS	Lunar Crater Observation and Sensing Satellite (LCROSS)
LEO	Low Earth Orbit
LEO	Low Earth Orbit
LEOP	Launch and Early Orbit Phase

Acronym	Definition
LERA	Lunar Exploration and Regolith Analysis
LERA-IB	Lunar Exploration and Regolith Analysis - Impactor Bus
LERA-IL	Lunar Exploration and Regolith Analysis - Impactor Launcher
LERA-IM	Lunar Exploration and Regolith Analysis - Impactor
LERA-O	Lunar Exploration and Regolith Analysis - Orbiter
LGA	Low Gain Antenna
Li-ion	Lithium-Ion
LILT	Low Intensity Low Temperature
LRO	Lunar Reconnaissance Orbiter
MAIT	Manufacture Assembly Integration and Testing
MAIT	Manufacture, Assembly, Integration and Testing
MASPEX	MAss SPectrometer for Planetary EXploration/Europa
MEO	Medium Earth Orbit
MLI	Multi-Layer Insulation
MMH	Monomethyl Hydrazine
MRO	Mars Reconnaissance Orbiter
NAC	Narrow Angle Camera
NASA	National Aeronautics and Space Administration
NEN	Near Earth Network
NMS	Neutral Mass Spectrometer
NS	Nominal Speed
OBC	OnBoard Computer
OS	Operating System
PXFA	Proportional xenon Feed Assembly
RCS	Reaction Control System
RFC	Regenerative Fuel Cells
RTG	Radioisotope Thermal Generator
SCAPE	Self-Contained Atmospheric Protective Ensemble
SDRAM	Solid Drive RAM
SSC	Swedish Space Systems
ST	Star Tracker
STK	Systems Tool Kit
STMD	Space Technology Mission Directorate
SUDA	SURface Dust Analyzer
TDM	Technology Demonstration Mission
THEMIS	THERmal EMission Imaging System
TPS	Thermal Protection System
TRL	Technology Readiness Level
TT&C	Telemetry, Tracking and Control
USD	United States Dollar
UTC	Coordinated Universal Time
WAC	Wide Angle Camera
WBS	Work Breakdown Structure

3 Executive Summary

Recently there has been an increase in the interest of prospecting planetary bodies within the Solar System for vital resources to human life, including water. The interest in this prospecting has been focused on the Moon, with an increase of missions investigating and analyzing the level of water and its base atoms; hydrogen and oxygen, on and within the surface of the Moon.

This report outlines Lunar Exploration and Regolith Analysis (LERA), a NASA Discovery unmanned mission to the Moon that aims to determine the location of water deposits in the Moon's south pole craters. The mission solution should be able to measure the ratio of water to regolith in at least two craters. A trade study has been performed of previous lunar missions to determine the best solution and mission configuration to achieve the mission objectives. A multiple satellite mission has been chosen which includes one satellite to fire Impactors at the Moon's surface to create ejecta plumes and another satellite to perform all scientific analysis by flying through the debris created by the plumes.

The requirements at the mission and system level have been identified as well as a detailed explanation of the mission overview. Once the upper-stage of the launcher has reached translunar orbit, it will deploy first the satellite, LERA-O (orbiter), into a circular orbit around the Moon. The second satellite, LERA-IB (impactor), will continue inside the upper-stage around the Moon in a cislunar orbit. Once LERA-IB is within close proximity of the Moon, six impactors (LERA-IM) will be detached simultaneously to perpendicularly impact the Moon.

The concept of operations is detailed next, with a detail of the telecommunications system between LERA-O, LERA-IB and ground control on Earth. The telecommunication system selected is chosen to maintain contact between elements at all stages of the mission lifetime. The Swedish Space Corporation (SSC) will be employed for telemetry and launch support service, tracking and control, and payload data services. The mission schedule has also been outlined from the beginning of mission development to the final stage of decommissioning both satellites.

Both LERA-O and LERA-IB will be integrated into the SpaceX Falcon 9 fairing. The LERA-IB will be integrated into the fairing adapter via a mechanical mating plate and will be permanently attached. The LERA-O will be mounted on top of the LERA-IB until deployment into lunar orbit. A thorough investigation and explanation of the science investigation will follow including the scientific goals and objectives, science implementation, and science mission. Although a minimum of two craters was required, LERA will be focusing on six craters: Cabeus, Shoemaker, Haworth, Faustini, Shackleton, and de Gerlache. It is recognized that in the polar regions of the Moon, any water that would be found would be in the form of ice. The collision created by the LERA-IM will create a plume to which any water from the surface will vaporize and eject plasma containing electrons, ions, and dust that may contain any of the 18 variations of the water molecule.

Two science objectives have been identified that will achieve the mission objectives and determine which scientific equipment is suitable. Regolith composition will analyze the gas and dust particles within the ejecta plume and surface topography will take visual and thermal images of the lunar surface before and after each impact. A trade off study was completed to determine the most suitable science instruments and only instruments with a technology readiness level of 8 and above were chosen for the design. Two pass spectrometers were chosen: MAss SPectrometer for Planetary EXploration (MASPEX) and SUrface Dust mass Analyzer (SUDA). For imaging, three cameras have been chosen: a narrow angle camera for the visible spectrum, a wide angle for the visible

spectrum, and a thermal imaging system.

The launch system and orbital mechanics of the mission have been outlined in detail and can be broken down into eight phases: upper-stage launch, upper-stage translunar injection, orbiter detach, orbiter lunar capture, upper-stage lunar flyby, impactor detach, and impact at lunar target. LERA-O and its subsystems will then follow in detail. The structure of LERA-O will implement heritage components in its structure from its spacecraft bus and thermal considerations. A brief paragraph detailing payload integration will be explained next and then the propulsion subsystem. Subsystem requirements have been outlined and a 15% contingency has been included in the calculation of propellant. A trade study was conducted for both an engine and propellant, and LERA-O will implement an Aerojet Rocketdyne Green Monopropellant Rocket Engine with AF-M315E, which is a hydroxyl ammonium nitrate blend. No significant risks are identified with respect to the propulsion system.

The Attitude Determination and Control System (ADCS) for LERA-O involved a trade study for the different attitude control methods that could be implemented, sensors that could be used for attitude determination, and equipment that could be used for control. Two Sinclair ST-16RT2 star trackers, four SolarMEMS nanoSSOC-D60 sun sensors, a Northrop LN-2005 inertial measurement unit, four Vectronic VRW-02 reaction wheels, and four QinetiQ T5 reaction control system thrusters were chosen.

Command and Data Handling (CDH) utilized mostly heritage components, chosen through trade studies and evaluating options against the mission and science objectives. The onboard computer will be the BAE Systems RAD 3U cPCI OBC, the data bus a MIL-STD-1553, and the data links will be SpaceWire IEEE 1355. The software chosen for LERA-O was VxWorks OS. Detail into the electrical architecture and risk aversion strategies are also included.

The electrical power subsystem (EPS) implemented heritage components and decisions were based on the peak power requirements of all subsystems on LERA-O, as well as a 30% contingency margin. The primary power source chosen were triple-junction solar cells from AZUR Space and will be deployable rigid panels. A secondary power source is required due events such as eclipses and a single Saft Specialist Battery Group VL48E battery will be used.

Details of the LERA-IB follow including a detailed explanation of the system architecture and system and subsystem requirements. Target characteristics are outlined including detailed outlines of reasoning behind crater selection and composition of lunar regolith. Detailed research of plumes is included, as well as ejecta mass distribution, ejecta volume distribution, and an explanation of how plumes were modelled. In the LERA-IB design section, pressure tank design is detailed including equations and calculations. The LERA-IB structure is outlined as well and includes a detailed CAD and its components. Delta V requirements are highlighted as well as considerations into any potentially contamination issues.

The mass of each LERA-IM will be limited to a wet mass of 30kg each. The final propellant tank design of LERA-IM and navigation and control instruments are outlined. LERA-IM will implement a Northrop LN-200S inertial measurement unit, an Adcole MAI-SS star tracker, an ATMEL AT697E processor, and a GS YUASA LSE 102 lithium-ion cell for power. The LERA-IL detachment mechanism design is given in detail including piston sizing, pressure tank sizing, and various CAD drawings to aid in the visualization of the system. The proposed design aims to achieve the mission and scientific objectives at a low-cost and within the specified time frame. Heritage and higher TRL components have been specifically chosen for most subsystems to ensure this and will aid in ensuring the success of the mission.

4 LERA Mission

4.1 Motivation and Mission Objectives

In any future crewed lunar base scenario, the transport of water from the Earth to the Moon would represent a major logistics burden. NASA, in one of their presentations on LCROSS, has revealed that transporting a gallon of water to the Moon would cost over \$100,000 [39]. Learning to live off the land would render human lunar exploration much easier and therefore efforts have been pursued to carry science missions to planetary bodies with the explicit goal of searching for water. Previous findings have uncovered that oxygen and hydrogen can be obtained from lunar soil. However, high energy level processes are required to extract such critical raw materials. If found in sufficiently large enough quantities, in-situ water deposits will provide the critical life support system required for manned space exploration missions. This will also greatly reduce the reliance of water supplies delivered from Earth. The primary mission objective of LERA is to provide a better understanding of the quantity, form, and distribution of water deposits (ratio of water to regolith) in permanently-shadowed regions near the south pole of the Moon. By evaluating the accessibility of water deposits on the Moon, LERA will help simplify future lunar mission architectures.

4.2 Mission Trade Study

When considering the overall approach to the Lunar Prospector mission there are numerous system architectures with potential to satisfy the proposal requirements. A high-level architecture analysis, outlined in 2, summarizes and compares the architectures based on five key factors: cost, innovation, risk, technology, and scientific evaluation.

Table 1: Possible mission architectures considered for LERA

Description	Cost	Innovation	Risk	Technology	Required Evaluation	Scientific
Lander/ Rover	Deployment of landing mechanism Large energy storage devices for movement in shadowed areas Larger in size and therefore will have higher launching costs	Low - performed many times before	Complexity of low-gravity environment Lack of sunlight in crater, need for high energy storage device	Landing strategy with consideration of the lack of atmosphere High energy storage devices High level communication devices 'Drilling' device to collect samples from under lunar surface	Very accurate characterization of regolith composition TRL 9	
Single CubeSat	Low-cost	High - start of field; technology and development only begun	New field places uncertainty on the reliability of the spacecraft Requires orbital and trajectory considerations due to low orbit requirement Small size means limited scientific instruments available	Development of new scientific instruments or adaptation of heritage	Heritage instruments TRL 4-9	scientific
Single large satellite	High complexity	Medium - similar to many other missions	Difficult system integration Trade off between scientific instruments, propulsion requirements and number of impactors available onboard	Release mechanism for impactors	Heritage instruments TRL 6-9	scientific
Multiple satellites	High complexity Relatively high launch costs	High - not many similar missions	Complex orbital requirements Reduces size due to the doubled requirement of two spacecrafts which may mean less scientific instruments available	Release mechanism for impactors Individual propulsion and attitude control systems	Heritage instruments TRL 6-9	scientific
Impacting 'Penetrator', which takes regolith samples after impact	High complexity	Takes an unconventional approach to this problem. Utilises high-g resistance technology	Unable to accurately guide to required location (Requires a pre-excavated area) Unable to slow down to a sufficiently low speed (Requires impact speeds of $\approx 600 [m/s]$) Destroyed on impact	G Resistance	TRL 2	

The possibility of a lander on the Moon was immediately disregarded due to the high costs involved in designing and ensuring that a lander can land safely on the Moon and has sufficient power required to navigate the rough surface of the southern hemisphere of the Moon and be able to communicate data obtained back to Earth. As the mission objective is to target the Moon's southmost craters for their water content, where craters are often shrouded in complete darkness regardless of the Moon's position from the Sun, it is likely that a lander would not be able to communicate unless an expensive nuclear-based power source is chosen. There have been single and multiple satellite missions to explore the presence of water on the Moon including Chandrayaan-1, Chang'E 1, Lunar IceCube, and LRO/LCROSS. The NASA Europa Clipper mission is also valuable to investigate as it was a mission that was able to analyze a vapor outgassing on Jupiter's Moon, Europa, which was identified as water vapor. A brief explanation of the scientific investigation will be conducted and a table summarizing the cost of each mission has been included in 2.

Table 2: Costiong of previous missions similar to LERA

Mission	Configuration	Mission Cost [USD ^{FY17}]	Launch Mass [kg]
Chandrayaan-1 (ISRO)	Orbiting satellite and single impact vehicle	\$65.7 [67]	1380
Chang'E 1 (CNSA)	Orbiting satellite	\$212.5 [58]	2350
Lunar IceCube (NASA)	CubeSat	N/A (\$7.9 awarded for further development)[98]	14
LADEE	Orbiting satellite	280 [2]	383
LRO/LCROSS (NASA)	Orbiting satellite and single impact vehicle	\$665 (LRO \$575 million, LCROSS \$90 million) [37]	1915/621
Lunar Orbiter 5	Orbiting satellite	<40 [1]	385.6

The Chandrayaan-1 was the ISRO's first planetary mission to the Moon and aimed to further understand the evolution of the Moon by mapping the geology of the surface at high resolution. At the beginning of lunar orbit, a Moon Impact Probe (MIP) will be released to impact the south polar region which then will allow for the satellite to collect information about the presence of water [15, 33]. The satellite continued to orbit the Moon and continue gathering information about the surface of the Moon and its composition. Chang'E-1 was China's first lunar spacecraft and aimed to determine the characteristics of the lunar surface through a satellite equipped with eight onboard scientific instruments [102]. The probe was originally scheduled to orbit the Moon only for a year, but the mission was later extended another year. The mission was able to create a full map of the Moon's surface. CubeSats offer a small-cost, small-scale mission solution for cislunar space that can be developed and completed in a much shorter time frame than traditional full-scale missions. The Lunar IceCube mission aimed to investigate the equatorial regions of the Moon and further develop the information known about the presence of water on the Moon [16]. Water measurements were taken at a low lunar orbit due to the capabilities of the onboard instruments. The mission is planned to be launched in 2019 and as part of NASA's NextSTEP program. It is planned to carry only one instrument to detect the presence of water in ice, liquid, and vapor forms, the Broadband Infrared Compact High Resolution Explorer Spectrometer (BIRCHES) [53]. The Europa Clipper mission aims to conduct a detailed investigation of Jupiter's icy Moon, Europa, and determine whether it processes the qualities to harbor life [96], including the presence of water. It has been found that beneath Europa's surface lies an ocean which scientists hope to further research with this mission. The mission will perform 45 flybys and collect information on the icy shell, surface geomorphology, and the composition of

the surface. A launch date has not been selected yet, but it is expected to fall between 2022 to 2025. The Lunar Crater Observation and Sensing Satellite (LCROSS) and Lunar Reconnaissance Orbiter (LRO) missions were developed as part of NASA's Exploration Systems Mission Directorate and were created to analyze the Moon's surface topography and geology as well as identify any useful resources [38]. On the LRO, the onboard scientific instruments were able to conduct their scientific investigation while remaining in orbit. The LCROSS was developed to impact the Moon's surface in the polar region right after the Centaur upper-stage and analyze the debris plume created by the impact for hydrogen and oxygen. This is completed using near-infrared spectrometers, a visible spectrometer, one visible camera, two near infrared cameras, and two mid-infrared cameras. Comparing the missions investigated above, there are a number of ways to be able to potentially investigate the presence of water on the Moon and other planetary bodies in space. The most popular and widely used solution currently is the use of satellites to analyze the composition of the lunar surface from orbit. However, a thorough and accurate analysis of the water content within the surface will be difficult to determine without attempting a mission that can penetrate the outer surface of the Moon. Both Chandrayaan-1 and LRO/LCROSS attempted this by impacting the southern regions of the Moon once and performed scientific analysis before impacting the Moon itself, which is not a viable option for the current mission proposed. In order to ensure that multiple sites are targeted, it would be suitable for the mission to have two separate spacecraft; one for conducting the analysis and the other for launching impactors at the chosen sites. Despite the complexity that a mission architecture composing of multiple satellites poses, the innovation aspect that presents itself is too rewarding and fascinating to disregard. Although the LRO/LCROSS mission cost is more than the cost requirement specified in Section 4.3, with the implementation of heritage components, it is expected that the LERA mission will be able to achieve the scientific objectives whilst remaining under budget. The mission's requirements are outlined in Section 4.3, which are derived from the mission's concept of operations, feasibility of the instruments in the given environment and the availability and reliability of components.

4.3 Mission Requirements

- Top Level Requirements
- The cost of the mission, including launch vehicles, shall not exceed US \$500 Million (in Financial Year 2017)
- The mission shall use technologies that are currently in the NASA development portfolio or a Technology Readiness Level (TRL) of 8 or higher
- The mission platform shall analyze samples from a minimum of two lunar craters
- The mission shall complete its primary scientific mission no later than December 31, 2024
- The mission shall be un-crewed and robotic
- The mission platform shall determine the locations of water deposits, measured by the locations' latitude, longitude, and depth
- The mission platform shall have sufficient thermal management to be able to withstand extreme temperature environments throughout the mission lifecycle

- The mission platform shall be able to withstand all vibrations (low, mid and high frequency bands) that it is expected to encounter to during the mission
- The mission platform shall be able to sustain the power requirements over the duration of the mission
- The mission platform shall be designed so that it is capable of remaining serviceable, under controlled conditions, for up to two years after expected manufacturing date
- The LERA-O and LERA-IB shall both fit in the upper-stage launch vehicle payload bay
- The LERA-O and LERA-IB shall not exceed a combined mass of greater than 3000 kg
- The mission platform shall be able to measure and determine the ratio of water to regolith within an absolute error of 5%

4.4 System Breakdown Structure

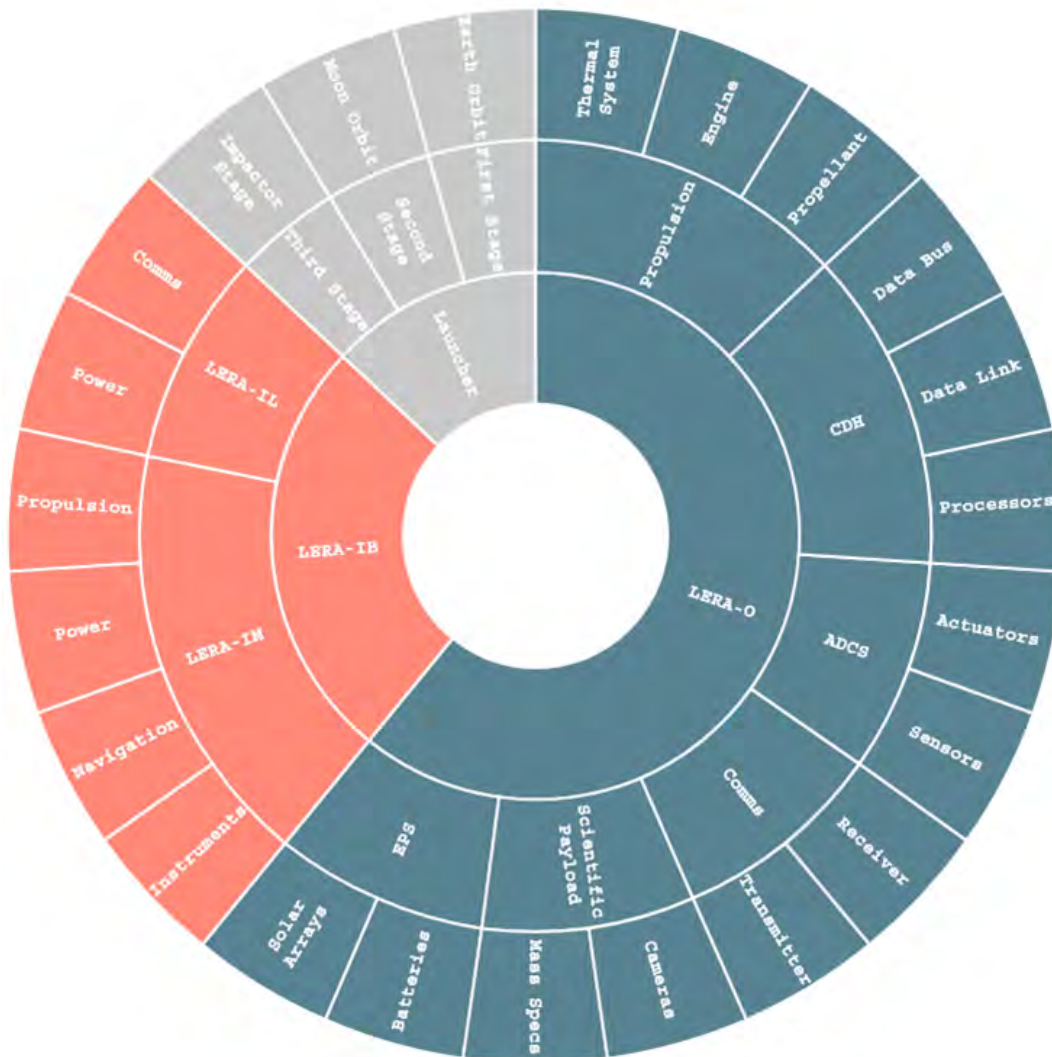


Figure 1: System breakdown structure

4.5 Cost Estimation

In comparison to other missions, the LERA mission has a considerably shorter mission duration of six years, nine months and 16 days. However, despite this, the LERA system as a whole is extremely complex in nature and must undergo a large development phase in order to account for lead times of components. As per the requirement, the LERA mission must not exceed \$500M USD, and thus, the total cost of the mission is of concern. This section discusses the costs associated with the LERA mission phases.

4.5.1 Work Breakdown Structure (WBS)

Figure 2 provides a visual representation of LERA's total cost trend with respect to the various milestone dates.

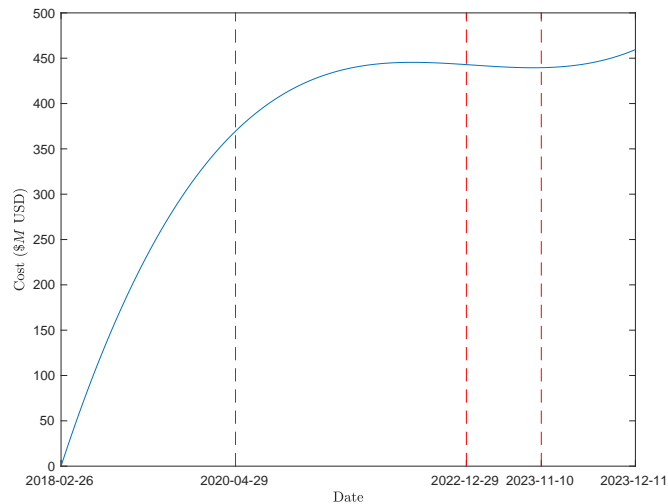


Figure 2: LERA Mission Cost Schedule

Planning The planning phase is the mission kickoff stage which begins at \$50M USD after signing the SpaceX launch vehicle contract.

Development The development phase is the most costly phase in the LERA mission. It involves component selection, procurement and development. Additionally are the manufacture, assembly, integration and testing (MAIT) of all subsystems and systems. Here all components will undergo the verification process which includes the evaluation of system compliance with regard to requirements, safety, quality, reliability and Federal Aviation Administration (FAA) Aeronautics and Space Transportation regulations.

Component Cost Modeling The cost estimation model used is based off a linear trend of a variety of space avionic components. It measures the required number of people working in a year to build the first unit of production, based on the mass of the components. The similarity multiplier, f , is a factor based on an engineer's estimate of how more or less difficult it is to produce a certain product compared to last time. The constant (c) ranks the difficulty to produce the product based on its similarity to components or products that have been previous developed and manufactured. Further the mass of the object is referred to as x . To determine

these costs Equation 1 is used.

$$Cost(\text{Man} - \text{Years}) = cfx^{xp} \quad (1)$$

Once calculated in man-years, these cost values have been converted with the assumption that an engineer will earn \$250K USD in FY18. A detailed cost breakdown of all components associated with the LERA design is presented in Appendix D.

Operations The operations costs of the mission are given a considerable allocation from the budget. It comprises of the costs of the mission control staff, ground network station usage, and in-space operations. It is assumed that at least 20 personnel at any one time are required to operate the ground stations.

Post-mission The post-mission tasks include the analysis of scientific data and the mission evaluation. This may take considerable resources and time to complete due to the complexity of the mission and the data outputs.

4.5.2 Mission Insurance

Within the mission budget, the mission insurance has been allocated \$25M USD. Combining the cost of both spacecraft and the launch, this insurance allocation will protect the mission against any launch failure.

4.5.3 Mission Contingency Cost

With a total cost budget of \$500M USD, a contingency factor of 5% has been added to account for any unforeseeable expenses that may occur over the duration of the mission. This could include, but is not limited to, incorrect or incomplete designs, defective components, human factors and unpredictable weather conditions.

4.5.4 Requirement Compliance

With a total cost budget of \$500M USD, the LERA mission complies with this requirement, even with an added 5% contingency factor and with mission insurance. A breakdown of this is illustrated in Table 3.

Table 3: Total LERA mission cost breakdown

Dates	Phase	Cost [M USD]
2/26/2018	Planning	2.00
4/29/2020	Development	391
12/29/2022	Operations	53.0
11/10/2023	Decommissioning	0.00
12/11/2023	Post-mission	4.00
12/11/2024	End mission	0.00
LERA Mission Cost		449
LERA Mission Cost + Insurance		474
LERA Mission Cost + Insurance + Contingency		499

4.6 Mass Estimation

A complete mass breakdown of LERA and its respective systems are outlined in Table 4. The mass of the subsystems and their components are known values given by manufacturers. Similarly to the cost estimation, an additional contingency factor based on the product's TRL has been added to the mass to account for any discrepancies that may occur during the development stage.

Table 4: Breakdown of the cost estimation for LERA

Component	Subsystem	Mass [kg]
LERA-IB	LERA-IM	198
LERA-IB	LERA-IB	292
LERA-IB	LERA-IL	384
	TOTAL WET	874
	TOTAL DRY	866
LERA-O	CDH + Comms	3.49
LERA-O	ADCS	53.8
LERA-O	EPS	33.7
LERA-O	Propulsion	115
LERA-O	Science	33.5
	TOTAL WET	239
	TOTAL DRY	137
	TOTAL Mass	1114

The only mission requirement which considers mass is that which requires the launch payload mass to be less than 6000 kg as specified by the launch vehicle provider, Space X. With a total payload mass of only 1114 kg, LERA clearly complies with this top-level requirement. The LERA payload integrated within the Falcon 9 upper-stage takes up approximately a third of the vehicle. Therefore, validating the mass estimation which approximates that the upper-stage payload can comfortably carry 3000 kg. For a detailed breakdown of the mass budget, please refer to Appendix D

4.7 Concept of Operations

4.7.1 Telecommunications

The telecommunications system for LERA is responsible for providing on-going data linkage between ground control on Earth and the LERA-O and LERA-IB spacecrafts. Not only must this system be capable of sending data to ground control operators pertaining to altitude, axial orientation, fuel consumption, net velocity, and other telemetric parameters, but it must also be capable of retaining data which is of paramount importance to LERA's mission objective - scientific regolith composition data. LERA will utilize Swedish Space Corporation's (SSC) launch support service and telemetry, tracking and control (TT&C), and payload data services which operate through their global station network. This network will provide around the clock services to both LERA-O and LERA-IB which comprises of launch and early orbit phase (LEOP) and key spacecraft health-related data such as axial orientation, attitude parameters, telemetric subsystem statuses, net velocity and temperatures and in-orbit support [83, 84].

Below is a list displaying various constraining requirements which drives the design and selection of LERA's telecommunication system.

-
- LERA must be capable of communicating with the Swedish Space System's (SSC) global network of ground stations during the entirety of its mission
 - LERA shall be capable of transferring data with a bit error rate (BER) of less than 10^{-5} incorrect symbols per second
 - LERA shall be capable of transferring data at a rate of no less than 1200 symbols per second (1.2 kbps)
 - LERA shall be capable of communicating with a link margin of greatest magnitude between either 4 dB or 30% of the E_b/N_0 required for linkage

As outlined above, these telecommunication requirements will ensure the selected system will be able to provide adequate signal at all stages of the mission lifetime. A minimum link margin of 5 dB ensures LERA has complete immunity from signal losses due to random activities affecting the received E_b/N_0 of the system [32]. E_b/N_0 selection is based purely and solely on the bit error rate of a selected modulation and error correction regime. If LERA is to transmit for one hour a day, an allowable bit error rate of 10^{-5} translates to one error per month; a negligible occurrence rate that would result in a simple retransmission of data in a timely manner as required. It is also worth noting that the extra power from establishing a link margin will lower the bit error rate from this expected value [32]. The minimum communication speed required for achieving a sufficient transfer rate of data is expected to be approximately 1200 symbols per second (1.2 kbps) which will further constrain the design selection process. Moreover, it is worth noting that LERA will be following the Consultative Committee for Space Data Systems (CCSDS) for recommendations regarding telemetry delivery for a telecommunications system which is designed for minimal data loss. Different mission operational phases will require different forms of telecommunication and have therefore been segmented below.

Ground Antenna Network SSC's antenna networks are located at eleven sites over the globe, including the Americas, Europe, Africa, Asia and Australia, with their coverage further expanded by eight additional stations through a collaborative agreement with industry partners. LERA will therefore have the ability to maintain communications and data handling by establishing a link to any of these antennas within the network [82]. The extensive global coverage and proven performance, combined with the low ongoing operation cost and greater coverage availability makes SSC's network far more desirable than those compared with other mission management services and their respective antennas.

Onboard Antenna As all uplink data pertaining to ground commands and downlink data pertaining to telemetry and scientific data transmission that is produced by LERA will be transmitted through these multi-frequency antennas, LERA will require a Low Gain Patch Antenna (LGA) which provides low amplification of radio frequency signals [30]. One of the benefits of a LGA antenna is that it is omnidirectional and is able to transmit and receive signals regardless of orientation. A single LGA is capable of transmitting data back to a SSC antenna on Earth when positioned within a tilt angle of $\pm 20^\circ$ [72]. This allows LERA and LERA-O to transmit data during orbit without needing to be axially reorientated through propulsive methods to accurately establish connection with ground-based antennae. For both LERA vehicles completing their respective orbits, their position and orientation may be such that it inhibits accurate pointing towards Earth and the ground stations. For this reason, integration of an omnidirectional antenna is

extremely beneficial as all communication can be maintained and data can be timely transmitted before the next round of scientific sampling. The key design parameters will be a link margin of minimum 4dB, minimizing power consumption, maximizing data rate, and minimizing geometry/mass. Table 5 outlines X and S Band antenna specifications [57, 85].

Table 5: Antenna frequency band specifications

Parameters	SSC Antenna	LERA LGA
Antenna Diameter [m]	13	0.0127
Frequency Band	X Band	S Band
Frequency [GHz]	2.2-2.4	8.0-8.4
Wavelength [cm]	13.63	3.75

Table 6 outlines the gain of each antenna during both up and downlink, given an antenna efficiency of 60%.

Table 6: Antenna gain specifications

Parameters	Transmission		Reception	
	SSC Antenna	LERA LGA	SSC Antenna	LERA LGA
Frequency Band	S Band	X Band	X Band	S Band
Antenna Gain [dB]	67	18	79	7
G/T [dB/K]	33	23	23	33

Ground network SSC antennas receive data at a rate of 70.25kbps and transmits at a rate of 1.5kbps, which enables the support of all data handling and processing. Please note that these data rates assume the maximum data rate of the instruments whilst fully operational, during the orbital period of 1.94 hrs and with a safety factor of 1.5.

LERA-O LERA-O will be fitted with four low gain patch antennas on a single surface plate which will enable data transmission at a sufficient rate to match that of which the SSC ground antenna can receive. Below is a table showing the specifications of the LERA-O telecommunications system.

Table 7: LERA-O telecommunications system specifications

Parameters	LERA-O Telecommunications System	Total
Number of antennae	4	-
Transmitting Power Budget [W]	10	40
Mass [kg]	0.186	0.744

This telecommunications system will enable frequent data transmission during launch and Earth's geostationary orbit through correspondance with the Near Earth Network (NEN) and SSC antennae for the remaining stages of the mission timeline.

Ground Operations Operating 24 hours a day, SSC will be contracted on the LERA mission for the duration of the 141 day mission. The data handled and processed through their systems will forward will forward through to communications link to NASA.

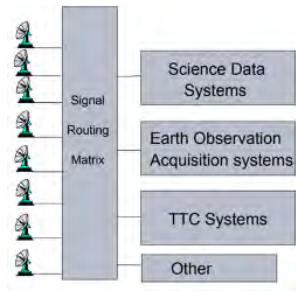


Figure 3: Ground Control system layout [72]

4.7.2 LERA-IB

The mission to be carried out is largely autonomous, and will thus require no operator input. However, there are two phases in which operator input is required. The phases of this mission include launch, flyby, LERA-O detach and target, LERA-IM detach and target, and termination/disposal. The only phase requiring operator input is the LERA-IM detach and target phase. This phase will be described in more detail below.

Impactor Delivery Phase This phase begins on 18 May 2023 10:40 UTCCG as the Falcon 9 upper-stage is on its approach to the Moon. This is the point at which the impactors are scheduled to detach from the Falcon 9 upper-stage to enter a collision trajectory for the target lunar site. At this stage, the operator will have the decision to choose which crater should be impacted and enter the Δv required to achieve this impact. The impactor is then launched by LERA-IL, making autonomous error corrections as appropriate until it impacts the lunar surface at approximately $3.19 [km/s]$. This process is repeated an additional five times at intervals of 1.94 hours corresponding with the time it takes LERA-O to complete a lunar orbit, ensuring that it is in position to take readings of the impact plume. The impactors are capable of detaching with any Δv up to and including $300 [m/s]$, which is assumed to be the maximum required for the last impactor to detach.

4.7.3 Mission Schedule

Table 8 provides a thorough overview on the LERA mission based on all phases of the project. All times are assumed to be in Coordinated Universal Time (UTC).

Table 8: Mission schedule

Date	Time	Phase	System	Task
02/26/2018	09 : 00 : 00	Planning	LERA	Preliminary Design Review (PDR)
05/26/2018	09 : 00 : 00	Planning	LERA	Concept generation
07/05/2018	09 : 00 : 00	Planning	LERA	Critical design review (CDR)
10/26/2018	09 : 00 : 00	Planning	LERA	Functional system design
12/26/2018	09 : 00 : 00	Planning	LERA	Trade studies
02/26/2019	09 : 00 : 00	Planning	LERA	Mission integration kickoff
04/29/2020	09 : 00 : 00	Development	LERA	Component selection (CS)
08/29/2020	09 : 00 : 00	Development	LERA	Component development (CD)
12/29/2020	09 : 00 : 00	Development	LERA	Subsystem integration and testing (SIT)
04/29/2021	09 : 00 : 00	Development	LERA	Subsystem verification
06/29/2021	09 : 00 : 00	Development	LERA	System integration and testing (SIT)
10/29/2021	09 : 00 : 00	Development	LERA	System verification
12/29/2021	09 : 00 : 00	Development	LERA	Completion of mission-unique design and analyzes
08/29/2021	09 : 00 : 00	Development	Ground Operations	TT&C, data handling and processing tests
04/20/2020	09 : 00 : 00	Development	upper-stage	Payload preparation
09/20/2022	09 : 00 : 00	Development	upper-stage	Launch campaign kickoff
10/20/2022	09 : 00 : 00	Development	upper-stage	Payload integration
12/20/2022	09 : 00 : 00	Development	upper-stage	Rollout readiness assessment
12/27/2022	09 : 00 : 00	Development	upper-stage	Launch readiness review
12/29/2022	05 : 56 : 46	Operations	upper-stage	Launch
12/29/2022	18 : 40 : 12	Operations	upper-stage	Flyby
12/31/2022	07 : 02 : 47	Operations	LERA-O	Detach and target (DT)
01/03/2023	15 : 03 : 03	Operations	LERA-O	Capture and circularize
05/19/2023	07 : 31 : 18	Operations	LERA-O	Science investigation
As needed		Operations	LERA-O	Plane change (max)
05/21/2023	08 : 31 : 18	Operations	LERA-O	Science investigation (SI)
05/19/2023	06 : 31 : 18	Operations	LERA-IM	Impactor release (IR)
11/10/2023	02 : 11 : 04	Decommissioning	LERA-IB and LERA-O	Terminal phase (TP)
10/11/2023	09 : 00 : 00	Post-mission	LERA	Scientific analysis
12/11/2024	09 : 00 : 00	Post-mission	LERA	Mission evaluation/ roll down

Planning The planning phase of the mission will involve the definition of top level requirements which are defined based on the mission objectives, as well as the generation, evaluation and selection of concepts. The most desirable concept will be chosen based on a combination of requirements, technical capabilities and design targets. It is within this phase that the system architecture will be formed.

Development During the development phase, individual components will first be selected through a trade study. Once selected, they will proceed to the procurement stage. Due to long lead times or the requirement of product development, this stage can often take many months. When the hardware is received, it will undergo testing, integration and verification at both a subsystem and system level. All verification stages include the evaluation of system compliance with regard requirements, safety, quality, reliability, FAA Aeronautics and Space Transportation regulations. Additionally, all launch schedule estimations have been constructed by the launch vehicle provider, Space X, where their specified milestone dates are to be contractually obliged [81]. These include mission unique requirements, readiness assessments both pre- and post- payload integration into the launch vehicle and prior to rollout onto the launch pad.

Operations The operations of the LERA mission take place over duration of 141 days. During this phase the integrated payload of LERA-O and LERA-IB will be launched within the upper-stage of the Falcon 9, after the release of LERA-O from the payload bay, LERA-IB will complete its cislunar orbit and will release a series of impactors into the selected lunar crater sites. Simultaneously, LERA-O will position itself into a circular lunar orbit and perform all scientific analysis on the ejecta plumes. Over the duration of the operations phase, it is assumed that all communications between the ground station and the spacecraft are established and functioning and all data, with respect to the spacecraft's attitude, axial orientation, fuel consumption, net velocity (TT&C) and scientific sampling, is processed and sent back to Earth. The timeline of tasks in which the upper-stage, LERA-O and LERA-IB perform are based on STK models.

Decommissioning Due to the mass and cost budget, neither LERA-O nor LERA-IB have the capabilities to crash onto the lunar surface as a means of disposal. For this reason, it is assumed that they will exhaust any remaining fuel to eject themselves into deep space.

Post-mission Concluding the mission will be the post-mission phase which involves the analysis of the scientific data, the mission evaluation and roll down.

4.8 Integration

LERA will be integrated in the standard SpaceX Falcon 9 fairing which will accommodate both the LERA-IB and LERA-O. Using a commercial launch vehicle requires the payload to be designed towards the manufacturer's specifications of the fairing [81]. In contrast to previous payload launches by the Falcon 9, the LERA-IB will be fixed to the launch vehicle adapter via a mechanical mating plate; hence permanently attached to the Falcon 9 upper-stage. Like the ride-sharing concept, the LERA-O will be mounted on top of the LERA-IB using the Mark II Motorized Lightband manufactured by Planetary Systems Corporation [27]. At the pre-determined moment, the separation mechanism will be activated, releasing the LERA-O into the Moon's orbit while LERA-IB and Falcon 9 upper-stage continues with its planned trajectory.

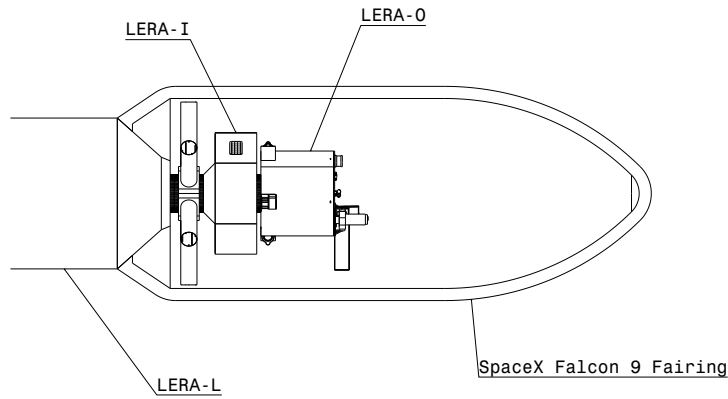


Figure 4: SpaceX Falcon 9 Fairing

5 Science Investigation

5.1 Science Goals and Objectives

5.1.1 Science Overview

LERA is a NASA Discovery class mission with the primary goal of determining both the location and quantity of water to regolith ratio in the Lunar craters known as Cabeus, Shoemaker, Haworth, Faustini, Shakelton, and De Gerlache. The subsystem LERA-O will support and control the scientific instrumentation and observation throughout the entirety of the mission. The scientific findings that LERA may uncover has the potential to significantly advance our knowledge for Moon mining and colonization could potentially be utilized for future deep space exploration missions as a Lunar resource station.

5.1.2 Specimen Analysis

With the water signature within the lunar regolith the focus of the LERA mission, the characterization of the expected water that the instruments will encounter in the ejecta plume is critical. There have been several other missions including landers, probes, and satellites that have searched for traces of ancient water in the solar system. Notable are the missions that accommodated instruments that were powerful and precise enough to obtain information about the subsurface chemistry of planets and Moons from orbit. Not only have these missions proved to be successful, but have also reduced mission costs due to the simplicity of not landing on the body.

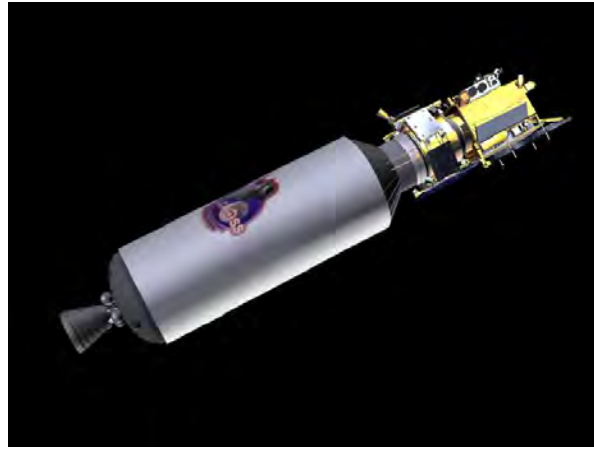


Figure 5: LCROSS Mission – NASA/JPL – This image or video was catalogued by Jet Propulsion Laboratory of the United States National Aeronautics and Space Administration (NASA).

The measurement objective of obtaining the ejecta plume data of six different lunar crater sites, rather than the minimum requirement of only two, creates a much higher likelihood of finding a water signature. This breakthrough generates the potential for investors to make a well-informed decision of where to place the first big lander or facility that will carry an in-situ propellant production capability.

Given the location of the craters that are under analysis, numerous sources suggest that it is frozen water ice that exists in the permanent shadows of the south pole, both on the surface and subsurface [73]. The collision of the impactor onto the surface of the Moon will vaporize the frozen water ice and will eject plasma containing electrons, ions, and dust that may contain all variations of the molecule, including rare isotopes that are not abundantly found on Earth. With only the naturally occurring and stable isotopes of hydrogen (H) and oxygen (O) in mind, there are 18 combinations of the water molecule that exist in three different states; vapor, liquid and solid. It is assumed that the instruments are capable of detecting all these variations, with the additional determination of other trace minerals and compounds including, but not limited to, acetylene (C_2H_2), ethylene (C_2H_4), ethane (C_2H_6), and methane (CH_4).

5.1.3 Objectives and Requirements

The science and measurement objectives which have been deemed critical to the success of the LERA mission are discussed below. The objectives originate from the top-level mission requirements and have been used to allocate the necessary hardware components recommended to close out these requirements.

Objective 1 – Regolith Composition

Measurement Objective In analyzing both the gas and dust particles that are present within the ejecta plume, there will be a greater understanding of the composition of regolith within the six target lunar crater sites. The benefit of incorporating the combined LERA-IB and LERA-O configuration into the mission allows LERA-O to focus solely on the analysis of the three potential sources of water on the Moon; cosmic impacts, solar wind implantation, and indigenous reservoirs. By aiming for a lower margin of error and

higher mass resolution than that of the LCROSS mission, a more precise estimation of water in all of its forms within specific lunar craters will be known and will assist in the future with Moon mining and deep space exploration missions.

Measurement Requirement The ejecta plume that LERA-O will fly through will consist of particles of a wide variety of shapes, sizes, and forms. This is owed to the composition of regolith at the impact site and the particles' relative proximity to the impact site. To ensure that the maximum amount of particulate is captured and analyzed, LERA-O will support a scientific payload which can assess a large range of particle sizes at a high mass resolution. Provided the instrumentation is robust, there will be a lower margin of error due to the repeatability of the sampling of six ejecta plumes. Additionally, with six lunar crater impacts, the payload must be reliable enough to perform the analysis of all six ejecta clouds that will transpire over the course of the mission without any risk of contamination tainting the results. With this in mind, the selected instruments must demonstrate that they are reliable and robust enough to provide accurate, uncontaminated results at all six crater sites.

Instrument Requirement The atomic masses of the most common water isotopes range from 18 to 24 *amu*. To guarantee that particulates within this range are accounted for, the instruments must have high resolution detectors which can distinguish atomic masses between at least 15 and 30 *amu*, therefore safeguarding the misrepresentation of the molecular structures of water in its different states.

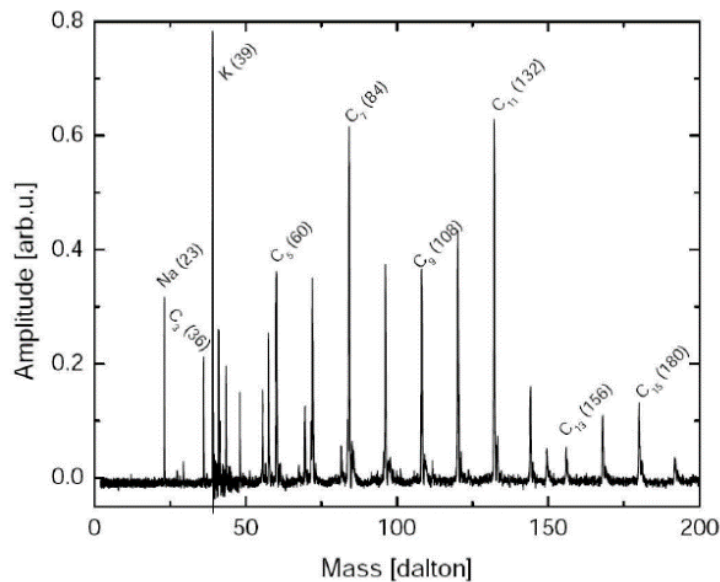


Figure 6: Mass spectrum from a graphite target with a series of carbon cluster lines – LAMA [87]

Objective 2 - Surface Topography

Measurement Objective Through the analysis and data collection of both visual and thermal images of the lunar surface before and after each impacting procedure, there will be substantial knowledge of the permanently shadowed regions of the lunar surface, their deep sunken craters, and the regolith plumes we seek to produce from the impacting projectiles. Imagine-type data acquisition

is especially critical for a mission of this nature with LERA-O expected to complete multiple flybys through multiple ejecta plumes, where VIS/IR imaging will be hindered by frequent, consecutive, and autonomously-segmented data intake. The method for surface topology analysis using visible and thermal imaging systems has been adopted from several heritage instrumentation used on previous missions such as LCROSS, LADEE, and Mars Odyssey. Furthermore, the goal of obtaining greater resolution surface images and lower error margin thermal images than the LCROSS and Mars Odyssey missions will aid in further understanding the water composition in specific PSR craters, supplementing the results obtained by LERA's high-precision spectrometer instrumentation through the multi-faceted validation of the ejecta plumes.

Measurement Requirement The surface topology of the six lunar craters of interest will be of critical importance for the LERA mission, as it will further an understanding of permanently shadowed region craters, provide greater resolution surface mapping of their topological features, and most of all, establish the foundation for result validation and accuracy assessment. As the LERA mission's craters of interest will lie on two orbital planes, it is also critical that the surface topography instruments have a degree of freedom in axes that allow for the repositioning/realignment of its field of view, with minimal dependence of the LERA-O's axial orientation. Moreover, the ejecta plume properties will need to be validated not only from geographical and geometrical aspects, but from a thermal aspect as well. The energy profile produced from the projectile impact and corresponding ejecta plume conical spread have been predetermined through computational simulation, however these expected profiles as they stand now are merely theoretical values which will need to be assessed against the actual findings. The energy profile produced by the impacting projectiles, and by extension, any discrepancies in their findings and hypothesized values, are expected to have substantial influence over the results produced by the spectrometer instrumentation in terms of how regolith composition disassociates upon impact and in the moments shortly after, and therefore the accuracy of these validation methods are substantially important.

Instrument Requirement In order to establish an accurate, yet feasible, topological data set, as well as to make use of technological advancement since the age of heritage missions, topological instrumentation will be sought to various resolutions and temperature precisions that seek to go beyond what has been captured historically where possible. The visible spectrum camera instrumentation will have a spatial resolution of, from a 50 kilometer altitude, at least 100 meters per pixel for a wide angle scope, producing surface mapping images with a high field of view. Moreover, it must also have a spatial resolution of at least 1 m/px for a narrow angle scope, producing high resolution images for smaller fields of view, such as an individual crater site. Additionally, the thermal infrared camera instrumentation must not only provide a spatial resolution of 20 m/px , but must also be capable of producing a thermal energy profile of within $\pm 3^\circ K$ to ensure accurate thermal validation for ejecta plume analysis.

Table 9: LERA's science objectives and the suitability of hardware to the top-level mission requirements and goals.

Science Objective	Measurement Objective	Measurement Requirement	Instrument requirement	Science Impact
Regolith Composition	Analyze particles in the ejecta plumes	Analyze gas and dust particles from 6 ejecta clouds	Detect elements with an atomic mass between 15 and 30 <i>amu</i>	Confirm the existence of water in the Lunar craters. Determine the subsurface composition of Lunar regolith
	Achieve composition accuracy with a lower margin of error than LCROSS mission	A margin of error of 2.9% by atomic mass	Maintain a high mass resolution for all ejecta plumes analyzed	More accurately determine the composition of lunar regolith
	Obtain clear and distinguishable spectrograph absorption peaks	Obtain accurate spectrographs from gas and dust particles found in 6 ejecta clouds	Provide a mass resolution of at least 3000 <i>m/dm</i> at FWHM for gas particulates and at least 150 <i>m/dm</i> at FWHM for dust particulates	Provide a clear distinction of what type of water is present on the Moon
Surface Topology	Analyze the topographic properties of the PSR deep lunar craters	Provide high resolution images of at least 1 <i>m/px</i> (NAC) and 100 <i>m/px</i> (WAC) at 50km altitude	Accurately map the lunar surface, particularly in permanently shadowed regions. Provide an accurate depiction of the crater topology and nearby terrain after impact	
	Analyze the thermal properties of the ejecta plumes	Obtain accurate thermal images of the 6 ejecta plumes	Provide thermal images accurate to within $\pm 3 K$	Validate the thermal intensity of the crater impact energy with respect to hypothesized calculations
	Assess the geometric properties of the ejecta plumes	Retrieve accurate data relating to the conical spread of the 6 ejecta plumes	Provide geometric images at a resolution of at least 20 <i>m/px</i> at 50 km altitude	Validate the geometric properties of the conical eject plumes with respect to hypothesized calculations

5.2 Science Instrumentation

5.2.1 Payload

The payload integrated onboard LERA-O consists of instruments that either have TRL of 8 and above or are part of NASA's technology development portfolio. It includes two high-resolution, time-of-flight mass spectrometers as well as a visible spectrum imaging system, comprising of a narrow angle camera, wide angle camera as well as a thermal imaging camera. All specifications are detailed in Table 9. The method in which the instruments were chosen was through a trade-off study, based on a 1 – 10 system where 1 was considered the most desirable and 10 the least. The instrument that obtained the lowest total score was deemed the most suitable when comparing various key performance parameters.

5.2.2 Mass Spectrometers

Gaseous Phase Mass Spectrometer The gaseous phase mass spectrometer will be responsible for collecting ejecta plume samples from particles of gaseous particulates during the LERA-O flybys. The selection process for the gas particle mass spectrometer was evaluated on the basis of several key design parameters such as mass, power budget required and dimensional volume, as well as several performance-indicating parameters such as particle size and mass resolution. The instruments shortlisted for the trade study were selected from the recent heritage missions: *Europa Clipper – MAss SPectrometer for Planetary EXploration (MASPEX)*, *Rosetta – Cometary Secondary Ion Mass Analyser (COSIMA)* and *Rosetta – Cometary Mass Analyser (COMA)*. These missions are amongst a small cluster of missions that share many similarities with LERA's mission instrumentation requirements whilst also bearing relatively new instrumentation technology.

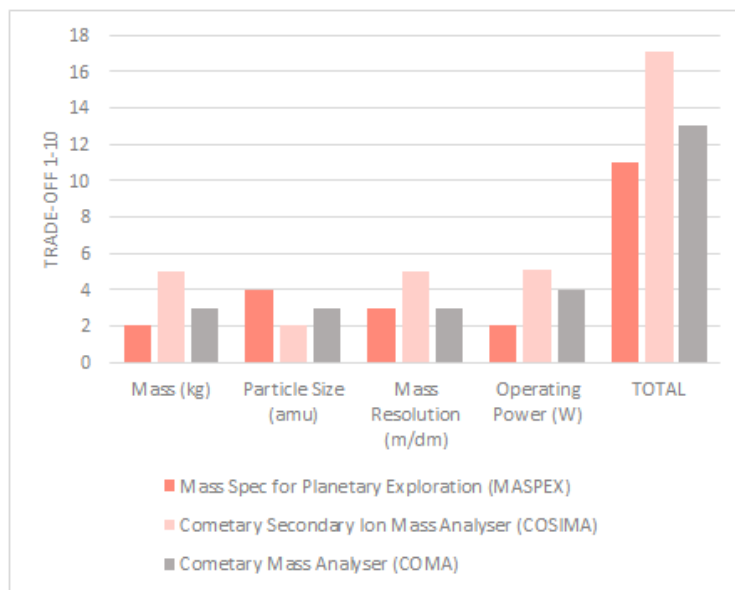


Figure 7: 1 – 10 Score trade-off study comparing similar mission instrumentation for gas particle mass spectrometers

From Figure 7 it was evident that despite its low mass, the MASPEX instrument far exceeded the performance of both COSIMA and COMA when comparing maximum incoming particle size, mass resolution, and operating power. With such a small mission

budget, instruments must be carefully considered. Although the maximum particle size the device that it can accurately analyze is 1/3 of that of COSIMA and COMA, the high mass resolution and low weight that MASPEX exhibits makes it the perfect candidate for analyzing the gas particles that LERA-O will encounter in the ejecta plumes.

Solid Phase Dust-Particulate Mass Spectrometer The solid phase dust-particulate mass spectrometer will be responsible for collecting ejecta plume samples from particles of dust particulates of smaller atomic size during the LERA-O flybys. The selection process for the dust particle mass spectrometer was also evaluated on the basis of several key design parameters such as mass, power budget required and dimensional volume, as well as several performance-indicating parameters such as particle size and mass resolution. The instruments shortlisted for the trade study were selected from the recent heritage missions: *Europa Clipper* - *Surface Dust mass Analyzer (SUDA)*, *Cassini* - *Neutral Mass Spectrometer (NMI)* and *Stardust* - *Cometary and Interstellar Dust Analyzer (CIDA)*. These missions are amongst a small cluster of missions that share many similarities with LERA's mission instrumentation requirements whilst also bearing relatively new instrumentation technology.

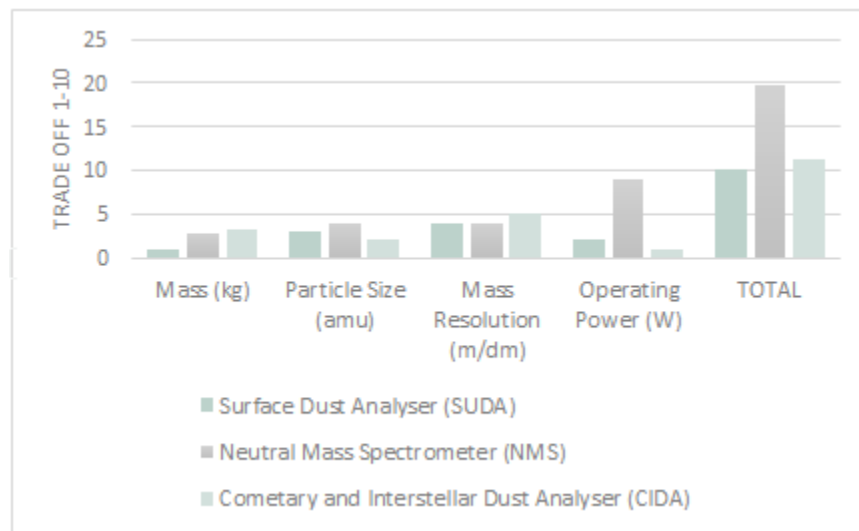


Figure 8: 1 – 10 Score trade-off study comparing similar mission instrumentation for dust particle mass spectrometers

Figure 8 illustrates the comparison between instruments that will be analyzing the incoming dust particles. With similar maximum particle size capabilities and mass resolution acceptance ranges, mass once again becomes the deciding parameter of the trade-off. Weighing at less than 2.5 times that of either competitor, SUDA is clearly the more desirable instrument to perform the task at hand.

LERA-O's mass spectrometers have both been selected from NASA's *Europa Clipper* mission [18, 55]. While both instruments currently hold a TRL of 6, with an expected launch date in the early 2020's, it can be assumed that these instruments will be ready for integration on LERA-O with a TRL of 8. The benefit of acquiring products that are already deep into the developmental stage provides solid evidence of its functionality, therefore severely reducing risk of failure when compared to commercial off-the-shelf components.

Table 10: Mass spectrometer instrument overview

Instrument	Mass [kg]	Power [W] Operational	TRL	Design Life
MASPEX	8	6.4	6	17
SUDA	4	8	6	17
Total	12	14.4		

Table 11: Performance specifications

Instrument	Mass [kg]	Particle size [amu]	Mass resolution [m/dm]	Peak width definition	Min particle speed [km/s]	Max particle speed [km/s]
MASPEX	8	2 – 1000	7000 – 24000	10% peak height	–	–
SUDA	4	1 – 250	150 – 200	FWHM	4	30

It is expected that there will be risks associated with continuation of the mass spectrometer instrument measurements within the 2 – 100 *amu* particulate size range if the appropriate propellant and propulsion system are not selected. We acknowledge the possibility of such contamination sources and have considered them vigorously during the propulsion system design and selection stages which is outlined in later sections of the report.

5.2.3 Imaging Systems

Visible Spectrum - Narrow Angle Camera The selection process for the narrow angle instrumentation was evaluated on the basis of several key design parameters such as mass, power budget required and dimensional volume, as well as several performance-indicating parameters such as wavelength band coverage, field of view and spatial resolution, determined from the pixel scale and orbiting altitude. As the primary purpose of the narrow angle camera is to generate high resolution images of the six selected craters before and after their respective impacts, as well as the ejecta plume conical spread geometries, parameters relating to the spatial resolution and geometry have been weighted with more prominence of other parameters such as wavelength coverage and field of view. The cameras shortlisted for the trade study were selected from the recent heritage missions: *Europa Clipper - Europa Imaging System (EIS)* and *LCROSS - Lunar Reconnaissance Orbiter Camera (LROC)*. These missions are amongst a small cluster of missions that share many similarities with LERA's mission instrumentation requirements whilst also bearing relatively new instrumentation technology.

Table 12: Narrow angle camera trade study

	Europa Imaging System (NAC)	Lunar Reconnaissance Orbiter Camera (NAC)
Wavelength band [<i>nm</i>]	390 – 700	400 – 750
FOV [<i>deg</i>]	2.3x1.2	2.85x2.85
IFOV [<i>μrad</i>]	10	10
Pixel Scale [<i>m/px</i>]	0.5	0.5
Swath [<i>km</i>]	2	5
Assumed spatial altitude [<i>km</i>]	50	50
Mass [<i>kg</i>]	6.6	8.2
Dimensions [<i>cm</i>]	68x26 (diameter)	70x27 (diameter)
Power [<i>W</i>] (Peak/Avg)	8.2 / 5.5	9.3 / 6.4

In Table 12, the specifications of each narrow angle camera has been tabulated. From this, it can be seen that whilst both cameras appear to have similar geometries, spatial resolutions, and wavelength; bands their masses, power consumption and fields of view differ relevantly. From Table 12, key specifications have been taken and weighted comparatively using the 1 – 10 trade off system and plotted below.

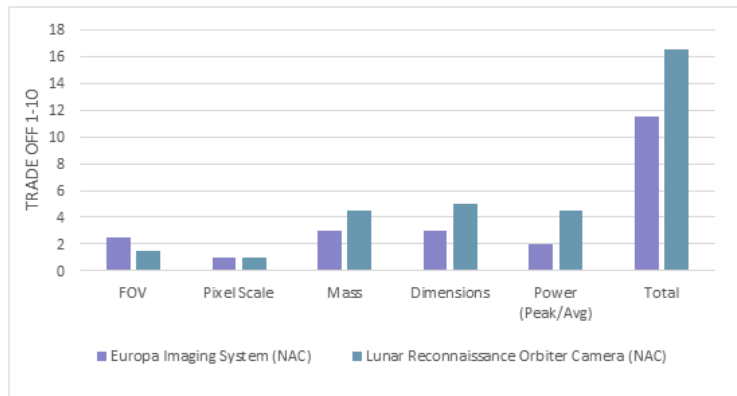


Figure 9: 1 – 10 Score trade-off study comparing similar mission instrumentation for narrow angle camera instrumentation

From Figure 9, it is evident that whilst LROC has a greater field of view, the EIS narrow angle camera is superior in terms of mass, geometric volume and power consumption, rendering it the clear dominant imaging instrument. Whilst the field of view is typically a critical parameter with high weighting, for the specific application of this narrow angle camera, it is not expected that the smaller field of view of the EIS will have any performance-limiting hindrances as not only the surface crater region is expected to be quite small, the spatial altitude was assumed at an altitude of 50 *km* for standardized comparative purposes, which will be substantially greater than the mission altitude LERA will be operating within, thus further alienating the field of view parameter.

Visible Spectrum - Wide Angle Camera The selection process for the wide angle instrumentation was also evaluated on the basis of several key design parameters such as mass, power budget required and dimensional volume, however the performance-indicating parameters that were assessed varied from those examined for the narrow angle instrumentation. This included a much greater emphasis on field of view than what was considered previously, and a lesser weighting on spatial resolution. As the primary

purpose of the wide angle camera is to generate lower resolution color images of the lunar surface map in regions surrounding the crater sites by taking advantage of its large image swath, parameters relating to the image swath distance and field of view have been weighted with more prominence of other parameters such as geometry and wavelength coverage.

Table 13: Wide angle camera trade study

	Europa Imaging System (WAC)	Lunar Reconnaissance Orbiter Camera (WAC)
Wavelength band(s) [<i>nm</i>]	6 color bands (370 – 1050)	7 color bands (321 – 689)
FOV [<i>deg</i>]	48 x 24	61 x 61
IFOV [<i>μrad</i>]	218	1500
Pixel Scale [<i>m/px</i>]	11	75
Swath [<i>km</i>]	44	60
Assumed spatial altitude [<i>km</i>]	50	50
Mass [<i>kg</i>]	1.1	0.9
Dimensions [<i>cm</i>]	14.1 x 28 x 38	15.8 x 23.2 x 32.3
Power [<i>W</i>] (Peak/Avg)	2.5/2.2	2.7/2.6

In Table 13, the specifications of each wide angle camera has been tabulated. From this, it can be seen that whilst both cameras also appear to have similar masses, geometries, and operating power consumptions; their spatial resolution, fields of view and wavelength bands differ drastically. From Table 13, key specifications have been taken and weighted comparatively using the 1 – 10 trade off system and plotted below.

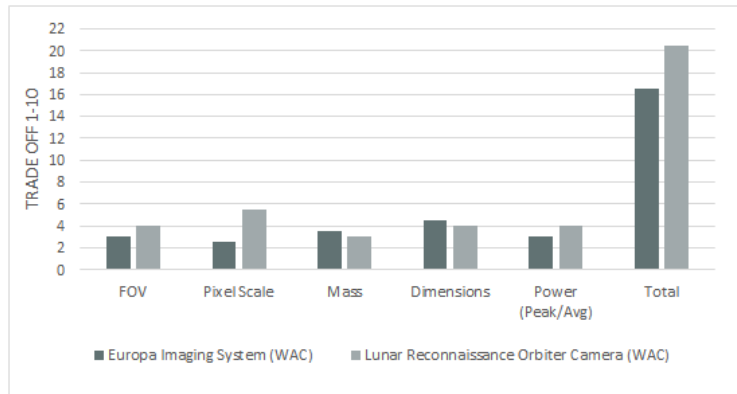


Figure 10: 1 – 10 Score trade-off study comparing similar mission instrumentation for wide angle camera instrumentation

From Figure 10, it is evident that whilst LROC has a greater field of view, lighter mass, and smaller volume, the EIS wide angle camera greatly surpasses it in spatial resolution and power consumption, which has ultimately rendered it as the chosen wide angle imaging instrument. The selection process for this instrument was quite difficult, as both the field of view and image swath for the LROC appeared superior, as well as being a critical parameter with high weighting for the application of this instrument. However the EIS WAC’s incredibly high spatial resolution of 18 *m/px* at a reputable field of view of 48° x 24° and image swath of 44 *km* provides it with a monumental weighting score, with the smaller FOV and shorter swath not expected to bear any performance-limiting hindrances or insufficiencies when compared to the specifications of the LROC. By selecting an instrument such as the EIS WAC with high spatial resolution across a sufficiently large field of view and long image swath, the LERA mission will be equipped

to provide greater high resolution lunar surface mapping over the permanently shadowed and surrounding polar regions.

Thermal Imaging System In much the same way as the visible spectrum imaging instrumentation, the selection process for the thermal imaging instrumentation was also evaluated on the basis of several key design parameters such as mass, power budget required and dimensional volume. This instrument was also evaluated on the basis of several performance-indicating parameters such as wavelength coverage, temperature precision, and spatial resolution. The primary purpose of the thermal imaging system is to scan the crater sites for thermal anomalies before, during, and after impact, as well as generate complete thermal energy profiles, geometric validations, and geographic validations of the ejecta plumes. As a result, parameters relating to the accuracy of the instrument in terms of temperature precision and spatial resolution are of paramount importance and therefore be weighted with more over other parameters such as wavelength coverage and instrument geometry. The thermal imaging systems shortlisted for trade study selection were chosen from the recent heritage missions: *Europa Clipper - Europa Thermal Emission Imaging System (E-THEMIS)* and *Mars Odyssey - Thermal Emission Imaging System (THEMIS)*. These missions also share many similarities with LERA's mission instrumentation requirements whilst also bearing relatively new instrumentation technology.

Table 14: Thermal imaging camera trade study

	Europa Thermal Emission Imaging System (E-THEMIS)	Mars Odyssey Thermal Emission Imaging System (THEMIS)
Wavelength band(s) [<i>nm</i>]	3 bands (7 – 70)	10 bands (6 – 15)
Temperature precision [<i>K</i>]	0.2 for 90 <i>K</i> surfaces 0.1 for 220 <i>K</i> surfaces 1 – 2.2 for 220 – 90 <i>K</i> surfaces	0.5 – 1 for all surfaces
Pixel Scale [<i>m/px</i>]	10	18
Assumed spatial altitude [<i>km</i>]	50	50
Mass [<i>kg</i>]	11.4	11.2
Dimensions [<i>cm</i>]	31 x 35 x 58	29 x 37 x 55
Power [<i>W</i>] (Peak/Avg)	13.8/12.6	14/12.8

In Table 14, the specifications of each thermal imaging system has been tabulated. From this, it can be seen that whilst the heritage instrument THEMIS has a slightly lighter weight, smaller volume and lower power consumption, the E-THEMIS is superior in all other aspects. Not only can the E-THEMIS produce higher resolution images at a given altitude, but it also covers a wider range of wavelength bands. From Table 14, key specifications have been taken and weighted comparatively using the 1 – 10 trade off system and plotted below.

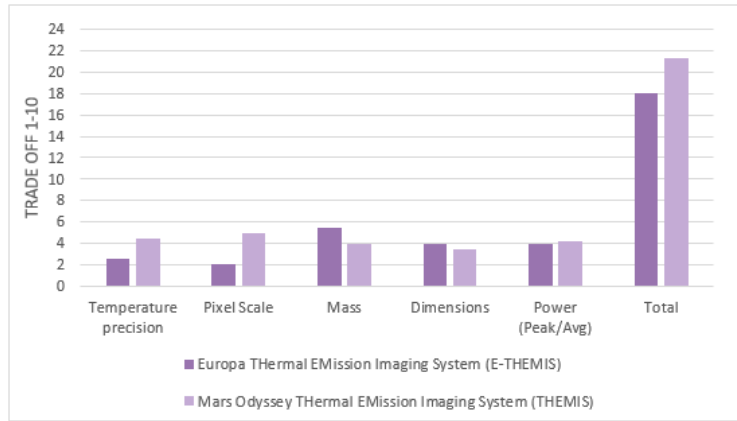


Figure 11: 1 – 10 Score trade-off study comparing similar mission instrumentation for thermal imaging instrumentation

From Figure 11, it is evident that the E-THEMIS surpasses the THEMIS when all key parameters have been considered according to their weighting with respect to the instrument requirements within this mission profile. Spatial resolution and temperature precision being the two most critical parameters, have ultimately rendered the E-THEMIS as the chosen thermal imaging instrument. By selecting an instrument such as the E-THEMIS, with high spatial resolution and accurate temperature profiling, the LERA mission will be equipped for more accurate validation instrumentation over the permanently shadowed crater regions and the ejecta plumes set to emanate from them post-impact. It is also worth noting that the E-THEMIS has been instrumentally equipped with a radiation-hardened integrated circuit which will be incorporated to meet the radiation requirements imposed by the mission environment.

The camera systems have all been taken from NASA’s Europa Clipper mission [69–71]. Currently with the launch date set for as early as 2020, the TRL for these instruments are between 6 and 7, with special reference to the heritage mission Mars Odyssey and upcoming mission OSIRIS-REx [74], which utilize similar inherited technologies. It is therefore feasible to consider integration of these instruments into LERA-O if operation launch date is not expected before 2023, allowing development time to further prepare these instruments for usage with increased TRL.

Table 15: Thermal imaging camera instrument overview

Instrument	Mass [kg]	Pixel Scale [m/px]	Wavelength band(s)	Power [W] (Peak/Avg)
EIS (NAC)	6.6	0.5	1 band (390 – 700 nm)	8.2/5.5
EIS (WAC)	1.1	11	6 color bands (370 – 1050nm)	2.5/2.2
E-THEMIS	11.4	10	3 bands (7 – 70µm)	13.8/12.6

Summary of Science Instrumentation Table 16 and Figure 12 below show the scientific instrumentation selected for the LERA mission onboard LERA-O.

Table 16: LERA-O science instruments

Instrument	Definition	Category	Function
MASPEX	MASS SPECTROMETER for Planetary EXPLORATION/Europa	Mass Spectrometer	Regolith composition analysis for gaseous region of the ejecta plumes
SUDA	SURFACE DUST ANALYZER	Mass Spectrometer	Regolith composition analysis for solid dust region of the ejecta plumes
EIS (NAC)	Europa Imaging System - Narrow Angle Camera	Visible Spectrum Camera	High resolution image capture for crater mapping and mission phase validation
EIS (WAC)	Europa Imaging System - Wide Angle Camera	Visible Spectrum Camera	Wide area image capture for surface mapping and scientific research
E-THEMIS	Europa - THERMAL EMISSION IMAGING SYSTEM	Thermal IR Camera	Thermal imaging camera for ejecta plume energy profile determination and mission phase validation

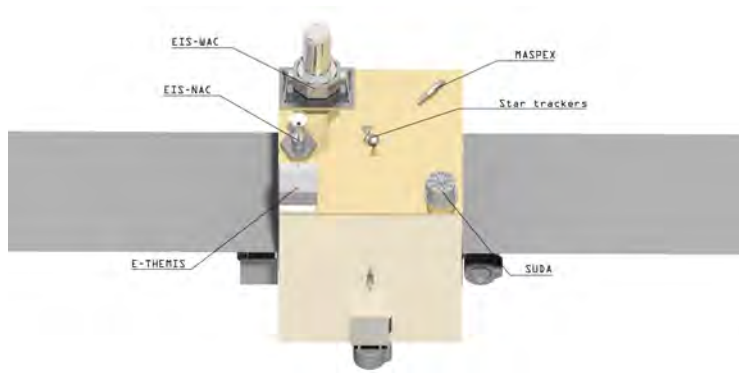


Figure 12: LERA-O Science Instruments

5.2.4 Instrument Testing, Integration, and Calibration

Testing For the instruments to be qualified to a TRL of 8, they must undergo a range of verification acceptance tests. These tests include but are not limited to: Vibration & shock testing; Temperature testing; Thermal cycle testing; Vacuum testing; Micro-gravity testing; Electromagnetic Compatibility/Interference (EMC/EMI) testing; Interface testing.

The instruments SUDA and MASPEX were originally intended for NASA’s mission, Europa Clipper, whereby the spacecraft is expected to perform 40 – 45 flybys of Jupiter’s icy Moon, Europa. With this in mind, it can be assumed that both instruments will have undergone rigorous testing that will ensure that they can withstand the expected conditions of the Europa mission and can, with ease, be reliable and robust enough to provide accurate, uncontaminated results at all six crater sites for the LERA mission.

Visible spectrum cameras EIS NAC/WAC and E-THEMIS will require minimal initial testing once in operation, with all testing done having been completed prior to integration. No additional testing of the instruments is required prior to integration onto LERA-O.

Integration The essential difference between science instruments selected for Europa and that of LERA, is that Europa flyby encounters will occur at some 4 *km/s*, whereas LERA-O will be flying through the artificial plume at some 1.6 *km/s*. Whilst SUDA is

thermal and electromagnetic radiation considerations are taken care of during their developmental periods. Contamination is the most concerning and probable risk that must be taken into consideration. This could occur from either:

- A build up for organic particulates may become lodged internally and blemish the data collected
- Ingestion of gases emitted by the propulsion and ADCS system

For this reason, in-flight calibration and background baseline sampling is critical in ensuring that minimal contamination takes place. Moreover, imaging instrumentation all face common risks associated with:

- FOV/axial orientation of the camera lens with respect to the ground surface during flybys
- Particle accumulation on the lens during flybys through ejecta plumes
- Lens degradation due to fast moving particulate/space junk collision Special considerations will need to be made by ground teams to monitor the health of these instruments.

5.3 Science Mission

LERA-O's mission timeline is based off the milestones that the spacecraft is expected to encounter over the duration of its mission, from separation from the Falcon 9 to the end of its proposed mission.



Figure 14: Mission Flowchart

5.3.1 Pre lunar orbit

The first stage of LERA-O's mission includes the separation from the upper-stage of the Falcon 9. The upper-stage of the Falcon 9 payload bay consists of LERA-O and LERA-IB. The launch vehicle will be travelling in a cislunar orbit where LERA-O will be released from the payload bay. Upon release, LERA-O's onboard propulsion system will insert the spacecraft into its proposed trajectory with a given ΔV .

5.3.2 Lunar orbit insertion

The Attitude Determination and Control System (ADCS) will be used to maintain the circular trajectory around the Moon at an altitude of 12.8 km and velocity of 1.67 km/s. The orbital period of LERA-O is 1.83 hrs. Before the impactors are released, LERA-O

will power on the scientific instrumentation to warm up their systems.

5.3.3 Impacts 1 – 3

LERA-O will analyze a total of six ejecta plumes, at the lunar crater sites listed above. Before any sampling is executed, the instruments, both the mass spectrometers and cameras, will take pre-plume baseline samples. This will allow any potential discrepancies in background particles to be eliminated during scientific evaluation.

5.3.4 Data collection & transfer

Once the instruments have performed their onboard analysis, the data will be transferred to the data storage component of the Onboard Computer (OBC) until communication with the ground station is reached. Once this communication is established, the data will be transferred to the ground station to be decoded and analyzed for scientific purposes. With an orbital period of 1.83 *hrs*, it is expected that the data transfer will be possible for half of this time while LERA-O is facing Earth.

5.3.5 Change in orbital plane

After LERA-O has performed the scientific analysis on four of the six crater sites, it must change orbital planes in order to be appropriately positioned for the next two sites. This will involve the onboard propulsion system to insert a specific ΔV . Additional attitude and navigation maneuvers will be performed by the ADCS.

5.3.6 Mission end

At the completion of the mission, the spacecraft will be decommissioned by the slow decay of its orbit until it impacts the surface of the Moon.

6 Launch System

The trade studies (Figure 15) for the launch systems are based on a 1-10 scale where 10 is highest favorable condition and 1 is least favorable. The maximum payload to GTO, lowest launch cost, and highest reliability are the most favorable conditions.

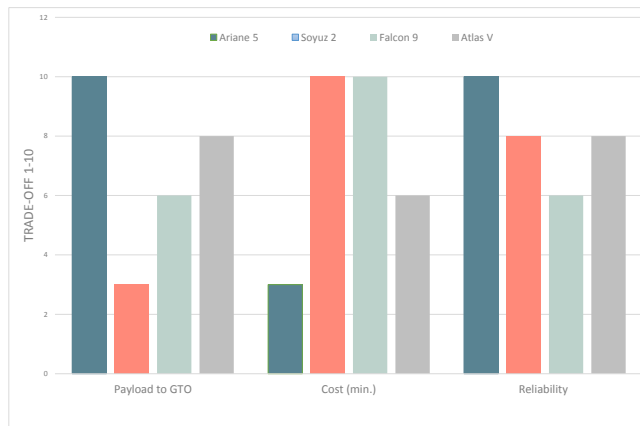


Figure 15: Launch system trade study

Although Ariane 5 is able to carry a heavier payload to GTO and has shown to be more reliable in the launch system trade off study (a breakdown of which is given in Figure 15), the Falcon 9 was chosen as the launch system for the LERA mission.

While having the lowest reliability, based on flight heritage and successful launch rates when compared to the other launch systems, the Falcon 9 is proving itself to be a formidable medium-lift rocket system having already successfully launched over 50 times and now flying resupply missions to the ISS. Furthermore, SpaceX has ushered in a new era of reusable rocket systems with its triumphant return of the Falcon 9's first stage to Earth on numerous occasions. It is envisioned the price of launch will drop by the time of the LERA launch as more Falcon 9s are produced and the reusability of the first stage has accumulated greater flight heritage. The cost of launch could even be further reduced if SpaceX's plan to make the second stage reusable is also achieved prior to launch [81].

Moreover, as the launch system was designed for future human transport to space, all of the Falcon 9's subsystems employ full redundancy, including triple-redundant avionics on the second stage, multiple redundant lithium-ion batteries on both stages, and extra redundant actuators used for the separation of stages. There also exists several failure / error aversion schemes such as multiple in-space start capabilities and autonomous engine cut-offs should a problem be detected during takeoff [81].

The low budget of the LERA mission requires innovative solutions to keep the cost of the mission down, so the future cost savings of the Falcon 9, while retaining a high level of launch reliability, make it of great advantage to LERA.

Risk of fault on the launch system could lead to catastrophic failure resulting from explosion. Should such an event take place, the entire mission would be lost. Launch system failures are out of control of the LERA team, however, the autonomous engine-out detection system of the Falcon 9 could help to reduce the likelihood of a mission ending defection.

7 Mission Breakdown

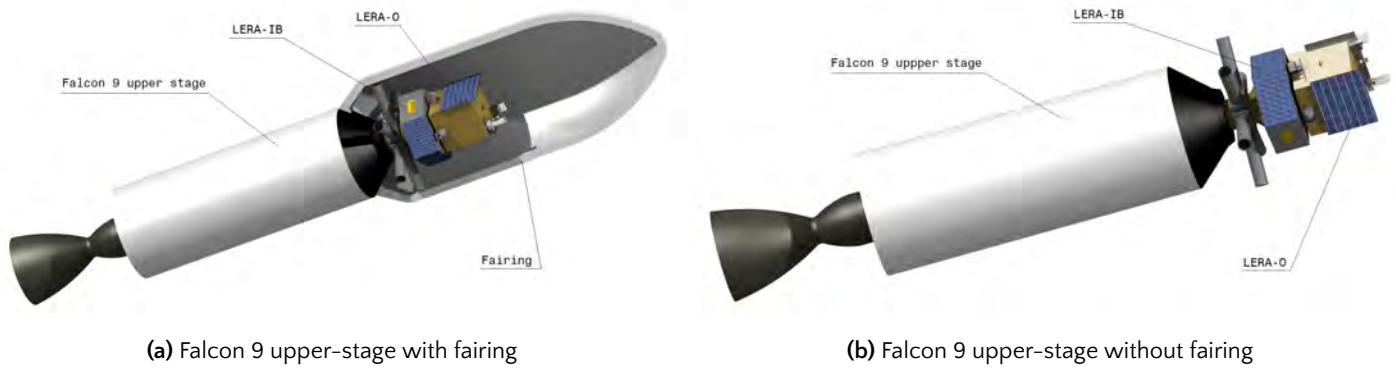


Figure 16: Falcon 9 upper-stage and payload

The LERA mission is to follow a similar orbit to the LCROSS mission. Upon translunar injection, the Falcon 9 upper-stage which is carrying both the LERA-O and LERA-IB systems, pictured in Figure ??, will be in a trajectory towards the Moon. At Point 1 in Figure 17, the LERA-O will be injected into a circular orbit around the Moon. Then, the Falcon 9 upper-stage, now only with the LERA-IB system attached to it, will continue in a larger orbit around the Earth and the Moon. After three large orbits, the Falcon 9 upper-stage will be in close proximity of the Moon in its fourth orbit, during which each of the six LERA-IM's can be detached simultaneously to achieve a close to perpendicular impact with the Moon. Point 2 in Figure 17 indicates the location from which the first of the six LERA-IM's will be released from the LERA-IB system. Further details on the mission architecture of both the LERA-IB and LERA-O systems are provided below.

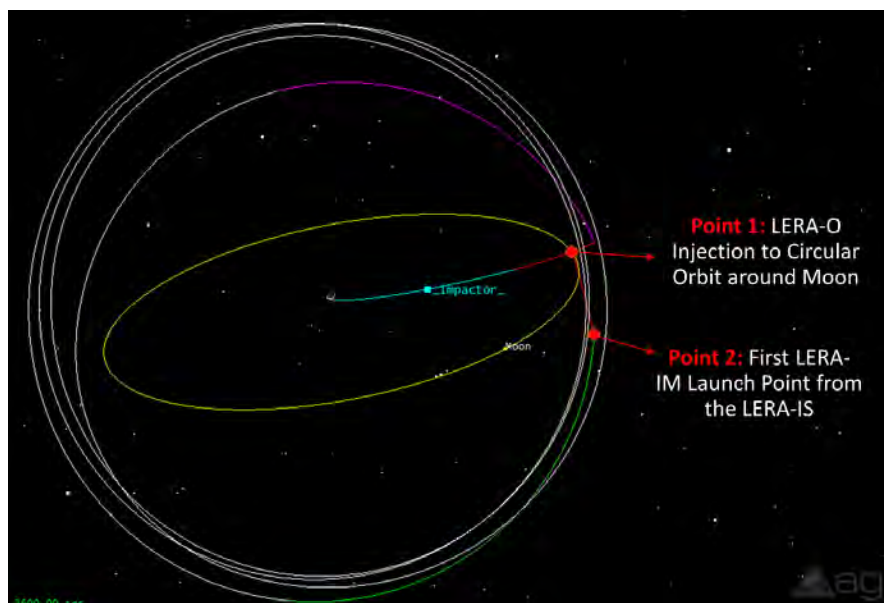


Figure 17: LERA mission breakdown

7.1 LERA-O Mission Overview

The LERA-O segment of the LERA mission will conduct all scientific investigation of the six south pole craters chosen. The LERA-O will perform the mission objectives, independent of the other systems once deployed into orbit. While LERA-O begins its orbit around the Moon, the solar panels will be deployed and the reaction thrusters will activate to ensure that the LERA-O is in the correct position to perform its mission objectives. LERA-O will continue in a circular orbit around the Moon until the LERA-IB segment of the mission begins. Then, it will analyze the ejecta plume created by each of the six LERA-IM's as it passes over them and then relays the data collected back to the ground control station. Further, the LERA-O will be making an orbital change after it collects data from the first four LERA-IM impacts as the next two craters are in a different orbital plane.

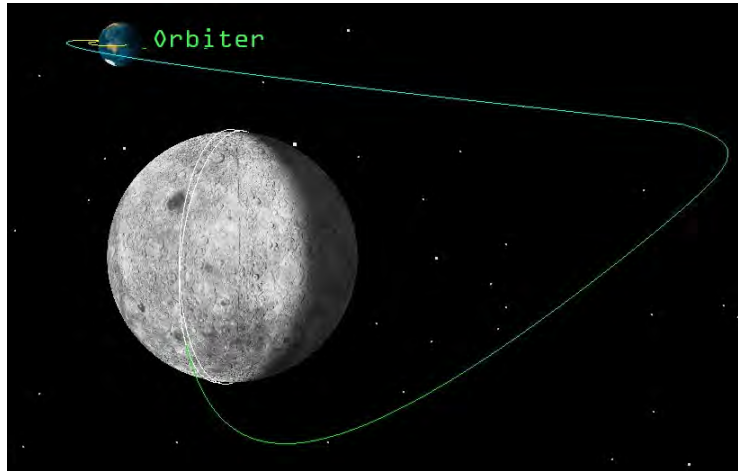


Figure 18: LERA-O mission breakdown

7.2 LERA-IB Mission Overview

The LERA-IB system consists of the the LERA-IM and the LERA-IL subsystems. The LERA-IB segment of the LERA mission consists of the systematic launch of the six LERA-IM's into six different craters in the south pole region of the Moon. The six LERA-IM's are initially attached to the LERA-IB, which is attached to the Falcon 9 upper-stage, and are detached one after another using the six LERA-IL's onboard. As the LERA-IB is at Point 2 (Figure 17), each of the six LERA-IM's are detached for impact on the Moon with an interval of 1.94 [hr] between them. This interval allows for the LERA-O system to complete one entire circular orbit around the Moon and be near the crater that will be impacted by the next LERA-IM. The timing of this is crucial as the LERA-O must be passing over the crater seconds after impact from a LERA-IM. Further, for the first launch of LERA-IM, the total trajectory time after detachment and before the impact on the Moon is approximately 20 [hr]. Thus, detaching one LERA-IM every 1.94 [hr] will mean the last LERA-IM detached will take approximately 8 [hr] to impact. Figure 19 represents the detachment of each of the LERA-IM's from the LERA-IB. Here, it is important to note that this Figure is not to scale.

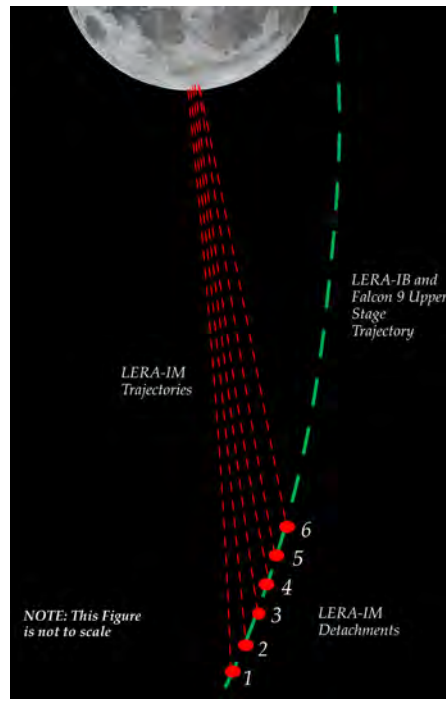


Figure 19: LERA-IB mission breakdown

A decision was made to have a circular orbit instead of an elliptical orbit. This was due to the fact that the entry angle for an elliptical orbit with unwanted precession would have required an excessive Δv to correct. A circular orbit, on the other hand, allows for a lower orbital velocity (1.66 [km/s]) which gives the mass spectrometers more time to recalibrate before the following sampling.

7.3 Trajectory Modeling

The mission architecture requires a complex orbital trajectory to be established for three separate vehicles, the upper-stage of the Falcon 9, LERA-O, and LERA-IB. The trajectory followed by the LERA mission can be broken down into seven distinct sequential phases, as follows:

- | | |
|-------------------------------------|---------------------------|
| 1. Upper-stage launch | 5. Impactor detach |
| 2. Upper-stage translunar injection | 6. Impact at lunar target |
| 3. Orbiter detach | 7. Orbiter lunar capture |
| 4. Upper-stage lunar flyby | |

In order to model how these phases act both independently and as a whole, a trajectory simulation was run using the STK AstrogatorTM software package from Analytical Graphics Inc.

First, the trajectory of the launch and lunar flyby of the upper body were modeled by setting the launch epoch, and Δv along the x-axis as control parameters. A multi-body equality constraints for the difference in declination and difference in right ascension on a B-plane targeting with the Moon, as the central body, were applied and a solution was converged upon that brought the trajectory in-line with the lunar plane.

Next, the trajectory of the orbiter was modeled as following the same path as the upper-stage up to a distance of $300 \times 10^3 [km]$ from the Earth. At this point, by using B-plane targeting, and geodetic equality constraints on latitude and longitude, and the Δv along the x, y, and z thrust axes, the orbiter targets a point that will provide the first required orbital inclination.

The propulsion required to place LERA-O in a circular orbit was done using a negative velocity vector burn that targeted an equality constraint of zero eccentricity. The change in orbital plane was then modeled by the y thrust axis burn, the ascending node of the orbit, and the Keplerian element inclination as equality constraints. This resulted in a solution for the second orbital plane. The altitude of LERA-O was fixed at 49.2 [m], with one orbit taking 113 [mins].

Following this, the trajectory of the upper-stage was modeled beyond the lunar flyby point. The decision was made to model the upper-stage trajectory on that of the LCROSS mission so the lunar flyby burn was used to put the upper-stage into a 90.0° inclined orbit relative to the Earth orbital plane [13]. The upper-stage orbits for approximately 4 months before detaching the impactor.

In order to model the impactor detachment and subsequent trajectory, a combination of b-plane targeting and geodetic elements were used in conjunction with x, y, and z thrust axis burns, and maneuver epoch set as control parameters. A trajectory was modeled, detaching approximately 20.0 [hrs] before impact, with an impact angle of 88.0°. However, the Δv required for this maneuver is far too high to be realistic. This is due to a large z-axis burn required to "catch up" to the Moon as it passes by on its orbital plane too early. It is believed that this burn can be reduced to below 150 [m/s] total Δv with further optimization to synchronize the timing between lunar orbit and upper-stage trajectory. Additionally, given that there is a period of approximately 12 [hrs] between the first and final impactor detachments, it is estimated that the Δv requirements of the final impactor detachment are twice the initial detachment, increasing the maximum Δv requirement for impactor detachment to 300 [m/s].

Table 17: Δv budget for orbital maneuvers

Vehicle	Maneuver	Δv [m/s] Budget
upper-stage	Launch	
	Translunar injection	3.12×10^3
	Flyby	983
	Total	4.10×10^3
Orbiter	Detach and target	132
	Capture and circularize	823
	Plane change (max.)	134
	Total	1.09×10^3
Impactor	Detach and target	300
	Impact	
	Total	300

8 LERA-O

8.1 Overview

Figure 20 below depicts the design of the LERA-O.



Figure 20: LERA-O System Architecture

8.2 LERA-O System Architecture

The LERA-O system architecture is provided in this section. The LERA-O subsystems include communication system, EPS, CDH, propulsion, instruments and ADCS. Each of these subsystems have various other subsystems linked to them. The flowchart in Figure 21 shows a summary of the systems and subsystems included in the LERA-O segment and the linkages between them.

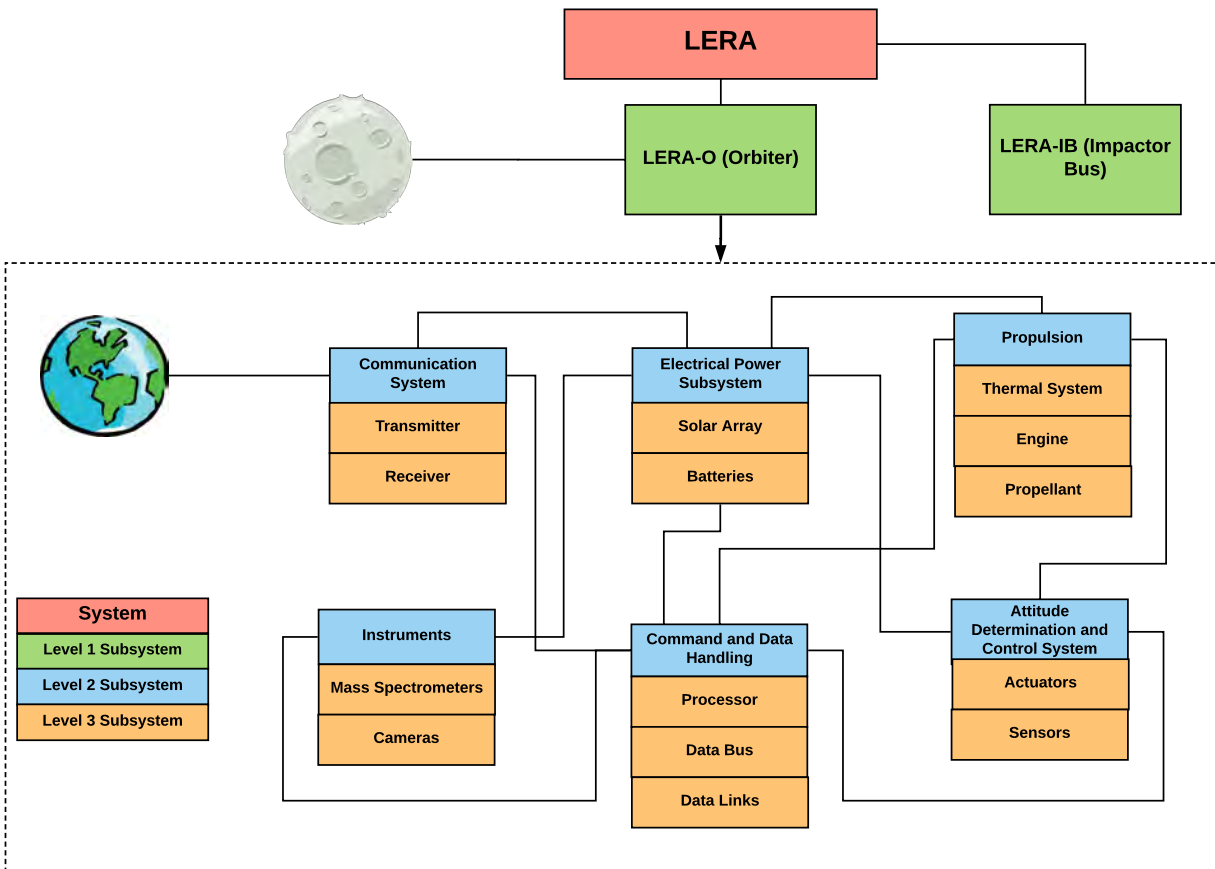


Figure 21: LERA-O system architecture

8.3 Structure

8.3.1 Spacecraft Bus

The structure of LERA-O will be based off a heritage product manufactured by Orbital ATK, GEOStar-2. The GEOStar-2 is typically implemented for small to medium sized communication satellites in GEO [6]. The GEOStar-2 bus is available for purchase as part of a full mission service including integration of payload, communications and propulsion. Since all subsystems will be specifically selected for the LERA mission, the GEOStar-2 bus will be purchased alone.

Table 18: Comparison between heritage batteries and the impact of using Li-ion Saft batteries [35]

Specification	Value
Dry Mass [<i>kg</i>]	1500 (weight includes Orbital ATK all payload except science payload)
Typical Mission Lifetime [<i>years</i>]	15
Compatible with Falcon 9	Yes
Dimensions [<i>m</i>]	1.75 m x 1.7 m x 1.8 m
Construction	Composite/Al

8.3.2 Thermal

Thermal management is important in the space environment because not only should the individual components within the bus have their own thermal management system, the spacecraft itself should also have its own thermal protection to ensure that the spacecraft is protected from the Sun's radiation, high temperatures from the Sun and low temperatures when in the shadow of the Earth or Moon. Thermal Protection Systems (TPS) are used to shield the spacecraft and can include passive thermal solutions such as Multi-Layer Insulation (MLI) [41]. MLI normally are comprised of a number of layers to minimise conduction between layers usually made from a material such as Nomex, with Kapton to be used as the outer skin on either side. These MLI blankets will cover the entire spacecraft bus, with spaces to leave the scientific payload exposed.

8.4 Propulsion

Figure 22 below shows the internal components of the LERA-O bus.

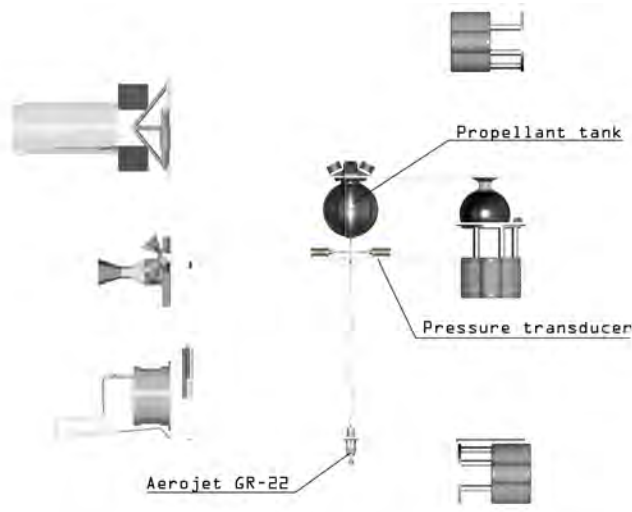


Figure 22: LERA-O system bus

8.4.1 Mission Requirements

Table 19: LERA-O propulsion system highlights

Property	Value
Total Δv [m/s]	1.25×10^3
Number of burns	3
Propellant type	Monopropellant
Feed system	Gas pressure
Propellant	AF-M315E
Pressurant	GN_2
Propulsion system dry mass [kg]	12.9
Propellant mass [kg]	101
Pressurant mass [kg]	1.05
Tank volume [l]	84.5

As per the mission architecture, LERA-O will deploy from the launch vehicle and then conduct a short engine burn to target the polar region of the Moon for insertion. Following this, the orbiter will conduct an extended burn in order to enter polar orbit. The orbiter propulsion system is to be used only to attain lunar orbit and achieve a one-time change in orbital plane. The propulsion system will not be used for orbital attitude control as exhaust emissions would contaminate sensitive measurements made by MASPEX during plume transits.

The full Δv budget for each maneuver and subsequent total fuel requirement are summarized in Table 20. A 15% contingency has been added to the Δv requirements in order to provide a level of tolerance for extra fuel required as a result of unforeseen events during operation. Mission fuel burn and burn duration were calculated using equations 28 to 34 in Appendix C.

Table 20: Δv budget and fuel requirements

Maneuver	Δv [m/s]	Δv contingency [m/s]	Δv total [m/s]	Fuel burn [kg]	Burn duration
Separation	132	19.8	152		
Lunar capture	823	123	946		
Orbital plane change	134	20.1	154		
Total	1.09×10^3	163	1.25×10^3	101	04:16:33

8.4.2 LERA-O Propellant Trade Study

As per Table 20, the orbiter propulsion system must be capable of providing it with a total Δv of 1.25×10^3 [m/s]. In order to determine the most appropriate propulsion system, a trade study was first conducted for propellant type. Five different propellant types were surveyed; hydroxyl ammonium nitrate (HAN) green propellant, hydrazine, liquid hydrogen, monomethyl hydrazine (MMH), and liquid methane. Cold-gas thrusters were not considered as part of the propulsion trade study due to their limited thrust capabilities. This is not a deep-space mission and requires a high Δv over a short time frame which could not be achieved with cold-gas propulsion. Each of the fuels studied was rated out of 10 in terms of its density-specific impulse, melting point, heritage, monopropellant capability, and toxicity. A total score was then calculated for each propellant type providing justification for a most appropriate propellant. The trade study evaluation is summarized in Table 21.

Table 21: Propellant suitability evaluation

Propellant	ρI_{sp} [kgs/m ³]	Score	Melting point [C°]	Score	Heritage	Score	Mono propellant capability	Score	Toxicity	Score	Total Score
AF-M315E (HAN)	3.62×10^6	10	-22	1	Low	2	Yes	8	Low	8	29
Hydrazine	3.40×10^6	9	1	1	Extensive	9	Yes	8	High	1	28
Liquid hydrogen	2.73×10^5	1	-259	10	Extensive	7	No	1	Low	9	28
MMH	2.90×10^6	8	-52	1	Moderate	6	No	3	High	1	19
Liquid Methane	1.25×10^6	3	-183	2	Moderate	4	No	1	Low	9	19

Density-specific Impulse The density-specific impulse is an important parameter for evaluating fuel type. It gives a measure of impulse per unit volume or thrust per time per volume. Of all the propellants evaluated, HAN had the highest density impulse. Therefore, a HAN-based propulsion system would require the smallest propellant tank volume per unit impulse. Subsequently, this would result in reduced overall mass and spacecraft size.

Melting Point The orbiter is required to travel through regions of space unexposed to the sun where temperatures can approach absolute zero (-273.15°C). A propellant with a low melting point will therefore require minimal preheating prior to combustion, therefore consuming less power. It should be noted that HAN cannot freeze as it has a glass transition [60].

Heritage Utilizing a propellant with extensive heritage on similar space missions is also a necessary consideration. Hydrazine has extensive heritage on spacecraft for primary launch propulsion systems and orbital attitude and station keeping propulsion systems. Liquid hydrogen has extensive heritage in use for the American space program, on the main engine of the space shuttle, the Ariane launcher and many commercial launches [101]. Monomethyl hydrazine has seen use as the propellant for the SpaceX-developed Draco thruster [78]. Liquid methane has a low heritage with use only in testing as the propellant for the SpaceX in-development Raptor engine [14] and the Blue Origin BE-4 engine [22].

Monopropellant Capability Propulsion systems with propellants which do not require an oxidizer for combustion offer the benefit of reduced complexity as only a single fuel tank is needed. Reduced cost and system mass are also potential benefits. Both methane and liquid hydrogen require liquid oxygen as an oxidizer which must be held at cryogenic temperatures, adding significantly to complexity, cost and power requirements. Aside from launch vehicle applications, longer duration missions utilizing liquid hydrogen or methane and oxygen would require extensive thermal management systems in order to maintain the necessary cryogenic state [68]. MMH also requires an oxidizer in dinitrogen tetroxide. Dinitrogen tetroxide does not need to be kept at cryogenic temperatures. HAN and hydrazine are capable as monopropellants, and only require contact with a catalyst in order to ignite.

Toxicity Toxicity is another important factor to consider for rocket propellants. A propellant with low toxicity means that less of a threat will be posed to those handling the substance when fuelling the rocket and less harmful pollution will be emitted to the environment. Both hydrazine and monomethyl hydrazine vapor are highly toxic requiring system handling and fuelling operations to be conducted by certified crews wearing self-contained atmospheric protective ensemble (SCAPE) suits [17]. This in turn significantly increases cost and adds complexity to mission scheduling. Hydrazine external leakage is classified with a "catastrophic" hazard rating as per MIL-STD-882E [29], whereas it is indicated that AF-M315E HAN propellant will likely be rated as "critical" or even "marginal" [60]. As a result of this lower hazard rating, the AF-M315E propulsion system will require only two seal-inhibits to leakage, reducing complexity, mass, and cost.

The US Air Force have tested and compared the toxicity results of AF-M315E with that of hydrazine to find that AF-M315E possesses significantly lower toxicity. Table 22 shows the toxicity testing results of AF-M315E and hydrazine when exposed to various test subjects. The toxicity level of AF-M315E is such that it may safely be handled in open containers for unlimited durations [60].

For NASA missions, the average contractual cost for conventional propellant loading is \$135,000 [60]. Current loading methods require one shift for setup (in SCAPE), a second shift waiting for propellant test confirmations, a third shift for loading, and a fourth shift for disassemble of the setup, during which other launch staff must wait posing a major interruption. Replacing hydrazine with AF-M315E green propellant could eliminate two shifts from the loading schedule as well as more than \$100,000 in costs associated with launch staff on standby during the fourth shift [60].

Table 22: Toxicity testing results of AF-M315E and hydrazine [17]

Property	AF-M315E	Hydrazine
LD50 (rat) [mg/kg]	550	60
Dermal Irritation (rabbit)	None - slight	Corrosive
Dermal Sensitization (guinea pig)	Non-sensitizer	-
Genotoxicity (Ames)	3 negative/2 positive	Positive

As per Table 21, hydroxyl ammonium nitrate AF-M315E propellant scored the highest in the trade study. A propulsion system based on this fuel is therefore selected.

8.4.3 Propulsion System Summary

The GR-22 AF-M315E (HAN blend) Green Monopropellant Rocket Engine by Aerojet Rocketdyne was selected for the propulsion system of LERA-O. The GR-22 is a 22 Newton thrust class rocket engine currently in development and scheduled for its first flight as part of the NASA Space Technology Mission Directorate's (STMD) Green Propellant Infusion Mission (GPIM) Technology Demonstration Mission (TDM) in June of 2018. The design of the engine is similar to that of a hydrazine-fueled rocket engine in that the single propellant flows over a high-temperature preheated catalyst bed in order to ignite combustion.



Figure 23: Aerojet prototype GR-22 thruster [59]

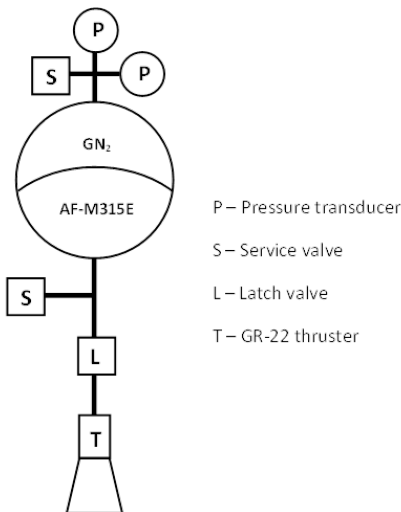


Figure 24: Propulsion system

Depicted in Figure 23, the thruster design consists of a valve, injector, catalyst chamber and nozzle all assembled in series. The LCH-240 catalyst is a bed of platinum group or transition series metal which when preheated ignites and decomposes the propellant upon contact, subsequently producing thrust [75]. The catalyst bed is preheated by an incorporated silicon carbide conductive medium which when heated provides uniform heating of the catalyst at 315C° for ignition [59].

The overall propulsion system is a single-string, blow-down system fed by a single fuel tank and containing a mixture of AF-M315E propellant and gaseous nitrogen (GN_2) as the pressurant gas [60]. Figure 24 depicts the propulsion system and its major components. The propellant and pressurant are separated within the tank by a diaphragm. As the propellant is depleted, the pressurant gas maintains sufficient pressure within the tank to feed the thruster with propellant. The mass of gaseous nitrogen pressurant was calculated using equations 37 and 38 in Appendix C.

Despite this, the propellant pressure reduces from its maximum of 3790kPa to its minimum of 690 kPa and thrust level subsequently also decreases from the thrusters rated maximum of 26.9N to its minimum of 5.7N [59]. The two pressure transducers are

"gas-side" and measure the tank pressure from the pressurant gas. Two service valves, one gas-side and one propellant side are required to load and drain the respective substances. A single latch valve controls the flow of propellant to the engine thruster. A single GR-22 thruster with an integral catalyst bed will contain the chemical reaction producing thrust.

Table 23 details the performance characteristics of the GR-22 thruster. Overall, the GR-22 thruster has comparably better performance to that of typical hydrazine 22 Newton class thrusters, albeit without the toxicity hazards associated with hydrazine propellant. The GR-22 thruster has a greater feed pressure range than the 590 - 2760kPa range of Aerojet Rocketdyne's MR-106L 22 N class thruster [76]. The GR-22 also compares favorably to the 235s specific impulse and of the $2.40 \times 10^6 \text{kgsm}^{-3}$ density specific impulse of the MR-106L thruster, however falls short of its 34N peak thrust.

Table 23: GPIM AF-M315E GR-22 thruster technical data

Thruster	GR-22
Propellant	AF-M315E
Thrust [N]	5.7 - 26.9
Feed pressure [kPa]	690 - 3790
Throughput [kg]	101
Pressure/Propellant ratio	0.22
Valve power [W]	15.9
Preheat power [W]	30
Thermal management [W]	277
Mass [kg]	0.59
Specific impulse [s]	248
Density specific impulse [kgs/m ³]	3.62×10^3

Table 24 details the component mass breakdown and total mass for the overall propulsion system. A 10% contingency factor has been added for each component as a tolerance to account for inaccurate estimations and mass increases as a result of further technology development prior to launch date. The most significant mass quantity is for the propellant. A contingency factor is not added for propellant mass a 15% contingency is already included within calculations. To calculate propellant tank mass, a linear interpolation was made between existing propellant tanks based on propellant volume and mass for the desired tank volume.

Table 24: LERA-O propulsion system mass breakdown

Component	Mass [kg]	Quantity	Total mass [kg]	Contingency %	Mass w/ contingency [kg]
Propellant	101	1	101	0	101
Pressurant	1.05	1	1.05	0	1.05
Tank	8.39	1	8.39	10	9.23
Thruster	0.59	1	0.59	10	0.65
Latch valve	0.40	1	0.4	10	0.44
Service valve	0.10	2	0.20	10	0.22
Pressure transducer	0.25	2	0.50	10	0.55
Tubing (1/4")	0.60	1	0.60	10	0.66
Filter	0.08	1	0.08	10	0.09
Electrical harness	1.00	1	1.00	10	1.10
Total			114		115

As green monopropellant propulsion systems are still in development, heritage is low and the components are not yet proven

as successful for flight missions. Table 25 summarizes the TRL of the major propulsion system components. All components are successfully flight proven for hydrazine as a propellant, but require minor modifications for compatibility with AF-M315E. The Green Propellant Infusion Mission is scheduled for launch aboard the next SpaceX Falcon Heavy launch in June of 2018. It is therefore assumed that all components are TRL 7 and ready for mission testing.

Table 25: Technology readiness of propulsion system components

Component	Manufacturer	TRL w/ AF-M315E	TRL w/ Hydrazine
Tank	Orbital ATK	7	9
Thruster	Aerojet Rocketdyne	7	9
Thruster valve	Aerojet Rocketdyne	7	9
Latch valve	RAFAEL	7	9
Service valve	RAFAEL	7	9
Pressure transducers	MOOG Bradford	7	9
Filter	RAFAEL	7	9

8.4.4 Propellant Thermal Management

AF-M315E does not freeze but, however it undergoes a glass transition phase at -85°C . The propellant must therefore be kept above -80°C for added tolerance. The rate of thermal conduction and subsequent required power for thermal management of propellant was calculated using equations 41 to 45 in Appendix C.

8.4.5 Risks

With respect to the orbiter propulsion system, the LERA mission is low risk. Table 26 summarizes the potential mission risks. It should be noted that it is assumed that the propulsion system will have been successfully proven as TRL 9 by LERA launch date due to the GPIM mission scheduled for launch in June 2018. As a result of this, main engine failure is unlikely and catalyst exhaustion is also unlikely as Aerojet LCH-240 catalyst will be mission proven. Propellant exhaustion is an unlikely event as a 15% contingency is already factored into Δv requirements. Impact with plume debris while in lunar orbit is highly likely. However, plume debris with comprise of only dust particles and gases. Puncture and subsequent leak is therefore highly unlikely.

Table 26: Propulsion system risks

Failure	Corrective action	Mission effect	Likelihood
Main engine failure	None	Failure	Low
Catalyst exhaustion	None	Failure	Low
Propellant exhaustion	None	Failure	Very low
Puncture from plume debris	None	Leak/spectrometry inaccuracy	Very low

8.5 Attitude Determination and Control System (ADCS)

The design process of the Attitude Determination and Control System (ADCS) for LERA-O took into consideration several factors in order to determine the subsystem's requirements. Such considerations included the control modes of the mission (see Table 27), the scientific investigation at hand, the duration of the mission and pointing accuracy requirements from other subsystems.

Table 27: Attitude control modes during the mission [86]

Mode	Description
Orbit Insertion	No spacecraft control
Acquisition	Initial determination of attitude and stabilization of spacecraft
On-Station	Station keeping maneuvers
Slew	Reorientation of the vehicle for change of orbital plane
Contingency or Safe	In case of emergencies, such as system failure or deactivation
Special	Used when flying through the ejecta plume

Following the abovementioned considerations, the ADCS must satisfy certain accuracy requirements, constantly maintain spacecraft stability, perform station keeping maneuvers and meet the estimated Δv requirements.

Table 28: ADCS subsystem requirements

	Requirements
Accuracy	Shall define attitude to within 0.05 degree accuracy Shall deliver attitude control to within 1 degree pointing accuracy
Capability	Shall maintain spacecraft stability at all times Shall sustain station keeping maneuvers during science investigation
Performance	Shall provide at least 184 m/s of Δv for attitude control

Desired accuracies outlined in the table above (see Table 28), derived from the accuracy requirements of the payload while the origins of the Δv value are explained later in Section 8.5.4. Table 29 below presents the various attitude control methods that were considered for LERA-O.

Table 29: Attitude control methods [86]

Type	Attitude	Typical Accuracy [deg]
Spin Stabilization	Repoint using precision maneuvers, such as torquers (slow) or thrusters (faster)	± 0.1 to ± 1 in 2 axes
Zero Momentum (Thruster Only)	No constraints, high spin rates possible	± 0.1 to ± 5
Zero Momentum (3 wheels)	No constraints	± 0.0001 to ± 1 (defined by sensors and processor)
Zero Momentum (CMG)	No constraints, high rates possible	± 0.001 to ± 1

LERA-O will be employing a three-axis stabilization, zero momentum attitude control technique with both reaction wheels and reaction control system (RCS) thrusters in order to achieve the accuracy required by the scientific payload and the necessary orientation of the solar panels. A three-axis attitude control method also provides a comparably faster maneuverability. Due to low budgetary requirements and time limitations, LERA-O will only adopt spaceflight proven heritage components for the ADCS. The various types of sensors explored to determine the attitude and orientation of the spacecraft are listed in Table 30.

Table 30: Types of sensor for attitude determination [99]

Sensor	Mass [kg]	Power [W]	Accuracy
Star Tracker	2-5	5-20	0.003-0.01 deg
Sun Sensor	0.1-2	0-3	0.005-3 deg
Inertial Measurement Unit	0.1-15	1-200	0.003-1 deg/hr
Magnetometer	0.3-1.2	<1	0.5-3 deg
Horizon Sensor	1-4	5-10	0.1-0.25 deg

A combination of star trackers, sun sensors, and an inertial measurement unit was selected for LERA-O due to their high accuracy and efficiency. Magnetometers and horizon sensors were disregarded as they tend to be less accurate and not as effective outside low earth orbit. Table 31, shown below, outlines the ADCS instruments that will be implemented in LERA-O in order to meet the relevant requirements and assist in mission success.

Table 31: Attitude determination and control instruments

Function	Instrument	Use	Quantity
Attitude determination	Star Tracker	Determine spacecraft attitude and orientation based on the relative location of specific stars	2
	Sun Sensors	Establish orientation based on the location of the sun	4
	IMU	Measures angular rate and acceleration of spacecraft	1
Attitude control	RCS Thrusters	Change attitude of spacecraft by providing thrust	4
	Reaction wheels	Control attitude of spacecraft by applying torque	4

The LERA-O attitude determination and control system employs star trackers as the primary instrument to establish spacecraft orientation and position. LERA-O shall have two star trackers onboard in order to achieve maximum accuracy on all three axes. Sun sensors shall determine attitude and orientation of the spacecraft in case of an emergency or star tracker failure. Moreover, sun sensors are of low weight, cost and power consumption and provide redundancy to the star trackers. The LERA-O ADCS also includes an Inertial Measurement Unit (IMU) responsible for measuring the rate of angular rotation and acceleration of the spacecraft. Such measurements help determine when and for how long to run the RCS thrusters in order to achieve the desired rotation. LERA-O will employ four reaction wheels and four RCS thrusters in order to control the attitude of the spacecraft. The four reaction wheels will be arranged in a pyramid configuration and will provide three-axis control. The fourth wheel will provide redundancy and will serve as a safety blanket in case another wheel fails.

The scientific investigation of the mission will be analyzing particles in the ejecta plumes to determine the ratio of water to Moon regolith. In order to do so LERA-O will be flying through the plumes carrying the appropriate scientific payload. As described in Section 5, the scientific payload mainly consists of mass spectrometers which will identify the compounds in the ejecta plume. Therefore, it is of vital importance for the ADCS to not contaminate the ejecta plumes during scientific measurements. Hence, the propellant used for the RCS thrusters had to be carefully chosen and only noble gases were considered. Due to its high efficiency compared to other noble gases xenon was selected. The scenario of only employing RCS thrusters was explored, however, minimum power and propellant weight is desired and RCS thrusters have high power consumption and xenon tends to be relatively heavy. Furthermore, reaction wheels can achieve small attitude and station keeping maneuvers which means RCS thrusters can

only be used for desaturation of reaction wheels and maneuvers that require higher torque. When in lunar orbit, station keeping maneuvers will be mainly performed by the reaction wheels or, if the need arises, the RCS thrusters. Repositioning of the spacecraft to prepare for the orbital change will have to be achieved by the RCS thrusters.

8.5.1 Sensors

Implementing spaceflight proven heritage components to the LERA-O ADCS eliminates the need for instrument development, component testing and system verification. This keeps the cost of the mission low, minimizes failure probability and helps ensure the success of the mission. Heritage components can also act as a risk mitigation strategy in the ADCS design process. Mass, power consumption and TRL were three of the key parameters that significantly affected the instrument selection process. Undeniably, the selected instruments should also meet the ADCS requirements outlined in Table 28.

Table 32: Potential star trackers for the LERA-O ADCS [51, 80, 93, 94]

Model	Mass [kg]	Power [W]	Accuracy cross bore-sight [arcsec]	Accuracy around boresight [arcsec]	Operating Temp. [°C]	Radiation Tolerance [krad]
Sinclair ST-16RT2	0.158	<0.5	<5	<55	-40 – 85	9
TY-Space NST Nano Star Tracker	0.150	<1	<7	<70	-30 – 60	30
BCT Extended NST	1.3	<1.5	<6	<40	-	-
Surrey Rigel-L	1.2	6.5	<3	<25	-20 – 50	5

Star Tracker All of the considered star trackers mentioned in Table 32 meet the accuracy requirements, however, the Sinclair ST-16RT2 was selected for LERA-O due to its low mass and power consumption and its higher accuracy and temperature operation range. The NST Nano star tracker scored the lowest mass and the highest radiation tolerance making it a close second but was disregarded since the advantages of the ST-16T2 outweighed the mass difference and radiation shielding performance between the two star trackers. Furthermore, the ST-16RT2 has achieved a TRL 9 making it the optimal star tracker for the mission. High TRL scores can contribute to the overall reliability of the ADCS, provide a level of reassurance to stakeholders as well as minimize risk of failure throughout the mission.

Table 33: Potential sun sensors for LERA-O ADCS [62–65, 91]

Model	Type	Mass [kg]	Power [W]	Accuracy [°]	Field of View [deg]	Radiation Tolerance [krad]	Operating Temp. [°C]	N ^o of Axes	TRL
SolarMEMS nanoSSOC-D60	Digital	0.006	0.115	<0.5	±60°	30	-30 - 85	2	9
SolarMEMS SSOC-D60	Digital	0.036	0.35	<0.3	±60°	30	-40 - 85	2	9
NewSpace Systems NFSS-411	Digital	0.035	0.038	<0.1	140°	10	-25 - 50	2	8
SolarMEMS nanoSSOC-A60	Analog	0.004	0.01	<0.5	±60°	>100	-30 - 85	2	9
SolarMEMS SSOC-A60	Analog	0.025	0.036	<0.3	±60°	>100	-45 - 85	2	9

Sun Sensors The sun sensors considered as viable options for the LERA-O ADCS are presented in Table 33. Once again, all sun sensors outlined meet the accuracy requirements. When comparing the digital sun sensors, the SolarMEMS nanoSSOC-D60 outperforms both the SolarMEMS SSOC-D60 and the NFSS-411. It weighs the least and has the highest radiation shielding and operational temperature range while also possessing a TRL 9. Even though the NFSS-411 sun sensor consumes less power and is more accurate than the SolarMEMS nanoSSOC-D60, more weight was attributed to the TRL during the decision making process. As discussed previously, the utilization of instruments with proven spaceflight heritage can help minimize development time and test-related costs. Analog sun sensors were also considered due to their comparably low weight and extremely low power consumption, however, they were deemed inappropriate due to the necessity of a digital signal in order to integrate the information into the onboard computer for data handling.

Table 34: Potential IMUs for the LERA-O ADCS [26, 28, 43, 79]

Model	Mass [kg]	Power [W]	Range [deg/sec]	Bias [deg/hr]	Angle Random Walk [deg-rt-hr]	Scale Factor [ppm]	Operating Temperature [°C]
Northrop LN- 200S	0.748	12	1000	<0.1	<0.07	300	-54 - 71
Honeywell MIMU	4.44	22	375	<0.005	<0.005	<1	-30 - 65
Airbus ASTRIX 200	13	6.5 per ON channel	5	<0.0005	<0.0002	30	-10 - 50
Micro Aerospace Solutions MASIMU03	0.15	1.3	-	0.78	-	-	0 - 70

Inertial Measurement Unit Even though all of the inertial measurement units explored met the accuracy requirements, the Northrop LN- 200S was regarded as the best option due to its considerably low weight, relatively low power consumption and vast operational temperature range. It was chosen over the MASIMU03 because of the non-compatible environmental survivability. When compared to the other IMUs, the LN-200S lacks in accuracy but can still meet the accuracy requirements for the ADCS operations.

8.5.2 Actuators

Table 35: Reaction wheels considered for the LERA-O ADCS [4, 23, 66, 95]

Model	Mass per wheel [kg]	Nominal Speed (NS) [rpm]	Angular momentum at NS [Nms]	Reaction torque at NS [Nm]	Power consumption [W]	Operating Temperature [°C]
VECTRONIC Aerospace VRW-02	1	± 5000	0.2	0.02	<3	-20 - 70
TELDIX RSI 01-5/15	<0.6	± 2800	0.12	0.005	<4	-20 - 60
Survey 10 SP-M	0.96	3000	0.42	0.011	<3.5	-20 - 50
Microwheel 200 MSCI	0.94	± 10000	0.18	0.03	<7	-30 - 60

Reaction Wheels When comparing all potential reaction wheels (see Table 35), the Vectronic VRW-0.2 reaction wheel was deemed the most appropriate for the LERA-O ADCS. Power efficiency was the main driving factor during the reaction wheel selection process. The VECTRONIC Aerospace reaction wheel possessed the lower power consumption of all options. A trade-off between the weight and angular momentum characteristics was then performed, where the VRW-02 was deemed to be the best option for LERA-O.

Reaction Control System Thrusters The potential RCS small thrusters were compared taking into consideration five main engine characteristics, including mass, thrust, specific impulse (I_{sp}), power consumption, and TRL. In order to meet the mission budget requirements, the RCS would need to be as light and power-efficient as possible. Another significant factor in the RCS small thruster decision making process was TRL. Malfunction of the thrusters could lead to mission failure since reaction wheels alone would not be able to compensate for orbital drift. Therefore, selecting a safe and spaceflight proven heritage system is of vital importance.

Table 36: xenon reaction control thrusters that were taken into consideration for the attitude determination and control system of the LERA-O [19, 34, 36]

Model	Mass [kg]	Thrust [N]	I_{sp} [sec]	Power [W]	TRL				
QinetiQ T5	2.5	0.025	>3000	700	9				
QinetiQ T6	8.3	0.23	>4000	5000	8				
Ariane Group RIT 10 EVO	1.8	145W 0.005	435W 0.015	760W 0.025	145W >1900	435W >3000	760W >3200	145-760	8
NSTAR	8.2	0.019- 0.092	1900- 3100	500- 2300	9				

Considering the effect that component TRL could have on mission success, thrusters with TRL lower than nine were instantly disregarded. The QinetiQ T5 outperformed all other thrusters possessing the lowest mass and power consumption when compared to other TRL 9 thrusters. The QinetiQ T5 thruster also has a high specific impulse and can achieve relatively high thrust values despite its low power consumption.

The ion propulsion RCS will also require an Ion Propulsion Control Unit (IPCU) and a Proportional xenon Feed Assembly (PXFA) in order to accurately control and measure xenon propellant flow [31]. These systems will contribute to the overall mass and power

consumption of LERA-O ADCS.

8.5.3 ADCS Overview

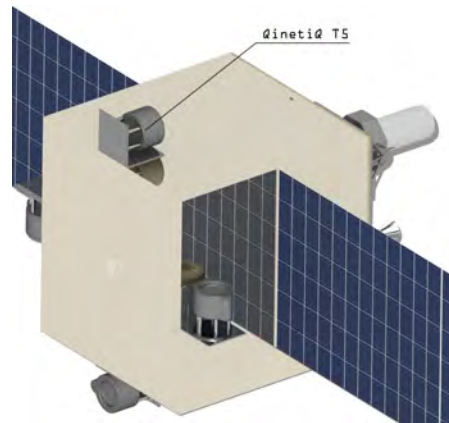


Figure 25: QinetiQ T5 thrusters mounted on LERA-O bus

Table 37: Attitude determination and control system overview

Function	Instrument	System	Quantity	Mass [kg]	Power [W]
Attitude determination	Star Tracker	Sinclair ST-16RT2	2	0.158	0.5
	Sun Sensors	SolarMEMS nanoSSOC- D60	4	0.006	0.115
	IMU	Northrop LN- 200S	1	0.748	12
Attitude control	Reaction wheels	Vectronic VRW-02	4	1	3
	RCS thrusters	QinetiQ T5	4	2.5	700
	IPCU	-	1	16.7	814
	PXFA	-	1	7.5	-
	Fuel	-	-	6.05	-
	Fuel tank	-	1	5.929	-
	Total				51.267

8.5.4 (Δv) Budget

A determining factor for the design of the ADCS is the amount of required impulse (also referred to as Δv) to perform station keeping maneuvers throughout the duration of the mission. In order to determine the Δv budget for the LERA-O ADCS the Systems Tool Kit (STK) software along with a three-body (Sun-Moon-Earth) propagator was utilized. The Cartesian (X, Y, Z, Vx, Vy, Vz) values were measured before and after the completion of one full orbit, which defined the consequential drift in each direction. Subsequently, the velocity vector ($|V|$) was identified. It was found that the $|V|$ increases by $0.2221m/s$ and LERA-O drops in altitude by $0.235m$ after one orbit. In order to maintain orbit, LERA-O will have to provide an anti-velocity vector of $0.2221m/s$ per orbit. Considering an orbital period of 1.83 hours and a calendar month of 30 days the Δv required was calculated to be $26.67m/s$ per month. Adding an extra 15% for margin of error results in a $30.67m/s\Delta v$ per month. The mission duration is estimated to be six months which translates to a total ADCS Δv budget of $184m/s$ for the entire mission. LERA-O will be orbiting the Moon at an altitude of as low as $50km$, where gravitational forces are relatively high, explaining the relatively high Δv required.

8.5.5 Fuel Mass Estimation

Once the Δv value for the ADCS was established the fuel mass required for the LERA-O control system was easily evaluated using the Tsiolkovsky rocket equation. Assuming a dry mass of 300 the xenon mass required to produce $184m/s\Delta v$ was calculated to be 6kg. Fuel mass estimations help define the required fuel tank size and wet mass of the spacecraft. The design material selected for the xenon fuel tank is titanium Ti-6Al-4V (Grade 5) due to its high tensile strength and strain.

Table 38: Given the mechanical properties of the chosen material the following characteristics relating to the xenon fuel tank were defined

Feature	Value
Pressure of propellant	91.27 MPa
Pressure on fuel tank material	781 MPa
xenon Fuel tank diameter	25.36 cm
xenon Fuel tank weight	5.929 kg

8.6 Command and Data Handling

The CDH subsystem of LERA-O contains the onboard computer, data bus, data links to all other LERA subsystems, and is responsible for the overall functioning of the LERA-O spacecraft. The trade studies for the OBC and data bus are based on a 1-10 scale where 10 is highest favorable condition and 1 is least favorable.

8.6.1 Hardware

Onboard Computer Figure 26 shows highest favorability for the lowest maximum power consumption, greatest operational temperature range, maximum total radiation dose tolerance, and maximum clock speed.

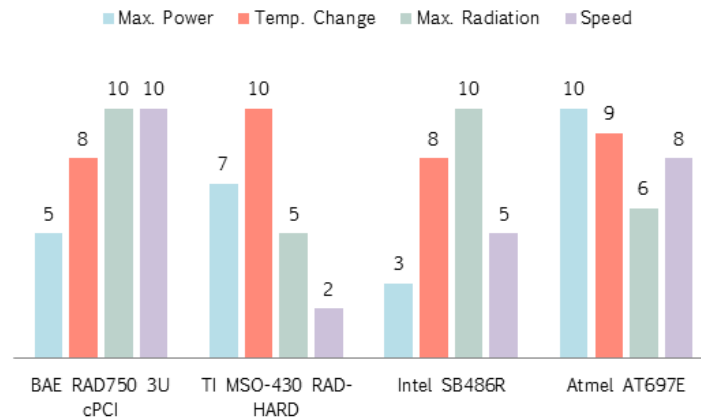


Figure 26: Onboard computer trade study

After completing a trade-off study on several different onboard computer systems with significant flight heritage which could be adapted to the LERA mission, it was decided to utilize the RAD750 3U cPCI OBC offered by BAE Systems. The complete specifications for the RAD750 are given in Figure 26. The high clock speed and high radiation hardness and resistance, along with its successful

spaceflight heritage (such as on the LADEE, LRO, and MRO missions), made the RAD750 the most appropriate for the LERA mission specifications [90].

Table 39: LERA-O instrument data rates

<i>Instruments</i>	MASPEX	SUDA	EIS NAC	EIS WAC	E-THEMIS	Total
<i>Data rate (kbps)</i>	57.0	3.50	2.52	2.88	4.34	70.3

Data Rates In order to calculate the required onboard data storage capacity required, it was assumed that 50.0% of the orbital period of LERA-O would be spent around the dark side of the Moon, resulting in loss of contact with the ground communication station. Taking the peak data rates from each of the spacecraft instruments (MASPEX, SUDA, EIS NAC, EIS WAC, and E-THEMIS), the maximum data size during the communication black out was calculated by halving the time of an orbit and multiplying it by the total data downlink rates from the instruments. Therefore, total storage required per orbit was calculated as 28.9[*MB*]. This was then multiplied by a safety factor of 1.50 to give the total data density of 43.3[*MB*]. Based on this value, the RAD7503U cPCI contains sufficient storage in its SDRAM memory to store the data from each orbit, with ample storage space left over for software and communications data.

Data Bus Figure 27 shows highest favorability for the lowest maximum power consumption, maximum total radiation dose tolerance, and highest data transfer rate.

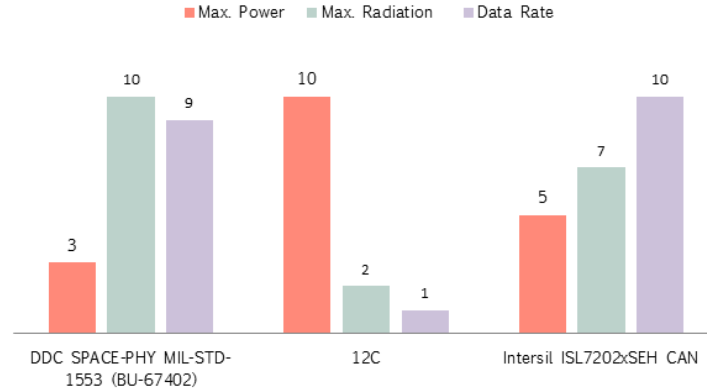


Figure 27: Data bus trade study

The radiation hardened MIL-STD-1553 data bus is a commonly used data bus for space applications (for example on the U.S. Laboratory Module, Zarya, the European Columbus Orbital Facility, and JEM on the ISS). It is highly tolerant to the large doses of radiation present in space and has a reasonably high data rate (as shown in Figure 27). Therefore, the MIL-STD-1553 was selected for use on LERA-O over the other data buses which were analyzed. The integrated transceiver/transformer of the BU-67402 helps to save space and the single package improves the reliability of the bus, while simultaneously simplifying its layout [25].

Data Links SpaceWire IEEE 1355 point-to-point data links have been selected to transfer data between the different LERA-O subsystems. The point-to-point connections provide low-latency data transfers and allow for controlled flow which in turn minimizes buffering and helps to avoid data losses. The IEEE 1355 is a high-speed data link capable of accommodating both the high-speed and low-speed data rates for input and output between the LERA-O subsystems. The IEEE 1355 has extensive flight heritage, developed by ESA, and used by NASA for missions such as for the James Webb Space Telescope, LRO, and LCROSS [24]. Ten data links are required to fully interconnect LERA-O.

8.6.2 Software

The VxWorks OS and software package is responsible for the CDH, EPS, and ADSC. Regarding CDH, VxWorks is responsible for sending commands to subsystems, receiving and storing payload data, memory management, and both internal and external telecommunications. Data from the payloads is initially stored in the Rad750 SDRAM before being transmitted to the ground communications station. For the EPS, VxWorks is responsible for distributing power to each subsystem as defined in Section 8.7. As for the ADSC, VxWorks regulates the propulsion systems based on the data received from the ADSC subsystem (described in Section 8.5). Furthermore, the VxWorks software performs housekeeping telemetry, such as error detection, instrument performance measurements, power level monitoring, data sequencing, and maintaining health reports of the overall system [92].

8.6.3 Risk Aversion

Shielding from radiation is vital for the CDH subsystem in order to avert a number of disruptive, or even mission-ending phenomenon which can occur when particle radiation interacts with the electronic systems. These phenomenon include, but are not limited to, charging, ionization, latch-up, and single event effects. Even though each CDH component is already radiation-hardened to aid in protecting from the volatile space environment, it was decided to place the OBC and data bus inside of a simple aluminum container to further safeguard the sensitive and delicate CDH processes.

8.6.4 Architecture

Based on a decision tree for the overall CDH subsystem architecture (Figure 28), it was decided to utilize a centralized master OBC rather than a distributed processing system in order to reduce its overall complexity and avoid the additional costs involved with implementing a distributed system. It was decided that payload data would take place at the ground control station instead of onboard by the OBC so as to reduce the onboard computing power required and avoid the need for a mass data storage device which would add to the complexity, cost, and weight of the system.

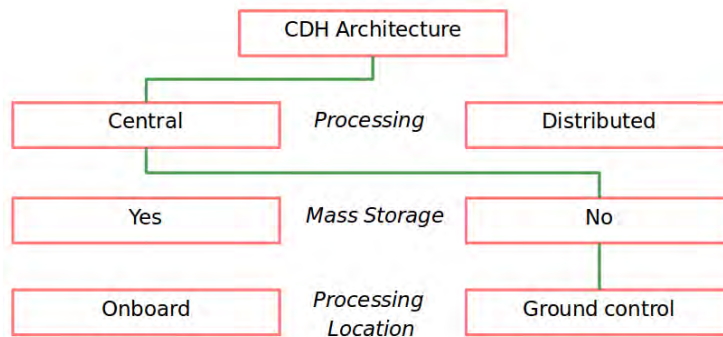


Figure 28: CDH architecture flowchart

8.7 Power

The Electrical Power System (EPS) of any spacecraft is important and its selection should take into consideration a number of factors including all power requirements from all subsystems, mission phases, any mass or cost limitations, mission life and spacecraft consideration. The EPS functions are usually classified as shown in Figure 29.

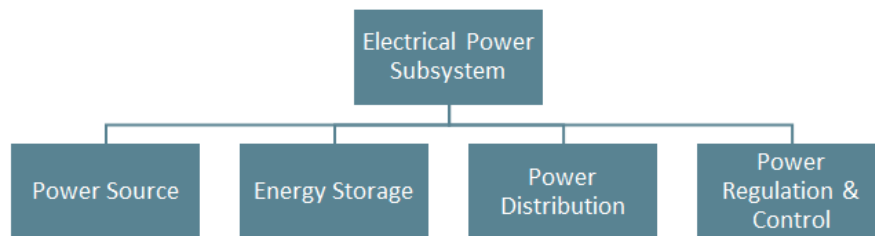


Figure 29: Electrical power subsystem and its functions [12]

Table 40: Power requirements for LERA-O

Electrical Power Subsystem Requirements

- The EPS shall be able to provide the orbiter sufficient power including periods of eclipse and anomalies
- The EPS shall be capable of providing the peak power required for all orbiter subsystems plus a safety margin of 30%
- The EPS shall be able to generate, convert and store energy for electrical power
- The EPS shall be able to manage all electrical power and distribute to subsystems
- The EPS shall be capable of providing subsystems a 20% safety margin for each new unit, 10% safety margin for each heritage unit and 5% safety margin for a recurrent unit
- The EPS system shall be able to be stowed during launch and post-launch and deployed if required
- The EPS system shall be capable of providing sufficient power until the end of the scientific phase
- The EPS system shall be capable of operating in temperatures between 0[°C] to 40[°C]

Table 41: Power budget for LERA-O

Subsystem	Component	Peak Power [W]	30% Margin	Total Power [W]
Command and Data Handling	Processor	11	3.3	14.3
	Data Bus	1.3	0.39	1.69
	Data Links	7	2.1	9.1
Scientific Payload	Mass Spectrometers	58.2	17.46	75.66
	Cameras	24.5	7.35	31.85
Attitude Determination and Control	Star Trackers	2	0.6	2.6
	Sun Sensors	2.92	0.876	3.796
	Inertial Momentum Unit	24	7.2	31.2
	Reaction Wheels	25	7.5	32.5
	Reaction Control System Thrusters	2800	840	3640
Propulsion	Valve	15.9	4.77	20.67
	Preheater	30	9	39
	Thermal	277	83.1	360.1
Communications	Antenna	80	24	104
Total		3358.82	1007.65	4366.47

8.7.1 Primary Power Source: Solar Panels

The power system generally occupies up to 30% of the spacecraft mass and can typically cost 20% of the spacecraft budget [12]. There are a range of different power sources that can be chosen and depend on the mission objective and how far away from the Sun the mission is completed. As the mission will be completed around the Moon, a solar array can be used as the primary source of power for all communications, telemetry, scientific instruments, control and navigation, and propulsion. The other prevalent power source is radioisotope thermal generators (RTG), generally used for missions outside the inner solar system where it would be difficult to utilize a solar panel so far from the Sun. There are a number of issues that prevent a mission such as LERA to use a RTG [52]. Those include high cost compared to solar panels and contamination of the Moon. Solar array selection is driven by power level, cost, risk, specific power, Low Intensity Low Temperature (LILT), natural frequency, strength and packaging. There are new and emerging solar array technologies which range from mid-TRL to TRL 9. At TRL 9, Orbital ATK's UltraFlex has been used for the Phoenix Mars mission and has demonstrated a specific power of 150 W/kg at beginning of life (BOL) and is lightweight [7]. At TRL 6, Orbital ATK's MegaFlex is currently in development for larger solar array requirements and potentially can replace UltraFlex for planetary missions [8]. Currently, and for use in Moon missions specifically, silicon (Si) or gallium arsenide (GaAs) solar cells are implemented due to their low cost and high success rate in heritage missions. Efficiencies for both can reach up to 29%, but GaAs have demonstrated efficiencies over 37%.

Table 42: Comparison of silicon and gallium arsenide solar cells

	Si	GaAs
		Better BOL AMO efficiencies
		Improved temperature coefficients
	Density is half of GaAs	Improved radiation resistance
		Good low light performance
Advantage	Material cost is 3 to 6 times less than GaAs	Excellent UV, radiation and moisture resistance
		Flexible and lightweight
		Smaller short-circuit current density
		Larger open-circuit voltage
		Higher conversion efficiency

As illustrated above, the GaAs solar cell advantages outweigh Si solar cell and therefore prove to be the suitable power source. Specifically, triple-junction GaAs solar cells are becoming the most common state-of-the-art and their multi-layered design allows for increased efficiency as well as decreased degradation due to radiation exposure [89].

Different mounting and structural platforms are available for solar arrays and depend on the mission requirements, power requirements, geometrical layout and thermal and radiation environment. Solar array platforms for triple-junction solar cells are compared in Table 43.

Table 43: Comparison of silicon and gallium arsenide solar cells [89]

Structural Platform	Maximum Power at 1 AU [kW]	Specific Power at 1 AU, BOL [W/kg]	Areal Power Density at 1 AU, BOL [W/m ²]	TRL
Body-mounted	2	N/A	314	9
Deployable rigid	25	80	330	9
Flexible fold-out	150	150	338	9
Flexible roll-out	25	150	338	7

While the characteristics above highlight flexible blanket arrays to be the best choice, there are a few other considerations that have been taken into account. Due to their low thermal mass and their tendency to have thermal expansion and contraction "mismatches" [52], flexible blanket systems can be susceptible to thermal snap. Thermal snap primarily occurs right after a solar array exits an eclipse period and is immediately subjected to illumination incidence. The lunar mission is vulnerable to many eclipse periods, particularly during the planned mission duration and therefore flexible blanket systems may be unreliable in a scenario where solar arrays are the main source of power. Deployable rigid solar arrays are currently utilized in the vast majority of space applications and have proven to be reliable. The deployable solar arrays will utilize a two-axis gimbal system to maintain orientation with the sun [52]. Motor and controller drive system can be configured to autonomously track the sun and these mechanisms rely on the star tracker and sun sensors on board. DC stepper motors are commonly used due to their "simplistic drive electronics" [52] and therefore are low in cost. There will be 36 m² of 30% triple junction GaAs solar cells from AZUR Space GmbH. Two deployable wings will be utilized so that they can be folded during launch and then deployed once orbit around the Moon has been established.

8.7.2 Secondary Power Source: Li-Ion Batteries

For solar powered missions, it is recommended that rechargeable battery systems are used as a secondary power source. The rechargeable battery should be reliable with appropriate cycle-life and low self-discharge. A secondary power source is required to provide power during launch and post-launch until solar panels can be deployed, when firing thrusters for attitude and trajectory control, during phases of cruise anomalies, during eclipses and times when the solar panels are unexposed to the sun [20]. Heritage missions have typically used nickel-cadmium (NiCd), nickel-hydrogen (NiH₂) or silver-zinc (AgZn) batteries. Lithium-ion (Li-ion) batteries have been utilized in recent missions due to their advantages over other rechargeable battery solutions [5]. Bugga et al. [20] have listed the four battery types and their useful characteristics, as seen in Table 44.

Table 44: Heritage batteries and useful characteristics [20]

System	Specific Energy [Wh/kg]	Energy Density [Wh/L]	Operating Temp. [°C]	Range Calendar Life [years]	Cycle Life
NiCd	100	200	-10 to +25	< 1	< 100
NiH ₂	35	100	-10 to 25	> 5	> 30,000
AgZn	40	80	-10 to 30	5 to 10	> 40,000
Li-ion	100	240	-30 to 40	4	1000

Li-ion batteries are beneficial due to their high energy density, specific energy, and operating temperature range. During the Spirit and Opportunity missions–simulation tests, Li-ion batteries demonstrated that 90% of initial capacity was retained. Li-ion batteries are also preferred due to their high efficiency, slow material degradation, lack of memory effect, low self-discharge and minimal maintenance requirements [97].

It is evident why current missions within the inner solar system employ the use of Li-ion batteries due to their long list of advantages, this can be compared to the types of batteries implemented in recent mission and past missions. More recent missions have mainly implemented Li-ion batteries, particularly for lunar missions, where solar arrays are used as the primary power source. Li-ion battery technology has advanced in recent years to allow for smaller and lighter batteries with less maintenance and improved ability to retain charge [35]. The SMART-1 lunar mission employed Saft Specialist Battery Group VES batteries and successfully completed a three year mission. As the mission to be completed by LERA will be more than MEO, the VL48E and VL10E batteries will be considered. Saft have developed specialized batteries, specifically for the US market and these will be used instead of the VES range. Technical specifications for both VL48E and VL10E are outlined in Table 46.

Table 45: Saft Li-ion cell technical specifications [35]

Specification	VL48E	VL10E
Guaranteed capacity [Ah]	48	10
Mean voltage at C/1.5	3.6	3.6
End of charge voltage V	4.1	4.1
Energy [Wh]	170	36
Specific energy [Wh/kg]	150	139
Height [mm]	250	129
Diameter [mm]	54	33.8
Weight [kg]	1.13	0.25
Status	Qualified	Qualified
Main application	GEO, LEO	GEO, LEO

As LERA-O will require a significant amount of power for all subsystems, VL48E batteries have been chosen. Only one VL48E battery will be required to support the spacecraft.

9 LERA-IB

This section discusses the LERA-IB component of the LERA mission in detail. The LERA-IB system is responsible for storage and launch of the LERA-IM. LERA-IB will be fixed to the launch Falcon 9 upper-stage adapter via a mechanical mating plate. Thus, the LERA-IB system will be permanently attached to the Falcon-9 upper-stage. The subsystems in the LERA-IB include the six LERA-IM's and the six LERA-IL's. The six LERA-IM's are all stored inside their respective LERA-IL tubes up until the instruction is provided to commence the launch/detachment sequence. Figure 30 highlights the LERA-IB system along with the two subsystems LERA-IM and LERA-IL.

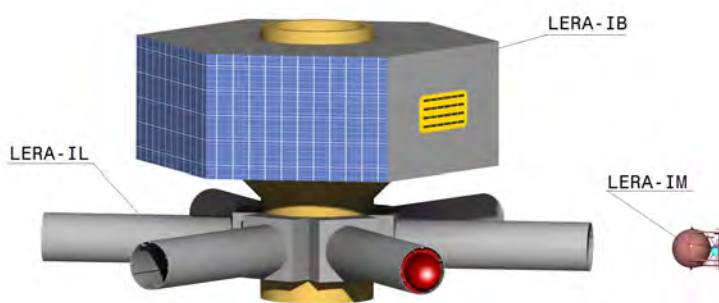


Figure 30: LERA-IM and LERA-IL Subsystems Attached to LERA-IB System

9.1 LERA-IB System Architecture

The LERA-IB system architecture is provided in this section. The LERA-IB system contains the LERA-IM and LERA-IL subsystems. Each of these subsystems have various other subsystems linked to them. The flowchart in Figure 31 demonstrates a summary of the systems and subsystems included in the LERA-IB segment and the linkages between them.

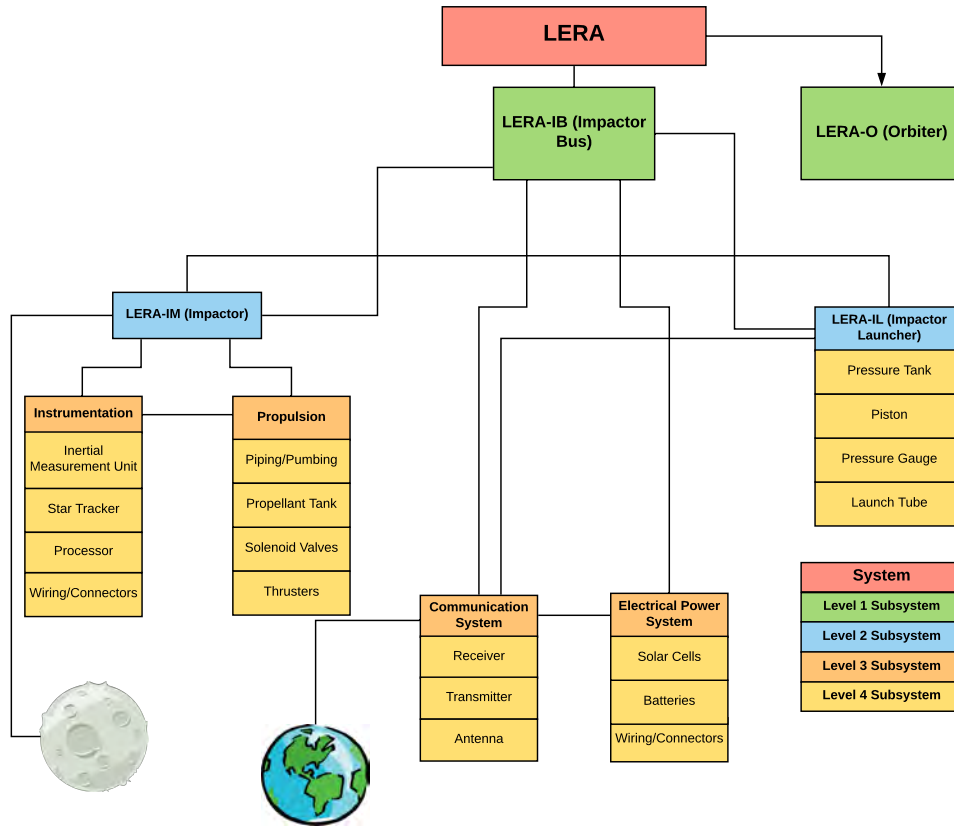


Figure 31: LERA-IB system architecture

9.2 LERA-IB Requirements

LERA-IB System Level Requirements

- The LERA-IB shall transmit and receive data at a minimum rate of 5 [kbps]
- The LERA-IB shall fit within the payload bay of the Falcon 9 upper-stage
- The LERA-IB shall be able to store six LERA-IL's and LERA-IM's
- The LERA-IB shall have an interface capable of connecting to the Falcon 9 upper-stage payload bay

LERA-IM Subsystem Level Requirements

- The LERA-IM shall create a plume detectable at 50 [km] altitude by MASPEX and SUDA
- The LERA-IM shall be able to impact the target location within an accuracy of 10 [km]
- The LERA-IM shall not contaminate the measurement samples by sharing a similar atomic weight of the volatiles of interest
- Each LERA-IM shall not exceed a total weight of 100 [kg]

LERA-IL Subsystem Level Requirements

- The LERA-IL shall be able to impart a maximum Δv 300 [m/s]

9.3 Target Characteristics

Primary research has shown that the highest concentration of water-ice is most likely to reside within the deep impact craters near the south pole region of the Moon [10]. Typically, these craters have extremely cold permanently shadowed areas, which are never exposed to the Sun during the Moon's orbit, make them the most viable regions on the Moon surface for water-ice existence. This section explores the composition of the Moon to highlight some important considerations for the LERA-IM design and provides a list of the selected six craters for impact.

9.3.1 Lunar Composition

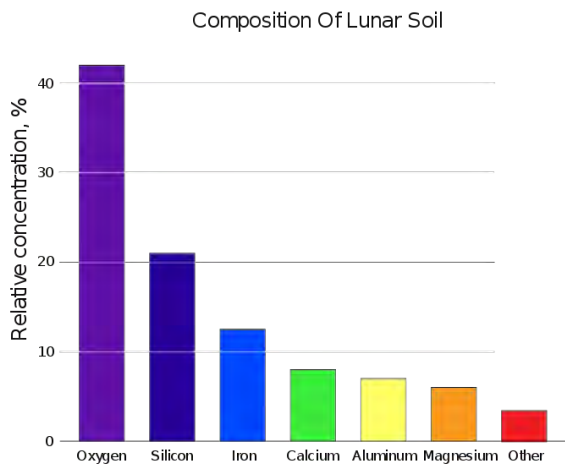


Figure 32: Lunar composition on the Moon [61]

The permanently shadowed regions of these craters, and perhaps the entire surface of the Moon, is covered by a layer of material, namely regolith, formed out of either dust, soil, or broken rock. This regolith layer is estimated to have an approximate depth of 4–5 metres in most areas of the permanently shadowed regions [11]. The potential existence of water-ice is envisaged to be below the surface regolith, and hence, a LERA-IM must be able to remove this layer and create a plume for the LERA-O that consists of particles from below the regolith layer.

A LERA-IM impacting in the permanently shadowed region of a crater near the south pole must avoid the contamination of the Moon. That is, the LERA-IM must not consist of any material that is typically found on the Moon. This allows the orbiter LERA-O to determine the origin

of the recorded particle (i.e. whether the particle came from the disintegrated LERA-IM or the Moon). Figure 32 below shows the typical materials composition found on the Moon.

9.3.2 Crater Selection

There are multiple craters in the south pole region of the Moon that have some permanently shadowed regions, and thus, a possibility of water-ice existence. An important consideration associated with crater selection is the orbital plane the crater aligns in. As per the mission plan of the LERA-IB, there will be six LERA-IM launches within approximately a twelve-hour period, with each of them separated by 1.94 [hr]. This provides the LERA-O only a short amount of time to ensure it is orbiting in the appropriate orbital plane so that it can collect data from the next impacted crater. Although the LERO-O may be able to conduct an orbital change after collecting data from an impact, it is predicted that doing so six times will require a significant amount of fuel. Thus, as an attempt to

minimise the required orbital changes from LERO-O, the six selected craters are aligned in a total of two orbital planes (as seen in Figure 33), requiring only one orbital change. Table 46 provides further details on the six selected craters. In addition to the orbital plane considerations, the Cabeus and the Shackleton craters are also partly chosen so that the LERA mission can provide validation of the previously collected data from the LCROSS or Chandrayaan-1 missions [21, 54].

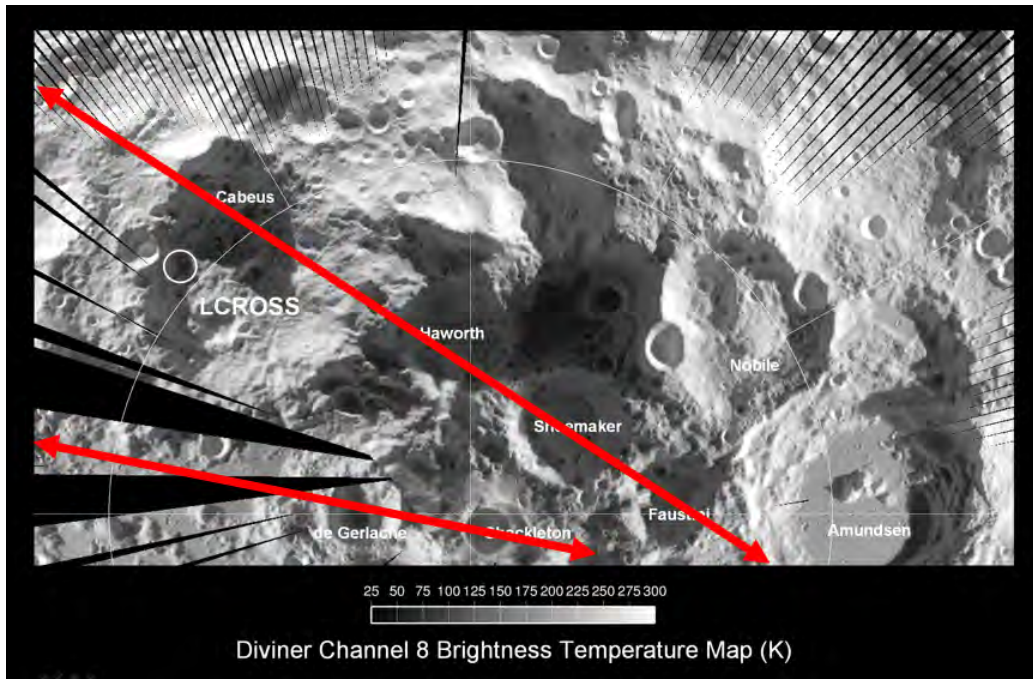


Figure 33: Selected craters and their orbital planes

Table 46: Details of six selected craters

Impacted Crater (In Order)	Location	Diameter [km]	Depth [km]
Cabeus [45]	85.33°S 42.13°W	100.58	4.00
Haworth [48]	87.45°S 5.17°W	51.42	--
Shoemaker [50]	88.14°S 35.91°E	51.82	--
Faustini [47]	87.18°S 84.31°E	42.48	--
De Gerlache [46]	88.5°S 87.1°W	32.40	--
Shackleton [49]	89.67°S 129.78°E	20.92	4.20

9.4 Plume

9.4.1 Background

On 9 October 2009, the Lunar Crater Observation and Sensing Satellite (LCROSS) experiment was declared a success after it impacted Cabeus Crater near the south pole region of the Moon [77]. The resulting excavation of surface material was observed by the trailing shepherding spacecraft that crashed into the surface of the Moon 250[secs] after the first impact. Onboard instruments were able to identify several different compounds of ice - assumed to be associated with permanent deposits of water ice - and hydroxyl molecules such as NH_2 and CO_2^+ [40]. Perhaps the most remarkable observation revealed by the LCROSS mission was

that the resulting ejecta plume consisted of two different components: a central steep-angle component and a surrounding low-angle cone-shaped component. Impact experiments at the NASA Ames Vertical Range Gun were conducted to investigate the LCROSS predictions. The experiments investigated the effect of using hollow projectiles on the resulting ejecta plume structure and were successful in replicating the bimodal morphology of the LCROSS debris plume. Experimental results demonstrated that the resulting low-angle component of the plume excavated a larger quantity of material from greater depths than the high-angle component [88]. Analysis of test results also showed that the volatile compounds excavated as part of the central plume remained aloft for a significant amount of time and well after the resulting crater finished forming. Based on these results, LERA will utilise hollow impactors to exploit the potential of the bimodal ejecta plume structure. This plume configuration will also maximise the amount of lunar volatile inventory. Finally, the hollow spherical impactor geometry will serve as a storing solution for the reaction mass meant to power the Reaction Control System (RCS) mounted on the impactor.

9.4.2 Characterization of the LERA Impact Plume

The following sections will use the nomenclature defined below to analyze, interpret, and derive the current knowledge of plume science within the available crater scaling theory to characterize the LERA impact plume.

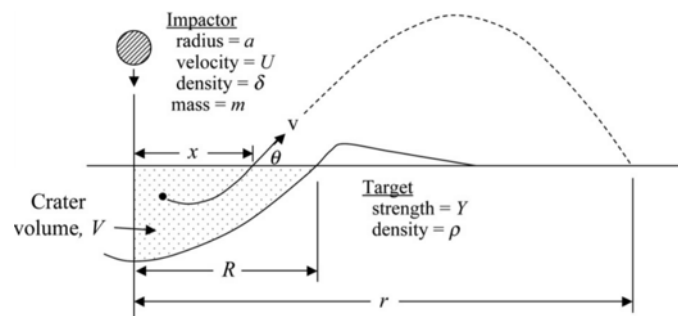


Figure 34: Definition of plume parameters

Following impact, the energy and momentum carried by the impactor will be transferred to the impact location, resulting in a crater growth which will be determined by either gravity or material strength. As the crater is forming, surface material will be displaced, moving in an upward and outward fashion along the bowl-shaped crater.

Ejecta Mass Distribution The following section acquaints the reader with the procedure that was followed to represent the resulting debris ejecta mass obtained above a certain altitude in terms of impactor mass. This was done by using scaling laws for crater ejecta widely available in the open literature. Analysis was commenced by identifying the regime in which the impact event is expected to happen. Housen, Schmidt, and Holsapple [44] define the parameter $Y/\rho gR$ and associate a small value of this parameter with an environment dominated by the strength regime, while a high value of $Y/\rho gR$ entails the prevalence of the gravity regime. This parameter is a direct measure of the work done to overcome target strength compared to the work performed to resist gravitational forces during crater formation. After substituting the relevant values, it appears that the target material displays little strength, which

allows the study to be conducted in this regime. It is useful to start by introducing that the volume of a crater following an impact event is dependent on the impactor radius a , impact velocity U , and mass density δ [42].

$$V = f[\{\rho, Y\}, \{a, U, \delta\}, \{g\}]$$

Dimensional analysis can then be used to establish a relationship between dimensionless combinations which include the cratering efficiency, the gravity-scaled size, and the strength group labelled as π_V , π_2 , and π_3 respectively. This relationship takes the following form:

$$\pi_V = \left\{ \pi_2 \times \left(\frac{\rho}{\delta} \right)^{\frac{6\nu-2-\mu}{3\mu}} + \left[K_2 \times \pi_3 \times \left(\frac{\rho}{\delta} \right)^{\frac{6\nu-2-\mu}{3\mu}} \right]^{\frac{2+\mu}{2}} \right\}^{-\frac{3\mu}{2+\mu}} \quad (2)$$

$$\pi_V = \frac{\rho V}{m}, \quad \pi_2 = \frac{ga}{U^2}, \quad \pi_3 = \frac{Y}{\rho U^2}$$

The constants K_1 (0.15) and K_2 (1) as well as the exponents ν and μ are determined from actual data in both the strength and gravity regime. Holsapple [42] assumes a value of 1/3 for ν in all cases, and a scaling exponent value of 0.41 for μ . Based on this equation, and after deriving the volume of surface ejecta in terms of impactor mass, a graph representing the mass of volatile compounds ejected above a certain altitude (Y axis) as a function of impactor mass (X axis) is shown in Figure 35 below. The impacting speed was calculated to be 2.5×10^3 [m/s] and the impact angle from the horizontal will be in the range of $85^\circ \pm 5^\circ$.

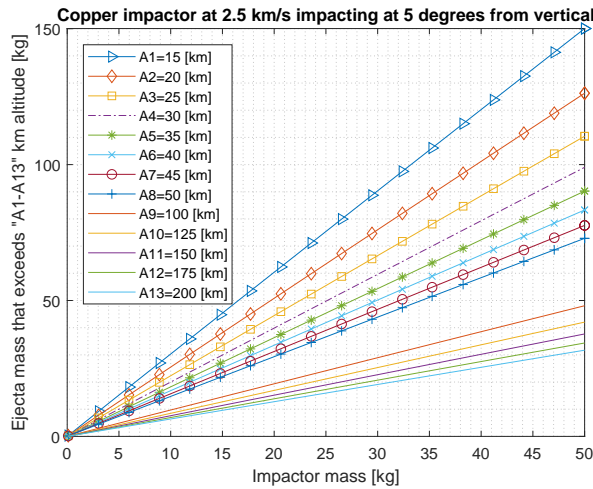


Figure 35: Ejecta mass obtained above the specified altitudes in terms of impactor mass

Ejecta Volume Distribution In this section, scaling relations are derived for surface volume discharged at velocities greater than specified surface ejecta velocities in terms of impactor mass. Housen, Schmidt, and Holsapple [44] introduce the following scaling relationship for the volume of ejecta with a velocity $>$ target ejection velocity:

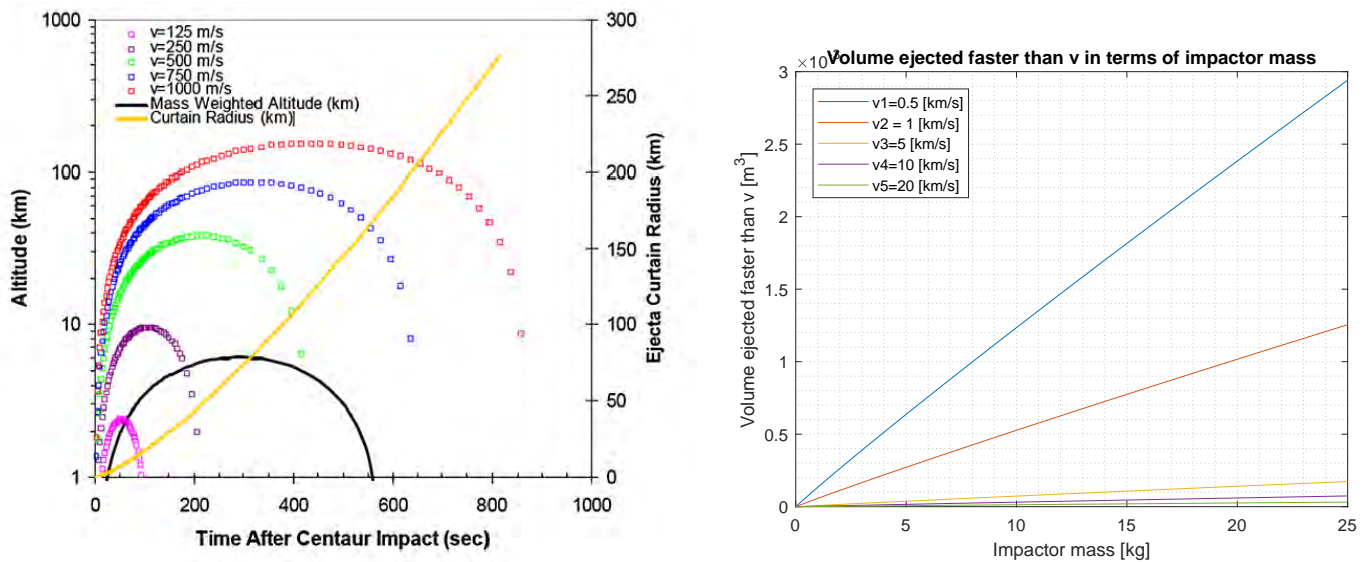
$$\frac{V_e}{R^3} \propto \left(V_{ejection_target} \times \sqrt{\frac{\rho}{Y}} \right)^{\frac{6\alpha}{\alpha-3}} \quad (3)$$

Equation 2 was then written in terms of resulting crater volume as a function of impactor mass and the crater volume presented in Equation 3 was rewritten in terms of crater volume using the equations below:

$$V_e \propto \left(V_{ejection_target} \times \sqrt{\frac{\rho}{Y}} \right)^{\frac{6\alpha}{\alpha-3}} \times \frac{3V}{4\pi} \quad (4)$$

$$V_{impactor} = \frac{4}{3} \pi R^3 \quad (5)$$

Housen, Schmidt, and Holsapple [44] recommend using a value of 0.51 for the exponent α , which is representative of experimental results obtained for impact events into lunar regolith. The behaviour of ejecta can then be presented in terms of volume of debris ejected faster than a given velocity as a function of the mass of the impacting body. This is illustrated in Figure 36b below:



(a) LCROSS altitude prediction for material with given velocities in (b) Resulting ejecta volume moving with velocity $> v$ in terms of impactor mass. LCROSS altitude prediction for impactor mass material with given velocities in terms of time after Centaur impact Heldmann et al. [39]

Figure 36: Predicted surface volume ejecta moving faster than velocity v for LERA and plume height for given velocities for LCROSS

Figure 35 also shows the predicted ejecta curtain radius obtained as a function of time following the Centaur impact. As it can be seen, all debris are expected to follow a ballistic trajectory originating from the impact location and land back on the lunar surface provided no disturbance of these trajectories occur. Material densities are expected to be at their maximum in the first 200[secs] following the Centaur impact eventHeldmann et al. [39].

Holsapple [42] introduces a relationship for the minimum possible ejection velocity in the strength regime that is independent of impactor mass. This variable is directly related to the density of the target medium and the target material strength value Y and can be represented as follows:

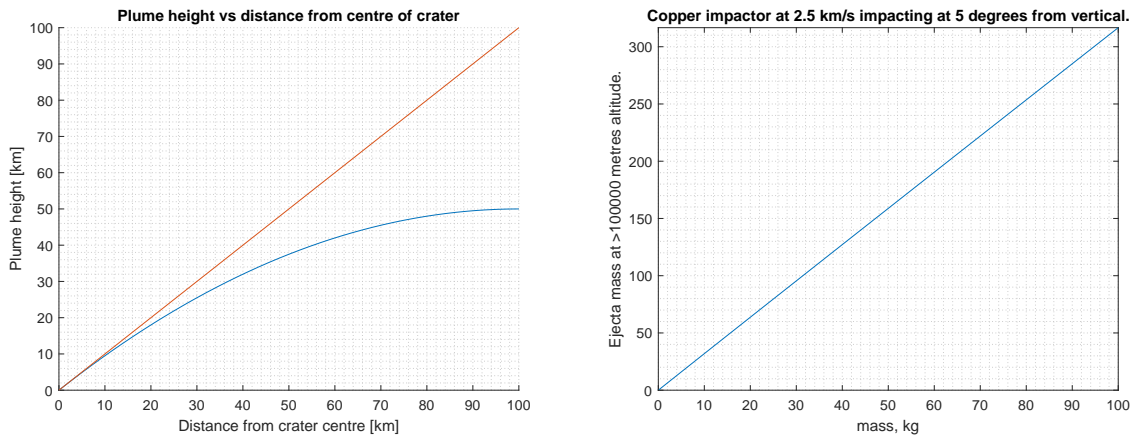
$$V_{ejecta_{min}} = \sqrt{\frac{Y}{\rho}} \quad (6)$$

This helps establish a threshold for the ejection velocity of surface material following an impact event. This value, $8.16 [m/s]$, is used at a later stage to construct the resulting multi-component ejecta plume structure to model the LERA impact plume.

Morphology of the Synthetic Plumes used to model the LERA Impact Plume The modeling of the synthetic plume consisted of a low-angle plume with ejection angles at 45° with respect to the lunar surface, but following a general ballistic trajectory and an independent 45° asymptote that extends to infinity. The latter is a theoretical limit that assumes a high-speed constant-angle (45°) migration of surface ejecta and acts as a lower bound of the low-angle plume structure. This was done in an effort to reproduce a plume that is morphologically similar to those produced by hollow impacting bodies. A review of maneuvers performed by the NASA LRO during the LCROSS mission unveiled that spacecraft's orbiter flew within $50 \times 10^4 [m]$ above areas located around the south pole of the Moon [77]. The water vapor plume at this altitude persisted for the remaining $4 [mins]$ duration of the Moon. Based on the success of this mission, and for the purpose of the calculations, a similar target altitude was chosen for the LERA-O in an aim to establish a minimum height threshold for plume detection.

Equation 7 below is the general ballistic equation used to model the trajectory of surface ejecta as a function of distance from the crater centre x :

$$h_{plume} = v_{0y} \left(\frac{x}{v_{0x}} \right) - 0.5g_{Moon} \left(\frac{x}{v_{0x}} \right)^2 \quad (7)$$



(a) Plume height in terms of distance from crater centre (b) Resulting ejecta mass above given altitude in terms of impactor mass

Figure 37: Morphology of the low-angle component of a synthetic plume

The molecular mass of a H_2O compound ($18.02 [amu]$) was used to determine a required density of $2.99 \times 10^{-16} [kg/m^3]$ by multiplying $m_{H_2O} \times C \times n$, where $C = 1.66 \times 10^{-27}$ and is the conversion factor between amu and kg , and where $n = 10^6$, representing the number of samples within a cubic metre. After integrating the area of the region formed by the two functions represented above

and multiplying by the required density, a resulting ejecta mass of 82.04 [kg] was obtained. This established a minimum cratering mass of 25.8 [kg] required to achieve the desirable plume density at an altitude of 50×10^4 [m].

9.5 LERA-IB Design

9.5.1 LERA-IB

Structure The LERA-IB structure will be a hexagonal prism with internal skeletal structures supporting the skin. The pressure tanks required for the detachment of the LERA-IM's, data processing unit, transmitter, receiver and battery will be integrated within the bus using mounts. The ergonomic layout of the bus interior allows a shorter profile, reducing overall volume. The bus skin will be made of a composite material sandwiching an aluminum honeycomb core. In addition to reducing cost and weight, the composite structure will provide overall structural integrity of the bus.

The LERA-IL will be constructed using a circular thin wall aluminum structure. The function of LERA-IL is to store the LERA-IM's prior to launch and to support the stress due to the build-up of pressure prior to the release of the LERA-IM's. Furthermore, the interior of the LERA-IL houses railings to hold and guide the LERA-IM's and stoppers to prevent the pistons from exiting the vehicle.

Layout Due to the LERA-IB being fixed to the Falcon 9 upper-stage, it was important to consider the orientation of the layout as the LERA-IB will be incapable of making maneuvers. The modular configuration of the LERA-IB was chosen to minimize complexity and assist with bottom up assembly of the subsystems. Immediately above the payload adapter is the LERA-IL which is connected to the pressure tanks inside the bus through plumbing to supply the compressed gas. The only exposed components onboard the LERA-IB are the patch antennas and the solar panels. Figure 38 represents the cross section view of the LERA-IB.

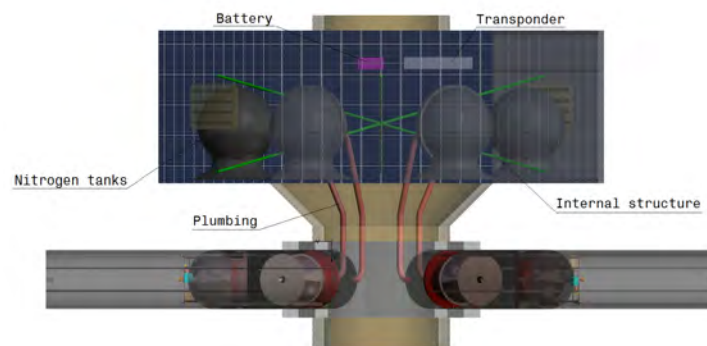


Figure 38: LERA-IB cross section

System Integration Once given the instruction from Earth to launch the LERA-IM, the data processing unit will send a signal to the pressure tank to open the valve. The compressed gas will flow towards the LERA-IL chamber where pressure is built up against the piston. Using a pressure gauge, once the pre-determined pressure is reached, an instruction will automatically be given to the piston stoppers to retract, and hence, detaching the LERA-IM. The transmitter located in the bus will then relay the status of the launch back to ground control. This process is repeated for each of the six LERA-IM detachments.

9.5.2 LERA-IM Design

The LERA-IM is specifically designed to meet the mission requirements of LERA. The purpose of the LERA-IM is to accurately impact in the permanently shadowed region of the desired crater so that a detectable plume is generated. To achieve accuracy within 10 [km], the LERA-IM consists of a RCS which entails guidance and navigation instruments to determine its position, as well as, a cold gas-based propulsion system to allow for any correction maneuvers required to impact on target. As per the mission architecture, there must be six LERA-IM's for six craters. Further, each of the six LERA-IM's must not exceed a mass of 100 [kg]. Figure 39 represents the final design of a the LERA-IM.

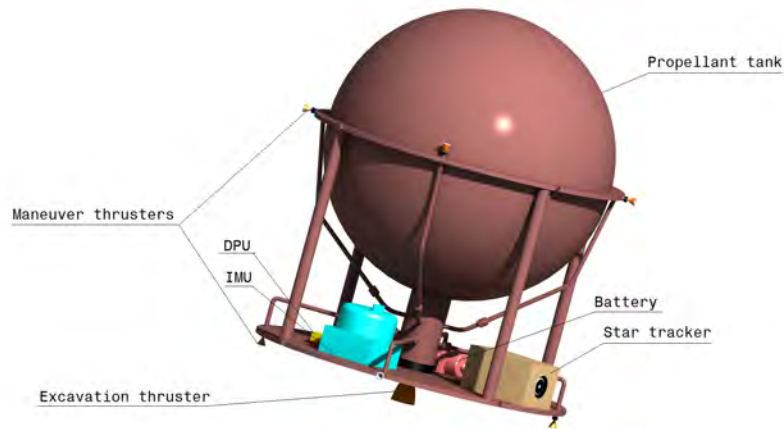


Figure 39: LERA-IM design

9.5.3 Δv Requirements

Each of the six LERA-IM's are placed in their respective LERA-IL's, which is a part of the LERA-IB. The LERA-IB is attached to the Falcon 9 upper-stage at all times of the mission, and hence, the orbital transfer requirements are satisfied by the upper-stage. Further, the Δv required to inject each of the LERA-IM's into their respective trajectories will also be provided by the upper-stage. This means, the LERA-IM is only required to maintain its trajectory and ensure an accurate impact by executing minor maneuvers (i.e. attitude control). Maintaining trajectory may require some Δv as there are a number of factors that can negatively impact a trajectory. For example, the gravitational pull from the Earth and the Moon may cause some deviation from the initial trajectory. Similarly, there may be inaccuracies in the control valves and thrusters used to make a maneuver. In light of these and considering a maximum trajectory time, or the trajectory time of the first LERA-IM, of approximately 20 [hr] for each of the six LERA-IM's, a conservative assumption of 12 [m/s] Δv is made. That is, the LERA-IM is designed so that it can achieve a total of 12 [m/s] Δv during its trajectory.

9.5.4 Contamination Considerations

The LERA mission consists of impacting the Moon with LERA-IM so that the LERA-O system can fly by the generated plume and detect the data. The impact will inevitably cause the plume generated to consist of both the particles from the Moon and the

disintegrated LERA-IM. Thus, to ensure an easy detection of particles that came from the Moon and the particles that came from the LERA-IM, it is considered essential to construct the LERA-IM with a material that is not typically found on the Moon. Various materials were investigated, however, copper was chosen as the primary material as there is no copper on the Moon. Copper is also easily detectable using the scientific instruments onboard the LERA-O. Further, the propellant used in the cold-gas thruster-based propulsion system must not contain any hydrogen as this may provide misleading data in terms of the existence of water on the Moon. Table 47 shows a comparison of the various cold-gas propellants that could be used for the LERA-IM propulsion system. Here, hydrogen is ruled out as an option as the purpose of the mission is to the water-ice existence on the Moon. Similarly, nitrogen has a molecular weight of 28 [kg/kmol] which is the same as silicon, leading to the LERA-O potentially not being able to detect silicon content along with the water. Xenon and sulfur hexafluoride have similar properties and are both deemed viable propellants with regards to contamination. However, as sulfur hexafluoride is not yet used in space missions, it does not meet the TRL requirements. Therefore, xenon is chosen as the propellant for the LERA-IM propulsion system.

Table 47: Comparison of LERA-IM propellants

Propellant	M_r [kg/kmol]	ρ [kg/m ³]	I_{sp} [s]
Hydrogen	2	20	272
Nitrogen	28	40	73
Xenon	131.30	2740	28
Sulfur hexafluoride	146.10	-	-

Further, to maximise the copper content in the LERA-IM, the propellant tank is made out of copper. The critical stress values of copper must not be exceeded by the hollow copper tank which holds the xenon propellant.

9.5.5 Initial Mass

To be able to impact six craters with six LERA-IM's, it was essential to keep the mass of each of the LERA-IM's at a minimal value. Whilst considering a sufficient plume generation, the total wet mass of each of the LERA-IM was limited to 30 [kg]. This satisfies the mass requirement of the LERA-IM subsystem.

9.5.6 Propellant Tank Design

The LERA-IM proposes the use of a copper-based hollow sphere to create a large enough plume upon impact. copper is used to prevent mass spectrometer contamination by isolating the artificial plume signal to a spike at 63.50 [μ]. As an attempt to minimize mass, the LERA-IM uses its copper-based hollow impactor sphere as its propellant tank to store the xenon. The methodology outlined in Appendix A is followed for the design of the copper-based xenon storage tank. The initial equations provided the mass of the propellant required by each of the LERA-IM's to achieve the desired 12 [m/s] Δv . The key mass values of the LERA-IM are provided in Table 48.

Table 48: Mass properties for LERA-IM

Property	Value
Final Dry Mass (m_f)	28.72 [kg]
Propellant Mass (m_p)	1.28 [kg]

Based on these mass values, the uncompressed volume of the xenon propellant and the tank size required to store the fuel at its uncompressed stage is found. When the propellant is compressed into a smaller tank, the propellant pressure will inevitably increase, and hence, the thickness and radius of the copper-based tank must be able to withstand the pressurized propellant. Thus, a range of radius and thickness values that are acceptable (i.e. the copper tank will not burst as the critical stresses are not reached) are plotted with the respective mass of the dry copper-tank (Figure 40a). For any of these thickness and radius combinations, the copper-tank will not burst due to high tensile and shear stresses up until temperatures of up to 436 [K]. From Figure 40a, whilst considering the total size and mass restrictions of the LERA-IM, the radius and thickness values are chosen, and the corresponding dry mass of the copper-tank is determined. It was ensured that the size of the copper-tank was not too large as this would have consequences on the number of LERA-IM's that could be fit in the Falcon 9 upper-stage. Figure 40b provides a schematic of the copper-based propellant tank design for the LERA-IM and Table 49 provides a summary of the characteristics of the designed propellant tank. It is important to note that the dimensions provided in Figure 40b are in [mm].

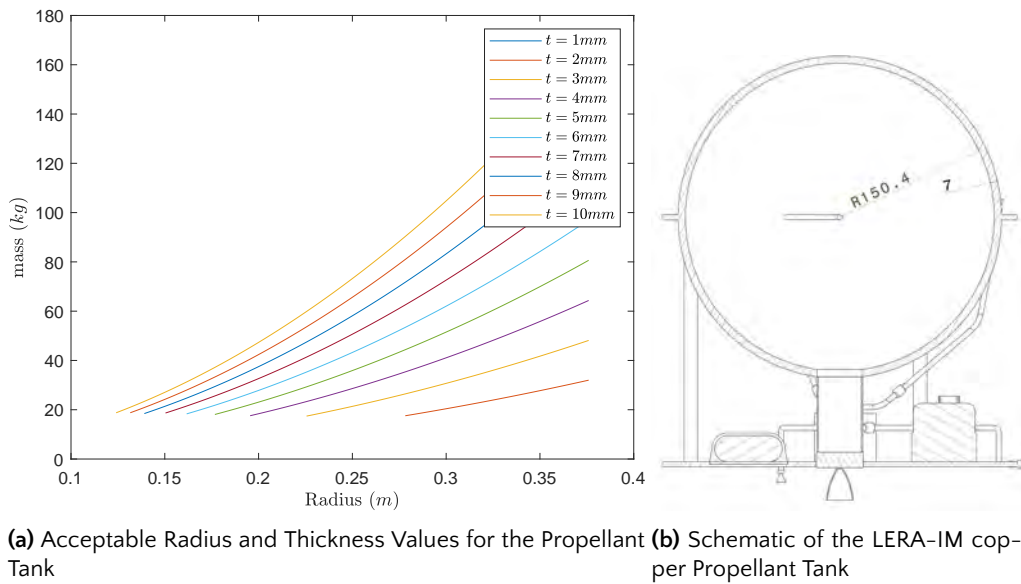


Figure 40: LERA-IM Design Characteristics

Table 49: LERA-IM propellant tank properties

Property	Value
Inner Radius (R_{inner})	15.04×10^{-2} [m]
Outer Radius (R_{outer})	15.74×10^{-2} [m]
Compressed xenon Pressure (P_c)	11.26×10^6 [Pa]
Compressed xenon Volume (V_c)	1.43×10^{-2} [m ³]
Empty copper Tank Mass (m_{empty})	18.67 [kg]

9.5.7 Navigation and Control Instruments

The maximum trajectory time of LERA-IM from the time of detachment to the time of impact is approximately 20 [hr]. Thus, the instruments used for navigation and Control of the LERA-IM must have sufficient battery. Each LERA-IM consists of a non-rechargeable battery that is used to power the instruments onboard during its trajectory. As an accurate impact is desired, the LERA-IM contains scientific instruments that allow it to determine its current position relative to its target location and make any alterations to the trajectory through the propulsion system. An important consideration has been to choose the smallest and lightest instruments that will be sufficient in meeting the purpose. To determine the orientation and attitude of the LERA-IM a Star Tracker is proposed. To determine the angular rate and specific force of the LERA-IM an Inertial Measurement Unit (IMU) is proposed. The IMU consists of three gyroscopes and three accelerometers which considers all degrees of freedom. Further, based on the measurements from the IMU and Star Tracker, the LERA-IM must be able to correlate the data and transfer the appropriate commands that are required to be made to the propulsion system. To do so, a Data Processing Unit (DPU) is proposed. The DPU will be used to compile the data from the IMU and Star Tracker and then transfer the appropriate commands to the solenoid valves in the nozzle in order to make appropriate maneuvers. Table 50 contains a list of the two instruments associated with navigation and control, the battery to power the navigation and control instruments, and the processor used to execute the commands and ensure adequate guidance of the LERA-IM.

Table 50: Navigation and control instruments onboard the LERA-IM

Instrument	Purpose	Manufacturer	Specifications
LN-200S [26]	Measuring or maintaining orientation or angular velocity Measuring accelerometer of LERA-IM	Northrop Grumman	12 [W] Nominal Power Operates ± 5 [VDC] and ± 15 [VDC] Space Qualified
MAI-SS Space Sextant: Miniature Star Tracker [3]	Precision attitude determination based on position of celestial bodies	Adcole Maryland Aerospace	5.7/27 [arcsec] accuracy Update rate of 4 [Hz] 5 [VDC] 1.5 [W] Nominal Power Consumption
ATMEL AT697E Processor [9]	Analyze data from IMU and Star Tracker Execute navigation commands to solenoid valves and hence thrusters	ATMEL	32 – bit Contains on-chip Integer Unit (IU) Contains Floating Point Unit (FPU) Idle mod
LSE 102 Lithium Ion Cells [100]	Ensure sufficient power for all three instruments	GS YUASA	421.04 [Wh] energy 114 [Ah] capacity

9.5.8 Thruster Design

The thruster design is an important part of the LERA-IM design as it ensures appropriate thrust is achieved from each of the thrusters on the LERA-IM to meet the Δv requirement of 12 [m/s] with the provided propellant mass, pressure, and volume. From the maxi-

imum trajectory of approximately 20 [hr] of the first LERA-IM, it is assumed that the thruster will be active for a maximum of 2 [%] of the trajectory time (1429.36 [s]). Hence, in the worst-case scenario, each of the thrusters must be able to, if fired individually, execute the desired thrust to achieve the whole 12 [m/s] Δv requirement. The process followed to design the required thrusters is provided in Appendix B.

The LERA-IM has two main types of thrusters: the maneuver thrusters and the excavation thruster. There are eight micro-thrusters onboard the LERA-IM to accommodate for the various maneuvers. The layout and orientation of these thrusters in the LERA-IM allows it to cover all six-degrees of freedom. These maneuver thrusters are made out of copper to minimize the use of any other material. Further, there is an excavation thruster that is proposed on the LERA-IM for exhausting any remaining propellant prior to impact in a matter of one second. This is considered to minimize any contamination of the Moon from xenon. The excavation of all remaining xenon through the excavation thruster (as seen in Figure 39) can also allow the LERA-IM to impact at a higher velocity, and perhaps, enabling a larger plume. The excavation thruster is also proposed to be made out of copper. Table 51 summarizes the process of thruster design and specifies the final values associated with the LERA-IM thrusters design.

Table 51: LERA-IM thruster design

Property	Maneuver Thruster	Excavation Thruster
Total Burn Time (t_{burn})	1429.36 [s]	1 [s]
Acceleration Required (a_{thrust})	0.084 [m/s^2]	6 [m/s^2]
Force Thruster (F_T)	2.52 [N]	180 [N]
Characteristic Velocity (C^*)	483 [m/s]	483 [m/s]
Exit Pressure (P_e)	1.12×10^7 [Pa]	1.12×10^7 [Pa]
Mach Exit (M_e)	0.0863	0.0863
Throat Area (A_t)	2.71×10^{-8} [m^2]	1.93×10^{-6} [m^2]
Exit Area (A_e)	2.24×10^{-7} [m^2]	1.60×10^{-5} [m^2]
Throat Radius (r_t)	9.28×10^{-5} [m]	7.85×10^{-4} [m]
Exit Radius (r_e)	2.67×10^{-3} [m]	9.04×10^{-3} [m]

9.5.9 LERA-IL Design

In order to give the impactor the required Δv to enter an impact trajectory, a detachment mechanism is required. As presented previously, this Δv requirement is estimated to be between 150 [m/s] for the initial impactor launch and 300 [m/s] for the final impactor launch. To achieve this requirement, a number of detachment mechanisms were explored including the use of a spring, explosives, and inducing an axial roll on the Falcon 9 upper-stage to utilise the corresponding angular momentum at the perimeter to detach the impactors. The selection that was made, however, was to use a pneumatic piston. This has the benefit of being able to impart a pre-determined Δv , which can easily be adjusted by increasing the pressure in the reservoir supplying the piston.

System Description This system is comprised of two primary components; the pressure reservoir and the piston. Figure 41 below shows the arrangement of these subsystems.

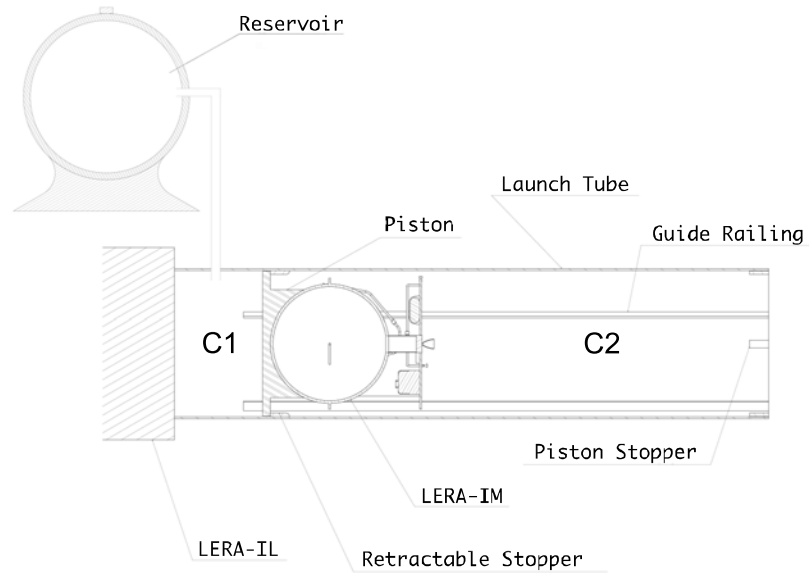


Figure 41: LERA-IL Configuration

Essentially, the pressure reservoir is connected to the piston chamber, segmented into two sections by a piston plate. As the valve is opened, pressurised nitrogen is allowed to flow from the reservoir and fill chamber C1. The piston plate is held in place by two switches, allowing the pressure in C1 to build. The pressure continues to build until a pressure sensor connected to C1 identifies that the chamber has a sufficient pressure to impart the required Δv . At this point, the switches holding the piston plate in place retract and allow the piston plate to move down the chamber, propelling the impactor out of the tube at the required Δv . Since this mission involves the launch of six impactors, six of these systems will be included on LERA-IB.

Piston Sizing In determining the allowable size of the piston, considerations included the diameter of the impactor, the internal dimensions of the upper-stage, and the distance required to accelerate the impactor to the required velocity. This yielded the design detailed in Figure 42 below:

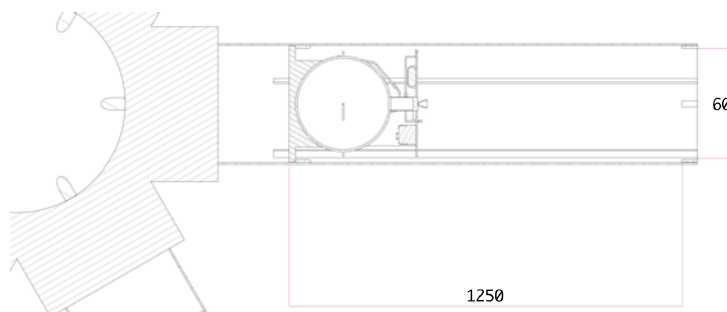


Figure 42: LERA-IL Configuration

9.5.10 Pressure-Tank Sizing

In order to determine the required pressure in the tank, Newtons second law of motion was used. Since the required $\Delta V = 300 [m/s]$, and the length of the launch tube is $d = 1.25 [m]$, the time to travel the length of the tube is $t = d/V = 0.31 [m]$. This corresponds to an acceleration of $a = V/t$, and since $F = ma$ this allows the calculation of the required force to accelerate the impactor to the required Δv value. Then, using $P_{req} = F/A$, where A is the cross sectional area of the piston plate, the required tank pressure was determined to be $2.28 \times 10^6 [Pa]$. In order to determine a feasible size and thickness of the tank to support this pressure, the process outlined in Appendix A above was used. The selected material for the tank was Aluminum-6061; selected for its low density and sufficiently high tensile and shear stress performance. The properties of Aluminum 6061 are captured in Table 52 below:

Table 52: Material properties of Aluminum-6061

Property	Value
σ_{CR}	$310 \times 10^6 [Pa]$
τ_{CR}	$207 \times 10^6 [Pa]$
ϵ_N	0.12
ν	0.33
ρ	$2.70 \times 10^3 [kg/m^3]$
E	$6.89 \times 10^{12} [Pa]$

As discussed previously, the pressure at a range of radii with varying levels of compression was analyzed, the results of which are shown in Figure 43a below. As the desire is to keep the size of this tank as small as possible, the selected radius of the tank was $0.233 [m]$, which corresponds to a tank pressure of $2.17 \times 10^7 [Pa]$, which is greater than the launch requirement of $2.28 \times 10^6 [Pa]$, so there is confidence that this reservoir will be able to provide sufficient force to achieve the target velocity. To determine if this pressure exceeded the stress requirements of Aluminum-6061, Figure 43b below was generated to compare the associated stress with design radius.

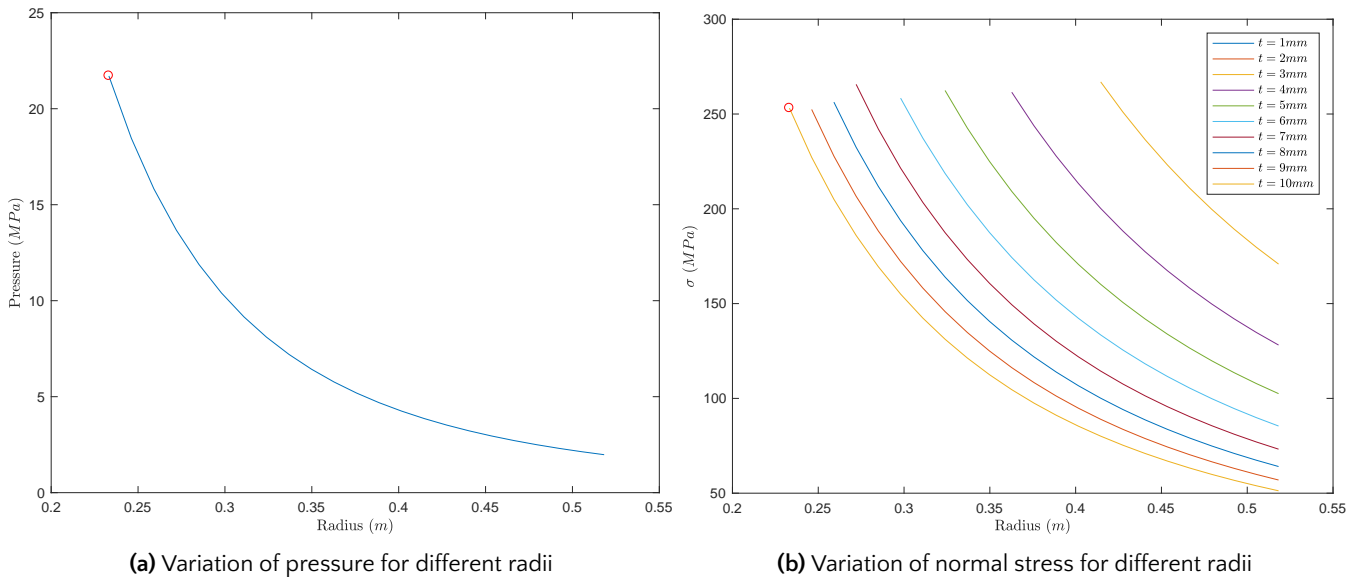


Figure 43: LERA-IL pressure and stress performance

As can be seen, the design point corresponds to a required thickness of $t = 1 \times 10^{-3} [m]$, which is achievable, and a normal stress of $2.53 \times 10^8 [Pa]$. Since $\sigma_{CR} = 3.10 \times 10^8 [Pa] > 2.53 \times 10^8$, this normal stress is acceptable. The same analysis was conducted for shear stress, shown in Figure 44a below. Figure 44b below also shows the relationship between radius and mass.

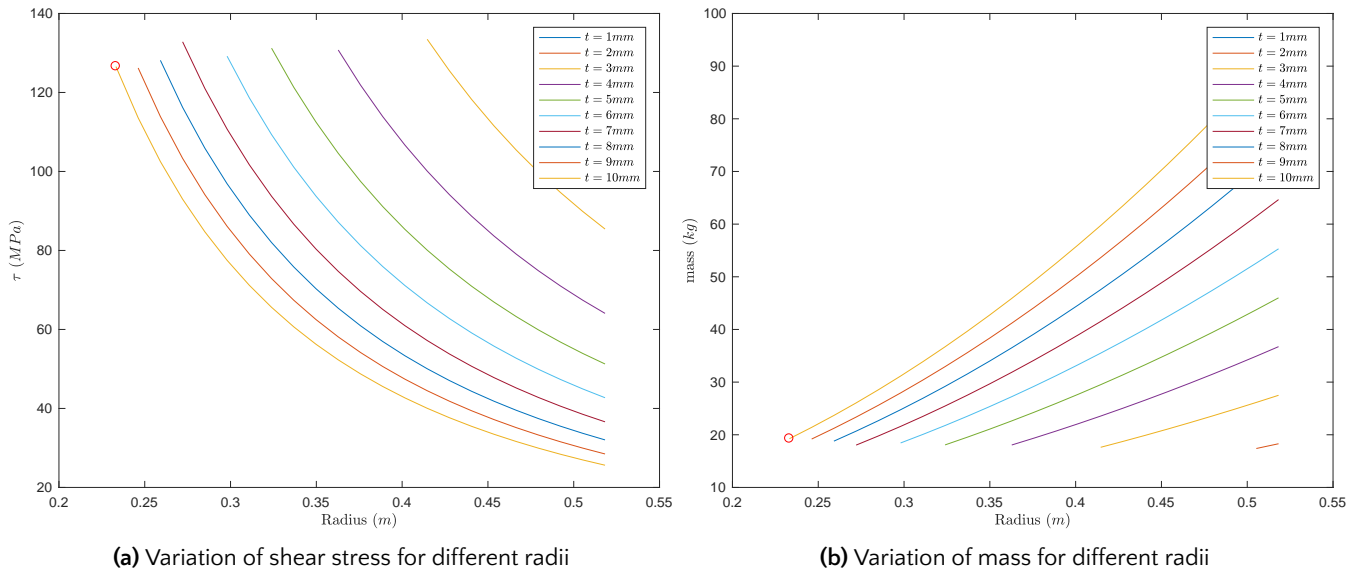


Figure 44: LERA-IL mass and shear stress characteristics

As it can be seen, the design point corresponds to a shear stress of $\tau = 1.27 \times 10^8 [Pa]$, which is less than the stated $\tau_{CR} = 2.07 \times 10^8 [Pa]$, and so there is confidence that this design will not experience material failure for this level of compression.

This means that for the design point selected, the mass of each tank is $m = 1.93 \times 10^1 [kg]$. The final design at the selected design point is illustrated in Figure 45 below:

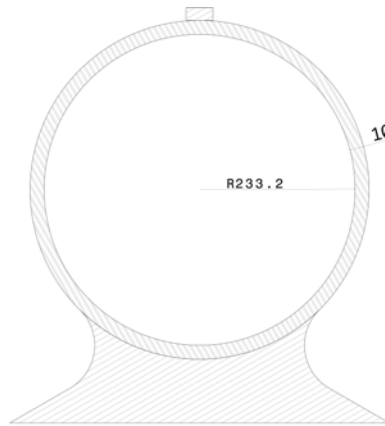


Figure 45: Dimensions of pressure tank at design point $r = 0.332 [m]$, $t = 10 [mm]$

9.5.11 Impactor Detachment Effect

The impact of this design on the Falcon 9 upper-stage at detachment can be predicted using the momentum equilibrium equations. This can be expressed as shown in equation 8 below:

$$m_{im}\Delta V_{im} = -m_{falcon}\Delta V_{falcon} \quad (8)$$

This states that the momentum induced on the impactor results in an equal and opposite momentum induced on the Falcon 9 upper-stage. Using $m_{im} = 30 [kg]$, $\Delta V_{im} = 300 [m/s]$ and the dry mass of the falcon 9, $m_{falcon} = 1.90 \times 10^3 [kg]$, the resulting velocity change on the Falcon 9 upper-stage can be calculated to be $\Delta V_{falcon} = 4.39 [m/s]$. This is considered an acceptable cost, and will be mitigated using the RCS of the Falcon 9 upper-stage.

9.6 Risk and Mitigation Strategies

Care was taken to identify all potential risks during the concept generation stage for LERA-IB. A proactive approach to mission threats was taken and mitigation strategies were identified in a bid to ensure continuous operational capability during the entire mission lifecycle. Several initiatives were taken to de-risk the mission architecture including but not limited to: leveraging design heritage by employing systems with flight-proven technology, designing in producibility to ensure conformability of components with the manufacturing system, and applying engineering management to establish quality, cost and time frameworks. The primary risks capable of jeopardising the integrity of the LERA-IB and its corresponding mitigation strategies are outlined in Table 53.

Table 53: LERA-IB risk and mitigation strategies

Risk Elements	Likelihood	Consequence	Mitigation Strategies
Failure of the pressurized LERA-IM propellant tank due to high pressure	Likely	High	Designing tank based on the internationally recognized pressure vessel safety codes
Failure of the pressurized LERA-IM propellant tank due to the force imparted by the piston in the LERA-IL	Likely	Very High	Designing the LERA-IM propellant tank with a reinforced girth weld and a mounting harness to distribute the force imparted
Failure of the onboard navigation and control instruments	Unlikely	Moderate	Using flight proven technology and utilization of heritage system architecture
Failure of systems due to environmental effects (exposure to excessive thermal profile, geomagnetic disturbance)	Unlikely	High	Using reliable components with flight proven technology or components that are currently in NASA's development portfolio

References

- [1] National Aeronautics and Space Administration. *Destination Moon: A History of the Lunar Orbiter Program*. Electronic Book. 2014. URL: <https://history.nasa.gov/TM-3487/contents.htm>.
- [2] National Aeronautics and Space Administration. *Lunar Atmosphere and Dust Environment Explorer (LADEE) Launch*. Report. 2013. URL: <https://www.nasa.gov/sites/default/files/files/LADEE-Press-Kit-08292013.pdf>.
- [3] Adcole Maryland Aerospace. *MAI-SS Space Sextant: Miniature Star Tracker*. Web Page. URL: <https://www.adcolemai.com/star-tracker-adacs-1>.

-
- [4] VECTRONIC Aerospace. *Reaction Wheel VRW-02*. Report. URL: <https://www.vectronic-aerospace.com/space-applications/reaction-wheel-vrw02/>.
- [5] Samina Asif and Yun Li. *Spacecraft Power Subsystem Technology Selection*. 2006. DOI: 10.1109/VPPC.2006.364275.
- [6] Orbital ATK. *GEOStar-2 Bus*. Report. 2014. URL: https://www.orbitalatk.com/space-systems/science-national-security-satellites/national-security-systems/docs/GEOStar2_Fact_Sheet.pdf.
- [7] Orbital ATK. *MegaFlex Solar Array*. Report. 2017. URL: https://www.orbitalatk.com/space-systems/space-components/solar-arrays/docs/MegaFlex_Solar_Array.pdf.
- [8] Orbital ATK. *UltraFlex Solar Array Systems*. Report. 2017. URL: https://www.orbitalatk.com/space-systems/space-components/solar-arrays/docs/UltraFlex_Factsheet.pdf.
- [9] ATMEL. *ATMEL AT697E Data Processing Unit*. Web Page. URL: <http://dtsheet.com/doc/235624/atmel-at697e>.
- [10] Edwin Barker et al. *Results of Observational Campaigns Carried Out During the Impact of Lunar Prospector into a Permanently Shadowed Crater near the South Pole of the Moon*. Vol. 31. 1999, p. 1583.
- [11] Gwen Bart et al. *Global survey of lunar regolith depths from LROC images*. Vol. 215. 2011, pp. 485–490. DOI: 10.1016/j.icarus.2011.07.017.
- [12] Pat Beauchamp et al. *Solar Power and Energy Storage for Planetary Missions*. Report. Jet Propulsion Laboratory, California Institute of Technology, 2015.
- [13] M. Beckman. "Mission Design for the Lunar Reconnaissance Orbiter". In: *29th Annual ASS Guidance and Control Conference*. American Astronautical Society, p. 4. URL: https://lunar.gsfc.nasa.gov/library/LRO_AAS_Paper_07-057.pdf.
- [14] Alejandro Belluscio. Web Page. Mar. 2016. URL: <https://www.nasaspaceflight.com/2016/10/its-propulsion-evolution-raptor-engine/>.
- [15] Narendra Bhandari. *Chandrayaan-1: Science goals*. Vol. 114. 2005, pp. 701–709. DOI: 10.1007/BF02715953.
- [16] Natasha Bosanac et al. "Trajectory design for a cislunar CubeSat leveraging dynamical systems techniques: The Lunar IceCube mission". In: *Acta Astronautica* 144 (2018), pp. 283–296. ISSN: 0094-5765. DOI: <https://doi.org/10.1016/j.actaastro.2017.12.025>. URL: <http://www.sciencedirect.com/science/article/pii/S0094576517307725>.
- [17] Adam Brand. *Reduced Toxicity, High Performance Monopropellant*. Report. US Air Force, 2011 2011.
- [18] T. G. Brockwell et al. "The mass spectrometer for planetary exploration (MASPEX)". In: *IEEE Aerospace Conference Proceedings*. Vol. 2016-June. DOI: 10.1109/AERO.2016.7500777. URL: <https://www.scopus.com/inward/record.uri?eid=2-s2.0-84978472525%5C&doi=10.1109%2fAERO.2016.7500777%5C&partnerID=40%5C&md5=1c42b57be909b011e51879439a31dce>
- [19] John R. Brophy et al. *Ion Propulsion System (NSTAR) DS1 Technology Validation Report*. Report. 1995. URL: https://pdssbn.astro.umd.edu/holdings/ds1-c-micas-3-rdr-visccd-borrelly-v1.0/document/doc_Apr04/int_reports/IPS_Integrated_Report.pdf.

-
- [20] R. Bugga et al. "Lithium Ion Batteries for Space Applications". In: *2007 IEEE Aerospace Conference*, pp. 1–7. DOI: 10.1109/AERO.2007.352728.
- [21] Bruce Campbell and Donald Campbell. "Regolith properties in the south polar region of the Moon from 70-cm radar polarimetry". In: *ICARUS 180* (2006), pp. 1–7.
- [22] Stephen Clark. *Spaceflight Now*. Web Page. 2017. URL: <https://spaceflightnow.com/2017/10/20/worlds-largest-methane-fueled-rocket-engine-test-fired-by-blue-origin/>.
- [23] Rockwell Collins. *RSI 01 Momentum and Reaction Wheel 0.1 Nms*. Report. URL: https://www.rockwellcollins.com/Products_and_Services/Defense/Platforms/Space/RSI_01_Momentum_and_Reaction_Wheel.aspx.
- [24] Data Device Corporation. *'Data Links and Networks in Space Applications – SpaceWire usage*. Report. 2005. URL: http://spacewire.esa.int/WG/SpaceWire/SpW-SnP-WG-Mtg4-Proceedings/Astrium_SpW_Usage.pdf.
- [25] Data Device Corporation. *SPACE-PHY Dual MIL-STD-1553 Transceiver/Transformer Device*. Report. 2017. URL: <http://www.ddc-web.com/Products/261/Default.aspx>.
- [26] Northrop Grumman Corporation. *LN-2005 IMU*. Report. Northrop Grumman Corporation, 2013. URL: <http://www.northropgrumman.com/Capabilities/LN200F0G/Documents/ln200s.pdf>.
- [27] Planetary Systems Corporation. *Mark II Motorized Lightband*. Web Page. URL: <http://www.planetarysystems.com/product/mark-ii-motorized-lightband/>.
- [28] Airbus Defence and Space. *ASTRIX 200*. Report. 2014. URL: http://www.space-airbusds.com/media/document/gnc_4_astrix-200_2015-v_std_b-def.pdf.
- [29] United States Department of Defense. *Department of Defense Standard Practice for System Safety*. Standard. 2012. URL: <https://www.system-safety.org/Documents/MIL-STD-882E.pdf>.
- [30] Oxford Dictionary. *Low Gain Antenna*. Web Page. 2018. DOI: 10.1093/oi/authority.20110803100116961. URL: <http://www.oxfordreference.com/view/10.1093/oi/authority.20110803100116961>.
- [31] C H Edwards et al. *The T5 Ion Propulsion Assembly for Drag Compensation on GOCE*. Report. European Space Station (ESA), 2004. URL: http://earth.esa.int/goce04/goce_proceedings/46_edwards.pdf.
- [32] Paul Gerin Fahlstrom and Thomas James Gleason. "Data-Link Margin". In: *Introduction to UAV Systems, Fourth Edition*. 2012. DOI: doi : 10.1002/9781118396780.ch14. URL: <https://onlinelibrary.wiley.com/doi/abs/10.1002/9781118396780.ch14>.
- [33] J. N. Goswami and M. Annadurai. *Chandrayaan-1: India's First Planetary Science Mission to the Moon*. Conference Paper. 2009.
- [34] Ariane Group. *Electric Propulsion Systems and Components: Radiofrequency Ion Propulsion For Orbit Raising, Station Keeping And Deep Space Missions*. Report. URL: <http://www.space-propulsion.com/brochures/electric-propulsion/electric-propulsion-thrusters.pdf>.

-
- [35] Saft Specialty Battery Group. *Rechargeable Li-ion battery systems: Light energy storage for space applications*. Report. 2006. URL: <http://www.houseofbatteries.com/documents/VES.pdf>.
- [36] Kevin Hall. *Gridded Ion Thruster developments*. Report. QinetiQ, 2017. URL: http://epic-src.eu/wp-content/uploads/23_EPICWorkshop2017_QinetiQ_EPIC_Madrid-2017.pdf.
- [37] William Harwood. *Atlas 5 rocket launches NASA moon mission*. Newspaper Article. May 2009. URL: <https://www.cnet.com/news/atlas-5-rocket-launches-nasa-moon-mission/>.
- [38] Grey Hautaluoma et al. *Lunar Reconnaissance Orbiter (LRO): Leading NASA's Way Back to the Moon; Lunar Crater Observation and Sensing Satellite (LCROSS): NASA's Mission to Search for Water on the Moon*. Press Release. 2009.
- [39] Jennifer L Heldmann et al. "LCROSS (Lunar Crater Observation and Sensing Satellite) observation campaign: strategies, implementation, and lessons learned". In: *Space science reviews* 167.1-4 (2012), pp. 93-140. ISSN: 0038-6308.
- [40] Brendan Hermalyn et al. "Scouring the surface: Ejecta dynamics and the LCROSS impact event". In: *Icarus* 218.1 (2012), pp. 654-665. ISSN: 0019-1035.
- [41] Scott A. Hill et al. "DRAFT Thermal Management Systems Roadmap". Washington DC, USA, 2010. URL: https://www.nasa.gov/pdf/501320main_TA14-Thermal-DRAFT-Nov2010-A.pdf.
- [42] K A Holsapple. "The Scaling of Impact Processes in Planetary Sciences". In: *Annual Review of Earth and Planetary Sciences* 21.1 (1993), pp. 333-373. DOI: 10.1146/annurev.ea.21.050193.002001. URL: <https://www.annualreviews.org/doi/abs/10.1146/annurev.ea.21.050193.002001>.
- [43] Honeywell. *MIMU: Miniature Inertial Measurement Unit*. Report. 2003. URL: <https://aerocontent.honeywell.com/aero/common/documents/myaerospacecatalog-documents/MIMU.pdf>.
- [44] KR Housen, RM Schmidt, and KA Holsapple. "Crater ejecta scaling laws: Fundamental forms based on dimensional analysis". In: *Journal of Geophysical Research: Solid Earth* 88.B3 (1983), pp. 2485-2499. ISSN: 2156-2202.
- [45] International Astronomical Union (IAU). *Planetary Names: Crater, craters: Cabeus*. Web Page. URL: <https://planetarynames.wr.usgs.gov/Feature/953>.
- [46] International Astronomical Union (IAU). *Planetary Names: Crater, craters: De Gerlache*. Web Page. URL: <https://planetarynames.wr.usgs.gov/Feature/1439>.
- [47] International Astronomical Union (IAU). *Planetary Names: Crater, craters: Faustini*. Web Page. URL: <https://planetarynames.wr.usgs.gov/Feature/1919>.
- [48] International Astronomical Union (IAU). *Planetary Names: Crater, craters: Haworth*. Web Page. URL: <https://planetarynames.wr.usgs.gov/Feature/14502>.
- [49] International Astronomical Union (IAU). *Planetary Names: Crater, craters: Shackleton*. Web Page. URL: <https://planetarynames.wr.usgs.gov/Feature/5450>.

-
- [50] International Astronomical Union (IAU). *Planetary Names: Crater, craters: Shoemaker*. Web Page. URL: <https://planetarynames.wr.usgs.gov/Feature/5494>.
- [51] Sinclair Interplanetary. *Second Generation Star Tracker (ST-16RT2)*. Report. 2015. URL: <http://www.sinclairinterplanetary.com/startrackers>.
- [52] P. A. Jones and B. R. Spence. "Spacecraft solar array technology trends". In: *IEEE Aerospace and Electronic Systems Magazine* 26.8 (2011), pp. 17–28. ISSN: 0885–8985. DOI: 10.1109/MAES.2011.5980605.
- [53] Lori Keesey. *Lunar IceCube to Take on Big Mission From Small Package*. Press Release. 2017. URL: <https://www.nasa.gov/feature/goddard/lunar-icecube-to-take-on-big-mission-from-small-package>.
- [54] J.W Keller et al. "The Lunar Reconnaissance Orbiter Mission – Six years of science and exploration of the Moon". In: *ICARUS* 273 (2016), pp. 2–24.
- [55] Sascha Kempf et al. *SUDA: A Dust Mass Spectrometer for Surface Mapping for the JUICE Mission to the Galilean Moons*. 2012, p. 1134.
- [56] Charles S. Leveritt and Nathan Klein. "Physical properties and molecular structure of the HAN-based liquid gun propellants". In: ed. by Anon. Publ by Fraunhofer–Inst fuer Treib- und Explosivstoffe, pp. 74.1–74.10. URL: <https://www.scopus.com/inward/record.uri?eid=2-s2.0-0025902086%5C&partnerID=40%5C&md5=543ee990185b6b98ca880e27f9d047fa>.
- [57] J. D. Lohn et al. "Automated synthesis of a lunar satellite antenna system". In: *IEEE Transactions on Antennas and Propagation* 63.4 (2015), pp. 1436–1444. DOI: 10.1109/TAP.2015.2404332. URL: <https://www.scopus.com/inward/record.uri?eid=2-s2.0-84927629826%5C&doi=10.1109%2fTAP.2015.2404332%5C&partnerID=40%5C&md5=e887ba5f810bb6d36b8fac11c6e83b8a>.
- [58] Tariq Malik. *Chang'e 1: China Gears Up for First Moon Mission*. Newspaper Article. 2007. URL: <https://www.space.com/3564-change-1-china-gears-moon-mission.html>.
- [59] R. K. Masse et al. "AF-M315E propulsion system advances & improvements". In: *52nd AIAA/SAE/ASEE Joint Propulsion Conference, 2016*. URL: <https://www.scopus.com/inward/record.uri?eid=2-s2.0-84983494279%5C&partnerID=40%5C&md5=a89ad868798a5c43a7321ba15b317071>.
- [60] R. Masse et al. "GPIMAF-M315E propulsion system". In: *51st AIAA/SAE/ASEE Joint Propulsion Conference*. URL: <https://www.scopus.com/inward/record.uri?eid=2-s2.0-84946031539%5C&partnerID=40%5C&md5=023771d724deb0688c782efafa464e>
- [61] S Maurice et al. *Distribution of Hydrogen at the Surface of the Moon*. Conference Paper. 2003.
- [62] Solar MEMS. *nanoSSOC-A60 Technical Specification, Interfaces & Operation*. Report. 2016. URL: <https://www.cubesatshop.com/wp-content/uploads/2016/06/nanoSSOC-A60-Technical-Specifications.pdf>.
- [63] Solar MEMS. *nanoSSOC-D60 Technical Specification, Interfaces & Operation*. Report. 2016. URL: <https://www.cubesatshop.com/wp-content/uploads/2016/06/nanoSSOC-D60-Technical-Specifications.pdf>.

-
- [64] Solar MEMS. *SSOC-A60 Technical specification, Interfaces & Operation*. Report. 2015. URL: <https://www.cubesatshop.com/wp-content/uploads/2016/06/SSOCA60-Technical-Specifications.pdf>.
- [65] Solar MEMS. *SSOC-D60 Technical specification, Interfaces & Operation*. Report. 2015. URL: <https://www.cubesatshop.com/wp-content/uploads/2016/06/SSOCD60-Technical-Specifications.pdf>.
- [66] MicroWheel. *Microwheel 200 MSCI*. Report. MicroWheel. URL: <http://www.msinc.ca/products/MicroWheel-200.pdf>.
- [67] Tamil Nadu. *Chandrayaan-1 mission completed in cost-effective manner, says top official*. Newspaper Article. 2011. URL: <http://www.thehindu.com/news/national/tamil-nadu/Chandrayaan-1-mission-completed-in-cost-effective-manner-says-top-official/article15461165.ece>.
- [68] NASA. *TA 14: Thermal Management Systems*. Report. NASA, 2015. URL: https://www.nasa.gov/sites/default/files/atoms/files/2015_nasa_technology_roadmaps_ta_14_thermal_management_final.pdf.
- [69] NASA. *The Europa Clipper Imaging System Narrow Angle Camera (EIS - NAC)*. Report. 2018.
- [70] NASA. *The Europa Clipper Imaging System Narrow Angle Camera (EIS - WAC)*. Report. 2018.
- [71] NASA. *The Europa Clipper Thermal Emission Imaging System (E-THEMIS)*. Report. 2018.
- [72] Björn Ohlson. "SSC – space expertise on high latitudes". In: *FMV Sensor Symposium*.
- [73] C. M. Pieters et al. "Character and spatial distribution of OH/H₂O on the surface of the moon seen by M3 on chandrayaan-1". In: *Science* 326.5952 (2009), pp. 568–572. DOI: 10.1126/science.1178658. URL: <https://www.scopus.com/inward/record.uri?eid=2-s2.0-70350502064%5C&doi=10.1126%2fscience.1178658%5C&partnerID=40%5C&md5=6a19041d78b7ad627a7e407efedb0622>.
- [74] Kagan Pittman. *New Thermal Imaging Technology to Look for Life on Jupiter Moon*. Web Page. 2015. URL: <https://www.engineering.com/DesignerEdge/DesignerEdgeArticles/ArticleID/10254/New-Thermal-Imaging-Technology-to-Look-for-Life-on-Jupiter-Moon.aspx>.
- [75] Jonothan Polaha. *Internal Resistive Heating of Catalyst Bed for Monopropellant Catalyst*. Patent. 2011. URL: <https://patentimages.storage.googleapis.com/ae/0a/62/5dccfb786aac19/US20110165030A1.pdf>.
- [76] Aerojet Rocketdyne. *Monopropellant Thrusters*. Catalog. 2006. URL: <http://www.rocket.com/files/aerojet/documents/Capabilities/PDFs/Monopropellant%20Data%20Sheets.pdf>.
- [77] Peter H Schultz et al. "The LCROSS cratering experiment". In: *science* 330.6003 (2010), pp. 468–472. ISSN: 0036-8075.
- [78] Emily Shanklin. *SpaceX Draco Thruster Performs Long Duration Firing and Restart*. Web Page. 2008. URL: <http://www.spacex.com/press/2012/12/19/spacex-draco-thruster-performs-long-duration-firing-and-restart>.
- [79] Micro Aerospace Solutions. *MASIMU03 Inertial Measurement Unit*. Report. URL: <http://www.micro-a.net/imu-tmpl.html>.
- [80] TY-Space. *Nano Star Tracker NST-1*. Report. URL: <https://www.cubesatshop.com/wp-content/uploads/2016/06/English-Flyer-logo.pdf>.
-

-
- [81] SpaceX. *Falcon 9 Launch Vehicle Payload User's Guide*. Report. 2015. URL: http://www.spacex.com/sites/spacex/files/falcon_9_users_guide_rev_2.0.pdf.
- [82] Swedish Space Corporation (SSC). *Ground Station Network*. Web Page. 2018. URL: <https://www.sscspace.com/services/leop/>.
- [83] Swedish Space Corporation (SSC). *Launch Support Service*. Web Page. 2018. URL: <https://www.sscspace.com/services/leop/>.
- [84] Swedish Space Corporation (SSC). *On-Orbit*. Web Page. 2018. URL: <https://www.sscspace.com/services/on-orbit/>.
- [85] Swedish Space Corporation (SSC). *USER'S HANDBOOK*. Web Page. 2011.
- [86] Scott R. Starin and John Eterno. *Attitude Determination and Control Systems*. Report. NASA, 2011. URL: <https://ntrs.nasa.gov/search.jsp?R=20110007876%5C&hterms=20110007876%5C&q=Ntx%3Dmode%2520matchallany%26Ntk%3DDocument-ID%26Ns%3DAcquired-Date%7C1%26N%3D0%26Ntt%3D20110007876>.
- [87] Z. Sternovsky et al. "The Large Area Mass Analyzer (LAMA) for in-situ chemical analysis of interstellar dust particles". In: *ESA - Workshop on Dust in Planetary Systems*, pp. 205–208. URL: <https://www.scopus.com/inward/record.uri?eid=2-s2.0-42549104311%5C&partnerID=40%5C&md5=00fe479dda4dc2ff0813003e19ee1bc6>.
- [88] Paul D Strycker et al. "Characterization of the LCROSS impact plume from a ground-based imaging detection". In: *Nature communications* 4 (2013), p. 2620. ISSN: 2041-1723.
- [89] Rao Surampudi et al. *Solar Power Technologies for Future Planetary Science Missions*. Report. NASA, 2017. URL: <https://solarsystem.nasa.gov/resources/548/solar-power-technologies-for-future-planetary-science-missions/>.
- [90] BAE Systems. *RAD750 3U CompactPCI*. Report. 2016. URL: <https://www.baesystems.com/en/download-en/20161103153137/1434555679066.pdf>.
- [91] NewSpace Systems. *NewSpace Fine Sun Sensor NFSS-411ñ Datasheet*. Report. URL: https://www.cubesatshop.com/wp-content/uploads/2016/06/NewSpace-Sun-Sensor_6a-1.pdf.
- [92] Wind River Systems. *VxWORKS*. Report. 2018. URL: <https://www.windriver.com/products/vxworks>.
- [93] Blue Canyon Technologies. *BCT Extended Baffle Nano Star Tracker*. Report. Blue Canyon Technologies. URL: http://bluecanyontech.com/wp-content/uploads/2015/12/Ext-Baffle-NST-Data-Sheet_1.1.pdf.
- [94] Surrey Satellite Technology. *Rigel-L Star Tracker*. Report. 2014. URL: http://www.sst-us.com/downloads/datasheets/rigel--star-tracker-datasheet_v112.pdf.
- [95] Surrey Sattelite Technology. *10SP-M Small Satellite Microwheel*. Report. URL: <http://www.sst-us.com/shop/satellite-subsystems/attitude-and-orbit-control-systems/10sp-m-small-satellite-microwheel-4-unit-package>.
- [96] Jay R. Thompson. *About Europa Clipper*. Web Page. 2016. URL: <https://europa.nasa.gov/about-clipper/overview/>.

- [97] Aditya Tulsyan et al. "State-of-charge estimation in lithium-ion batteries: A particle filter approach". In: *Journal of Power Sources* 331 (2016), pp. 208–223. ISSN: 0378-7753. DOI: <https://doi.org/10.1016/j.jpowsour.2016.08.113>. URL: <http://www.sciencedirect.com/science/article/pii/S0378775316311338>.
- [98] Morehead State University. *MSU's 'Deep Space Probe' selected by NASA for Lunar Mission*. Press Release. 2015. URL: https://web.archive.org/web/20150526085021/http://www.moreheadstate.edu/News/2015/April/MSU_s__Deep_Space_Probe__selected_by_NASA_for_Lunar_Mission/.
- [99] J R Wertz, D F Everett, and J J Puschell. *Space Mission Engineering: The New SMAD*. Microcosm Press, 2011. ISBN: 9781881883159. URL: <https://books.google.com.au/books?id=a1FNMAEACAAJ>.
- [100] GS YUASA. *Lithium ion cells for satellites applications LSE series*. Web Page. URL: http://www.gsyuasa-lp.com/SpecSheets/GSYuasa-LSE50_100_175.pdf.
- [101] Kathleen Zona. *Liquid Hydrogen—the Fuel of Choice for Space Exploration*. Web Page. 2010. URL: https://www.nasa.gov/topics/technology/hydrogen/hydrogen_fuel_of_choice.html.
- [102] Wei Zuo, Chunlai Li, and Zhubin Zhang. "Scientific data and their release of ChangE-1 and ChangE-2". In: *Chinese Journal of Geochemistry* 33.1 (2014), pp. 24–44. ISSN: 1993-0364. DOI: 10.1007/s11631-014-0657-3. URL: <https://doi.org/10.1007/s11631-014-0657-3>.

Appendix A Pressure Tank Design

In undertaking the design of both the detachment system (LERA-IL) and the impactor system (LERA-IM), the design of pressure tanks was required. The following is a presentation of the general methodology followed to determine the size, mass and thickness of the tanks to withstand required stress, strain and pressure requirements. For a specified initial mass (m_i), a required change in velocity (Δv), and the specific impulse (I_{sp}) of the chosen propellant, the final vehicle mass (m_f) can be found:

$$m_f = m_i \times e^{-\frac{\Delta v}{g I_{sp}}} \quad (9)$$

Using this, the mass of the propellant (m_p) can also be determined:

$$m_p = m_f \left(e^{\frac{\Delta v}{g I_{sp}}} - 1 \right) \quad (10)$$

The uncompressed volume of the propellant can be determined using m_p and the propellants density ρ_p using the relation:

$$V_{uc} = \frac{m_p}{\rho_p} \quad (11)$$

From here, is it trivial to determine the radius of a sphere with this volume:

$$r = \left(\frac{3V_{uc}}{4\pi} \right)^{\frac{1}{3}} \quad (12)$$

This radius is then compressed to a set of radii (r_c) by multiplying it with a set of adjustment factors (R):

$$r_c = \{R\} \times r \quad \forall 0.05 \leq R \leq 1, R \text{ mod } 0.01 = 0 \quad (13)$$

These new compressed radii, r_c , can be used to calculate the volume of the gas after compression (V_c):

$$V_c = \frac{4}{3}\pi r_c^3 \quad (14)$$

In order to determine the pressure of this compressed gas, the temperature of the gas in space must be calculated. This temperature is assumed to be the same as that of the enclosing tank, the calculation of which is as follows:

$$T = \left(\frac{(S + S_r) \times \frac{a_v}{\epsilon_{IR}} + E_{IR}}{4\sigma_{SB}} \right)^{\frac{1}{4}} \quad (15)$$

Where S is the solar flux, S_r is the solar flux reflected from Earth, a_v is the absorptivity of the tank material, ϵ_{IR} is the emissivity of the tank material, E_{IR} is the Earth's infrared flux and σ_{SB} is the Stefan-Boltzmann constant. This allows for the calculation of the pressure of the gas in the volume V_c :

$$P_c = \frac{m_p RT}{V_c} \quad (16)$$

The consideration however, is how this pressure affects the tensile stress of the tank. For a given thickness (t), this can be determined:

$$\sigma_t = \frac{P_c r_c}{2t} \quad (17)$$

This stress value can then be compared with the critical stress for the material (σ_{CR}) to determine if the material will fail. A similar process can be followed for the shear stress induced on the tank, using the following equation:

$$\tau = \frac{P_c r_c}{4t} \quad (18)$$

This value is compared with the critical shear stress for the material (τ_{CR}) to determine if the material will fail. Provided that neither σ_{CR} or τ_{CR} is exceeded, this radius and thickness can provide the volume (V_{tank}) and dimensions for an acceptable tank:

$$V_{tank} = \frac{4}{3}\pi(r_c + t)^3 - \frac{4}{3}\pi r_c^3 \quad (19)$$

V_{tank} can then be used to determine the mass of the tank (m_{tank}) when multiplied by the density of the tank material (ρ_{tank}):

$$m_{tank} = V_{tank}\rho_{tank} \quad (20)$$

Appendix B Thruster Design Equations

To determine the thrust required to achieve a maneuver, the acceleration (a_{thrust}) must be found using the following equation.

$$a_{thrust} = \frac{\Delta V}{t_{burn}} \quad (21)$$

The acceleration (a_{thrust}) is then used in conjunction with the initial mass (m_i) to determine the Thrust (F_T) required from each of the thrusters. Here, the m_i is the initial wet mass.

$$F_T = m_i a_{thrust} \quad (22)$$

The characteristic velocity C^* is determined using the following equation.

$$C^* = \frac{a_0}{\gamma \left(\frac{2}{\gamma+1} \right)^{\frac{\gamma+1}{2(\gamma-1)}}} \quad (23)$$

Where g is the gravity on the Earth, γ is the ratio of specific heat of the propellant being used and a_0 is the sonic velocity of the gas. This is then implemented to find the pressure of the propellant at the exit of the thruster (P_e).

$$I_{sp} = \frac{C^*}{g} \gamma \left\{ \left(\frac{2}{\gamma-1} \right) \left(\frac{2}{\gamma+1} \right)^{\frac{\gamma+1}{\gamma-1}} \left(1 - \frac{P_e}{P_c} \right)^{\frac{\gamma-1}{\gamma}} \right\}^{\frac{1}{2}} \quad (24)$$

Here, P_c is the internal pressure of the compressed gas in the tank. Though as the volume decreases this will drop, it has been assumed to remain constant. The Mach number (M_e) at the exit of the nozzle can now be determined.

$$\frac{P_e}{P_c} = \left(1 + \frac{\gamma-1}{2} M_e^2 \right)^{\frac{-\gamma}{\gamma-1}} \quad (25)$$

Now, using all the characteristics calculated, the following two equations can be simultaneously solved to obtain the area of the nozzle throat (A_t) and the area of the nozzle exit (A_e).

$$F = A_t P_c \gamma \left[\left(\frac{2}{\gamma-1} \right) \left(\frac{2}{\gamma+1} \right) \left(1 - \frac{P_e}{P_c} \right) \right] + P_e A_e \quad (26)$$

$$\frac{A_e}{A_t} = \frac{1}{M_e} \left[\left(\frac{2}{\gamma+1} \right) \left(1 + \frac{\gamma-1}{2} M_e^2 \right) \right]^{\frac{\gamma+1}{2\gamma-1}} \quad (27)$$

The throat area (A_t) and exit area (A_e) of the designed nozzle can then be converted to throat radius (r_t) and exit radius (r_e), respectively.

Appendix C LERA-O Propulsion

C.1 Parameters

Table 54: LERA-O propulsion parameters

Parameter	Value
m_e [kg]	150
Δv [m/s]	1.25×10^3
I_{sp} [s]	248
g_0 [m/s ²]	9.81
F_{max} [N]	26.9
F_{min} [N]	5.70
ρ [kg/m ³]	1.46×10^3
$R_p, estimate$	0.20
P_{max} [kPa]	3.79×10^3
P_{min} [kPa]	690
T [K]	193
M_N [g/mol]	14.0
M_H [g/mol]	1.00
M_O [g/mol]	16.0
N_A [1/mol]	6.02×10^{23}

C.2 Maneuvers

The LERA-O dry mass m_e was calculated from the system mass breakdown. A total fuel burn and thrusting duration was calculated for separation, orbital capture and orbital plane change maneuvers. Fuel mass m_f is calculated using the ideal rocket equation:

$$m_f = m_e e^{\frac{\Delta v}{v_{eq}}} - m_e \quad (28)$$

Where Δv is the change in velocity required and v_{eq} , the equivalent exhaust velocity is calculated by:

$$v_{eq} = I_{sp} g_0 \quad (29)$$

Where I_{sp} is specific impulse and g_0 is the gravitational acceleration on Earth. The total wet mass m_w of the orbiter can therefore be calculated.

$$m_w = m_e + m_f \quad (30)$$

In order to calculate the total fuel burn duration, the average acceleration required across all three maneuvers must first be calculated. In order to calculate acceleration the average orbiter mass and average thrust must be calculated.

Average mass m_{av} is given by:

$$m_{av} = \frac{m_e + m_w}{2} \quad (31)$$

Average thrust F_{av} is given by:

$$F_{av} = \frac{F_{max} + F_{min}}{2} \quad (32)$$

Average acceleration a_{av} is given by:

$$a_{av} = \frac{F_{av}}{m_{av}} \quad (33)$$

Total mission thrusting duration t can then be calculated:

$$t = \frac{\Delta v}{a_{av}} \quad (34)$$

C.3 Tank requirements

The propellant tank contains liquid AF-M315E propellant and gaseous nitrogen pressurant. In order to calculate the total required propellant tank volume, both the volume of propellant and pressurant required must be calculated. Propellant volume V_f is calculated by:

$$V_f = \frac{m_f}{\rho} \quad (35)$$

Where ρ is propellant density. The pressurant volume V_p is then calculated by first estimating an initial pressurant to propellant volume ratio $R_{p,estimate}$. Most diaphragm tanks for monopropellants have a pressurant-to-propellant ratio of 0.2 – 0.25. The initial pressurant volume is then calculated:

$$V_p = R_p V_f \quad (36)$$

The pressurant mass m_p is calculated twice, once with regard to the minimum tank pressure condition and once with regard to the maximum tank pressure condition. The minimum $m_{p,min}$ and maximum $m_{p,max}$ are calculated as:

$$m_{p,min} = \frac{P_{min}(V_f + V_p)}{RT} \quad (37)$$

$$m_{p,max} = \frac{P_{max}V_p}{RT} \quad (38)$$

Where P_{min} and P_{max} are minimum and maximum pressure respectively, R is the universal gas constant of and T is the tank internal temperature.

The initial estimate of R_p is then adjusted until $m_{p,min}$ and $m_{p,max}$ equalize and a solution is found. V_p is also recalculated given the final value of R_p .

Total tank volume V can then be calculated as the sum of the initial pressurant and propellant volumes.

$$V = V_p + V_f \quad (39)$$

The diameter D of the spherical propellant tank is:

$$D = \sqrt[3]{\frac{3V}{4\pi}} \quad (40)$$

C.4 Propellant thermal management

AF-M315E has a glass transition of $-85C^\circ$ [56]. For an added tolerance, the propellant temperature is to be maintained above $-80C^\circ$. The power required to keep the propellant was to be calculated. This calculation was based on the rate of thermal conduction Q from the fuel to ambient temperature. The molar mass M of hydroxyl ammonium nitrate NH_3OHNO_3 was first calculated by:

$$M = \sum_i x_i M_i \quad (41)$$

Where x_i is the mole fraction and M_i is the molar mass of each element. Molar volume V_m is calculated by:

$$V_m = \frac{M}{\rho} \quad (42)$$

The speed of sound c in hydroxyl ammonium nitrate is approximated using the formula [56]:

$$c = 1966 - 1.703T \quad (43)$$

Where T is the propellant temperature in C° . The conductivity constant λ is then calculated:

$$\lambda = 2.8 \left(\frac{N_A}{V_m} \right)^{\frac{2}{3}} kc \quad (44)$$

Where N_A is Avogadro's number and k is Boltzmann's constant. The rate of thermal conduction is then calculated as:

$$Q = \frac{\lambda A (T_1 - T_2)}{d} \quad (45)$$

Where A is the internal tank surface area, T_1 and T_2 are the desired propellant temperature and the ambient external temperature respectively.

Appendix D Cost and Mass Estimation

SYSTEM	SUBSYSTEM	COMPONENT	Qty	MASS (each) [kg]	MASS (total) [kg]	CONTINGENCY [%]	MASS + CONTINGENCY [kg]	TRL	f	Constant	CI	Cost [\$M USD]	
LERA-IB													
Impactor	LERA-IM	Copper Tank	6	18.67	112.02	5	117.62	9	0.10	0.86	7.93	11.90	
Impactor	LERA-IM	Propellant (Xenon)	6	1.28	7.70	5	8.08	9	0.93	0.86	5.80	8.89	
Impactor	LERA-IM	Maneuver Thrusters	48	0.06	2.88	5	3.02	9	1.00	0.86	2.45	29.39	
Impactor	LERA-IM	Venting Thruster	6	0.20	1.20	5	1.26	9	1.00	0.86	1.07	1.60	
Impactor	LERA-IM	LSE 102 Li-Ion Battery Cell	6	2.77	16.62	5	17.45	9	1.00	0.86	12.95	19.42	
Impactor	LERA-IM	MAI-SS Miniature Star Tracker	6	0.28	1.69	5	1.78	9	1.00	0.86	1.48	2.22	
Impactor	LERA-IM	Northrop LM-2005	6	0.75	4.49	5	4.71	9	1.00	0.86	3.73	5.60	
Impactor	LERA-IM	Piping/Plumbing	6	2.00	12.00	5	12.60	9	0.10	0.86	0.95	1.43	
Impactor	LERA-IM	Structural Harness	6	5.00	30.00	5	31.50	9	1.00	0.86	22.69	34.04	
Impactor	LERA-IM	ATMEL AT697E Data Processing Unit	6	0.01	0.05	5	0.06	9	1.00	0.86	0.06	0.08	
TOTAL							198.08					114.37	
Impactor	LERA-IB	Structure	1	250.00	250.00	5	262.50	9	1.00	0.86	170.08	42.52	
Impactor	LERA-IB	Patch Antenna	2	1.00	2.00	5	2.10	9	1.00	0.86	1.73	0.87	
Impactor	LERA-IB	Solar Panel	4	5.00	20.00	5	21.00	9	1.00	0.86	15.44	15.44	
Impactor	LERA-IB	8PSK X-Band Transmitter	1	1.37	1.37	5	1.44	9	0.50	0.86	0.60	0.15	
Impactor	LERA-IB	TTC X-Band Flexible Transponder	1	3.60	3.60	5	3.78	9	0.50	0.86	1.51	0.38	
Impactor	LERA-IB	V48E Li-Ion Battery	1	113	113	5	119	9	0.50	0.86	0.50	0.13	
TOTAL							292.01					59.48	
Impactor	LERA-IL	Launch Tube	6	30.00	180.00	5	189.00	6	0.10	0.86	12.45	18.67	
Impactor	LERA-IL	Piston Reservoir	6	19.26	115.56	5	121.34	6	0.80	0.86	65.37	98.05	
Impactor	LERA-IL	Propellant (Nitrogen)	6	10.62	63.71	5	66.90	9	1.00	0.86	46.41	69.61	
Impactor	LERA-IL	Piston	6	1.10	6.60	5	6.93	6	0.10	0.86	0.54	0.81	
TOTAL							384.16					187.14	
TOTAL FOR LERA-IB							874.31						360.29
LERA-O													
Orbiter	CDH	BAE RAD750 3U cPCI	1	0.55	0.55	5	0.58	9	1.00	0.86	0.51	0.06	
Orbiter	CDH	DDC MIL-STD-1553	1	0.01	0.01	5	0.01	9	0.20	0.86	0.00	0.00	
Orbiter	CDH	SpaceWire IEEE 1355	10	0.00	0.03	5	0.03	9	0.20	0.86	0.01	0.02	
Orbiter	CDH	Aluminium Casing	1	0.74	0.74	5	0.77	9	0.10	0.86	0.07	0.02	
Orbiter	CDH	Patch Antenna	2	1.00	2.00	5	2.10	9	1.00	0.86	1.73	0.87	
TOTAL							1.30					0.96	
Orbiter	ADCS	Sinclair ST-16RT2	2	0.16	0.32	5	0.33	9			0.12	0.24	
Orbiter	ADCS	SolarMEMS nanoSSOC- D60	4	0.01	0.02	5	0.03	9			0.00	0.02	
Orbiter	ADCS	Northrop LN- 2005	1	0.75	0.75	5	0.79	9	1.00	0.86	0.68	0.17	
Orbiter	ADCS	Vecronic VRW-02	4	1.00	4.00	5	4.20	9	1.00	0.86	3.35	3.35	
Orbiter	ADCS	QinetiQ TS	4	2.50	10.00	5	10.50	9	1.00	0.86	7.99	7.99	
Orbiter	ADCS	Ion Propulsion Control Unit (IPCU)	1	16.70	16.70	5	17.54	9	1.00	0.86	13.01	3.25	
Orbiter	ADCS	Proportional Xenon Feed Assembly (PXFA)	1	7.50	7.50	5	7.88	9	1.00	0.86	6.08	1.52	
Orbiter	ADCS	Propellant (Xenon)		6.05	6.05		0.00		1.00	0.86		0.01	
Orbiter	ADCS	Propellant tank	1	5.93	5.93	5	6.23	9	0.10	0.86	0.49	0.12	
TOTAL							53.83					16.67	
Orbiter	EPS	Triple-junction solar cells	1	30.96	30.96	5	32.51	9	1.00	0.86	23.38	5.85	
Orbiter	EPS	V48E Li-Ion Battery	1	112	112	5	118	9	1.00	0.86	1.00	0.25	
TOTAL							33.68					6.09	
Orbiter	Propulsion	Propellant	1	100.86	100.86	10	100.86	7	\$10/kg			0.00	
Orbiter	Propulsion	Pressurant	1	1.05	1.05	9	1.05	9	1.00	0.86	0.90	0.22	
Orbiter	Propulsion	Tank	1	8.39	8.39	10	9.23	7	0.10	0.86	0.71	0.18	
Orbiter	Propulsion	Thruster	1	0.59	0.59	10	0.65	7	1.00	0.86	0.57	0.14	
Orbiter	Propulsion	Latch valve	1	0.40	0.40	10	0.44	7	1.00	0.86	0.39	0.10	
Orbiter	Propulsion	Service valve	2	0.10	0.20	10	0.22	7	1.00	0.86	0.20	0.10	
Orbiter	Propulsion	Pressure transducer	2	0.25	0.50	10	0.53	7	1.00	0.86	0.49	0.24	
Orbiter	Propulsion	Tubing (1/4")	1	0.60	0.60	10	0.66	7	0.10	0.86	0.06	0.01	
Orbiter	Propulsion	Filter	1	0.08	0.08	10	0.09	7	1.00	0.86	0.09	0.02	
Orbiter	Propulsion	Electrical wiring/harnessing	1	1.00	1.00	10	1.10	7	1.00	0.86	0.94	0.23	
TOTAL							114.85					1.26	
Orbiter	Science	SUDA	1	8.00	8.00	12	8.96	6	1.00	0.86	6.87	1.72	
Orbiter	Science	MASPEX	1	4.00	4.00	12	4.48	6	1.00	0.86	3.56	0.89	
Orbiter	Science	NAC	1	6.60	6.60	5	6.93	9	1.00	0.86	5.38	1.35	
Orbiter	Science	WAC	1	1.10	1.10	5	1.16	9	1.00	0.86	0.98	0.25	
Orbiter	Science	E-THEMIS	1	11.40	11.40	5	11.97	9	1.00	0.86	9.05	2.26	
TOTAL							33.50					6.46	
TOTAL FOR LERA-O (Dry)							137.44						31.44
TOTAL FOR LERA-O (Wet)							239.31						31.44
Operations													
Operations		Launch	1					9				50.00	
Operations		Ground Operations	1									3.00	
Operations		Post-mission	1									4.00	
Other		Mission insurance	1									25.00	
Other		Mission contingency	1									25.00	
TOTAL FOR LERA mission												694.43	